


12-2016

ROS regulation of axonal mitochondrial transport

Pin-Chao Liao
Purdue University

Follow this and additional works at: https://docs.lib.purdue.edu/open_access_dissertations

 Part of the [Biology Commons](#), [Cell Biology Commons](#), and the [Neuroscience and Neurobiology Commons](#)

Recommended Citation

Liao, Pin-Chao, "ROS regulation of axonal mitochondrial transport" (2016). *Open Access Dissertations*. 966.
https://docs.lib.purdue.edu/open_access_dissertations/966

This document has been made available through Purdue e-Pubs, a service of the Purdue University Libraries. Please contact epubs@purdue.edu for additional information.

**PURDUE UNIVERSITY
GRADUATE SCHOOL
Thesis/Dissertation Acceptance**

This is to certify that the thesis/dissertation prepared

By Pin-Chao Liao

Entitled

ROS REGULATION OF AXONAL MITOCHONDRIAL TRANSPORT

For the degree of Doctor of Philosophy

Is approved by the final examining committee:

Peter J. Hollenbeck

Chair

Jean-Christophe Rochet

Henry C. Chang

Daniel M. Suter

To the best of my knowledge and as understood by the student in the Thesis/Dissertation Agreement, Publication Delay, and Certification Disclaimer (Graduate School Form 32), this thesis/dissertation adheres to the provisions of Purdue University's "Policy of Integrity in Research" and the use of copyright material.

Approved by Major Professor(s): Peter J. Hollenbeck

Approved by: Christine A. Hrycyna

Head of the Departmental Graduate Program

8/16/2016

Date

ROS REGULATION OF AXONAL MITOCHONDRIAL TRANSPORT

A Dissertation

Submitted to the Faculty

of

Purdue University

by

Pin-Chao Liao

In Partial Fulfillment of the

Requirements for the Degree

of

Doctor of Philosophy

December 2016

Purdue University

West Lafayette, Indiana

ACKNOWLEDGEMENTS

I would like to thank my advisor, Dr. Peter Hollenbeck for his great guidance and support in these years. He is a great advisor and mentor I've ever met. His attitude toward science affects me a lot. Data tell the story! I enjoy the way how he guides students. When we have questions, instead of giving us answers directly, he usually asks us "what do you think?" Then he provides unique insights into our questions. In addition, I really appreciate that he is never mean with vacations for students, so I can maintain my long-distance relationship with my wife. I am grateful to have this excellent advisor in my PhD career, and really enjoy working in this lab. I would also express my thanks to my committee members, Dr. Daniel Suter, Dr. Henry Chang, and Dr. Chris Rochet. During committee meetings, they gave me their valuable comments, suggestions, and feedback. These suggestions guided me on the right track of my research. I also appreciate their comments on my manuscript. Without them, I would definitely encounter more difficulties in my PhD career.

I would also like to thank our lab members, Swathi Devireddy, Hyun Sung, Elisabeth Garland-Kuntz and Doris Kemler. Swathi and Hyun are great fellow graduate students. They answered tons of my questions no matter about lab or life. They also gave me many suggestions about my research. Liz is the best technician I've met. She maintained our lab extremely well and helped our graduate students a lot. Doris also helped us a lot for maintaining our fly stock and lab supplies. I also thank my undergraduate students, Lauren Tandarich and Mazz Arif, for helping me analyzing data, and thank all Suter lab members for questions and discussion about my research.

I thank my friends at Purdue for your companion. Life here was not boring with these party times, and numerous nights chatting about life trivial. Your helps and companions in my PhD life lightened up this period that most of people would struggle.

Last, I would like to express my great thanks to my family. Thank my parents for fully supporting me to study abroad. I am sorry that I can't accompany you these years. Thank my wife, Shao-Chin Hung, for accompanying me for 11 years. I didn't even think about going abroad without you. Although maintaining a long-distance relationship for more than 6 years is not easy, I will keep my promise with you in the rest of my life.

Thank you for all of people I mentioned. I couldn't complete my PhD without any of you in my life.

TABLE OF CONTENTS

	Page
LIST OF TABLES	viii
LIST OF FIGURES	ix
LIST OF ABBREVIATIONS.....	xi
ABSTRACT.....	xv
CHAPTER 1. INTRODUCTION	1
1.1 Mitochondrial transport in neurons	1
1.1.1 Importance of mitochondrial transport in neurons	1
1.1.2 Behaviors of mitochondrial transport	2
1.1.3 Key proteins for mitochondrial transport	2
<i>1.1.3.1 Microtubule-based motor proteins – kinesin and dynein</i>	2
<i>1.1.3.2 Actin-based motor protein – myosin</i>	3
<i>1.1.3.3 Microtubule-based docking protein -- syntaphilin</i>	4
<i>1.1.3.4 Motor adaptor proteins – Miro and Milton</i>	5
1.1.4 Regulation of mitochondrial transport.....	6
<i>1.1.4.1 Cytosolic Ca²⁺ in the regulation of mitochondrial transport</i>	6
<i>1.1.4.2 Signaling pathways in the regulation of mitochondrial transport</i>	7
<i>1.1.4.3 PINK1/Parkin in the regulation of mitochondrial transport</i>	8
<i>1.1.4.4 Interrelationship of mitochondrial metabolic state, fission-fusion dynamics, and transport</i>	9
1.1.5 Mitochondrial transport and neurodegenerative diseases.....	10
1.2 Reactive oxygen species (ROS)	15
1.2.1 Reactive oxygen species (ROS) and antioxidants	15
1.2.2 Major sources of ROS	16

	Page
1.2.2.1 Mitochondria	16
1.2.2.2 NADPH oxidase (Nox) family.....	17
1.2.3 ROS and transport-related cell signaling.....	18
1.2.3.1 JNK signaling pathway.....	18
1.2.3.2 PI3K/Akt/GSK3 β signaling pathway	19
1.2.4 ROS and Ca ²⁺ homeostasis.....	20
1.2.4.1 Effects of ROS on plasma membrane Ca ²⁺ channels and pumps	21
1.2.4.2 Effects of ROS on intracellular Ca ²⁺ channels and pumps.....	22
1.2.5 ROS and neurodegenerative diseases	23
1.2.6 ROS and mitochondrial axonal transport	24
CHAPTER 2. MATERIALS AND METHODS.....	28
2.1 Materials and chemicals	28
2.1.1 Materials for <i>in vivo</i> studies.....	28
2.1.2 Materials for <i>in vitro</i> studies.....	28
2.1.3 Chemicals for <i>in vivo</i> studies.....	28
2.1.4 Chemicals for <i>in vitro</i> studies	29
2.2 <i>Drosophila</i> lines and maintenance	29
2.3 Preparation of primary neuronal cell culture and dissected larvae for live imaging.....	31
2.3.1 Preparation of <i>Drosophila</i> larval primary neuronal culture	31
2.3.2 <i>Drosophila</i> larval dissection for live imaging	31
2.3.3 ROS induction <i>in vitro</i> and <i>in vivo</i>	32
2.4 Analysis of mitochondrial and dense core vesicle (DCV) transport.....	33
2.4.1 Acquisition of time lapse confocal images.....	33
2.4.2 <i>In vitro</i> analysis of mitochondrial and DCV transport	33
2.4.3 <i>In vivo</i> analysis of mitochondrial and DCV transport.....	33
2.5 Measurement of mitochondrial membrane potential	36
2.5.1 TMRM treatment in cell culture	36
2.5.2 Imaging and quantification of TMRM intensity.....	36

	Page
2.6 Quantification of mitochondrial density and lengths	36
2.6.1 Quantification of mitochondrial density	36
2.6.2 Quantification of mitochondrial length	37
2.7 Measurement of Ca²⁺ levels and analysis of transport affected by Ca²⁺	37
2.7.1 Ca ²⁺ chelation and release in cell culture.....	37
2.7.2 Imaging and quantification of Ca ²⁺ levels	38
2.7.3 Imaging the effects of Ca ²⁺ on transport	38
2.8 Statistics	38
CHAPTER 3. RESULTS	40
3.1 Mitochondrial transport in axons is reduced in response to oxidative stress ..	40
3.1.1 Mitochondrial transport is reduced <i>in vitro</i> in response to oxidative stress ..	40
3.1.2 Mitochondrial transport is reduced <i>in vivo</i> in response to oxidative stress ...	40
3.2 Overexpression of SOD attenuates defects of mitochondrial transport under oxidative stress conditions	42
3.2.1 Overexpression of SOD rescues ROS-induced defects of mitochondrial transport <i>in vitro</i>	42
3.2.2 Overexpression of SOD rescues ROS-induced defects of mitochondrial transport <i>in vivo</i>	42
3.3 Transport of neuropeptide-bearing large DCVs is barely affected in the presence of ROS	47
3.3.1 DCV transport is barely affected in response to oxidative stress <i>in vitro</i>	47
3.3.2 DCV transport is not affected in response to oxidative stress <i>in vivo</i>	47
3.4 Endogenous Nox and Duox play roles in the regulation of mitochondrial transport	50
3.5 Mitochondrial fission-fusion balance and inner membrane potential are both diminished by ROS treatment	53
3.5.1 Mitochondrial length is reduced under oxidative stress conditions.....	53
3.5.2 Mitochondrial membrane potential is reduced under oxidative stress conditions.....	53

	Page
3.6 ROS-induced defects of mitochondrial transport are caused by Ca²⁺ levels ...	56
3.6.1 ROS elevate intracellular Ca ²⁺ levels.....	56
3.6.2 Elevated Ca ²⁺ levels inhibit mitochondrial transport specifically	56
3.6.3 ROS-induced defects of mitochondrial transport is mediated by Ca ²⁺ levels	57
3.6.4 Ca ²⁺ homeostasis is required for mitochondrial transport	58
3.6.5 Ca ²⁺ homeostasis is required for mitochondrial transport	58
3.7 The JNK pathway plays a role in the regulation of mitochondrial transport in axons by oxidative stress	64
3.7.1 Mitochondrial transport is not affected by JNK signaling <i>in vitro</i>	64
3.7.2 The JNK signaling pathway plays a role in the regulation of mitochondrial transport under oxidative stress <i>in vivo</i>	64
3.7.3 Activation of the JNK pathway shows a decrease of mitochondrial density	66
3.8 Activation or down-regulation of the JNK pathway does not affect intracellular Ca²⁺ levels	71
CHAPTER 4. DISCUSSION	73
4.1 Mitochondrial transport is preferentially affected by ROS	73
4.2 ROS homeostasis is required for mitochondrial transport	75
4.3 The ROS-induced effects on mitochondrial transport is mediated via changes of Ca²⁺ levels	76
4.4 The ROS-induced defects of mitochondrial transport is mediated by the signaling pathway.....	77
4.5 How might Ca²⁺ and the JNK pathway interact in the ROS regulation of mitochondrial transport?	78
4.6 Mitochondrial fission-fusion, metabolic state, and transport are interrelated in response to ROS	79
LIST OF REFERENCES	81
VITA.....	100

LIST OF TABLES

Table	Page
2.1 Genotypes of flies in this study.....	30

LIST OF FIGURES

Figure	Page
1.1 Mitochondrial transport in axons	12
1.2 Models of Ca ²⁺ regulation in mitochondrial transport	13
1.3 Recent model of PINK1/Parkin regulation in mitochondrial transport	14
1.4 ROS and antioxidant systems	26
1.5 ROS regulation of the JNK and the PI3K/Akt/GSK3 β pathway	27
2.1 Steps of <i>in vivo</i> larval dissection.....	32
2.2 GFP expression of mitochondria or DCVs <i>in vivo</i> and <i>in vitro</i>	35
3.1 The percentage of moving mitochondria is reduced in response to ROS and rescued by SOD overexpression <i>in vitro</i>	44
3.2 ROS change mitochondrial motility mainly by reducing flux and velocity <i>in vivo</i> ...	45
3.3 ROS modestly affect mitochondrial duty cycle, run length, and percentage of moving mitochondria <i>in vivo</i>	46
3.4 DCV transport is nearly unaffected by ROS treatment <i>in vitro</i>	48
3.5 DCV transport is unaffected by ROS treatment <i>in vivo</i>	49
3.6 Endogenous ROS affect mitochondrial flux and velocity <i>in vivo</i>	51
3.7 Endogenous ROS affect mitochondrial duty cycle, run length, and the percentage of moving mitochondria <i>in vivo</i>	52
3.8 Mitochondrial length and membrane potential are reduced in response to ROS	55
3.9 Elevated Ca ²⁺ levels are induced by H ₂ O ₂	60
3.10 Elevated Ca ²⁺ levels inhibit mitochondrial transport.....	61
3.11 Ca ²⁺ homeostasis is required for normal mitochondrial transport	62
3.12 Ca ²⁺ homeostasis is required for normal mitochondrial morphology.....	63

Figure	Page
3.13 The percentage of moving mitochondria is not affected by the JNK pathway under oxidative stress conditions <i>in vitro</i>	67
3.14 The JNK pathway plays a role in the regulation of mitochondrial transport <i>in vivo</i>	68
3.15 Mitochondrial duty cycle, run length, and percentage of moving are not affected by the JNK pathway <i>in vivo</i>	69
3.16 Activation of the JNK pathway shows a decrease of mitochondrial density	70
3.17 Activation or down-regulation of the JNK pathway does not affect intracellular Ca ²⁺ levels	72

LIST OF ABBREVIATIONS

- A4: Abdominal segment 4
- ALS: Amyotrophic lateral sclerosis
- ANF: Atrial natriuretic peptide
- APP: Amyloid precursor protein
- ASK1: Apoptosis signal-regulating kinase 1
- ATP: Adenosine triphosphate
- BNIP3: Bcl-2 E1B 19-KDa interacting protein 3
- Bsk: Basket
- Ca²⁺: Calcium ion
- CaM: Calmodulin
- CCCP: carbonyl cyanide *m*-chlorophenylhydrazone
- Cu: Copper
- cyt bL: Low-potential cytochrome b
- dDuox: *Drosophila* Duox
- DA: Dopaminergic
- DCV: Dense core vesicle
- DHC: Dynein heavy chain
- DIC: Dynein intermediate chain
- DLC: Dynein light chain
- DLIC: Dynein light intermediate chain
- DNA: Deoxyribonucleic acid
- dNox: *Drosophila* Nox
- DRG: Dorsal root ganglion
- Drp1: Dynamin related protein 1

Duox: Dual oxidase
DuoxA: Duox activator
EC: Extracellular
EGTA: Ethylene glycol-bis(β -aminoethyl ether)-N,N,N',N'-tetraacetic acid
ER: Endoplasmic reticulum
FBS: Fetal bovine serum
Fc: Cytoplasmic fluorescence
FCCP: Carbonyl cyanide-4-(trifluoromethoxy)phenylhydrazone
Fm: Mitochondrial fluorescence
FOXO: Forkhead box O
G α 12: Alpha subunit of the heterotrimeric G protein G12
GSH: Glutathione
GSH Px: Glutathione peroxidase
GSK3: Glycogen synthase kinase 3
GTP: Guanosine triphosphate
H₂O₂: Hydrogen peroxide
Hep: Hemipterous
HL6: Hemolymph-like
IP3: Inositol 1,4,5-triphosphate
IP₃R: Inositol 1,4,5-trisphosphate receptor
JIP: JNK-interacting protein
JNK: c-Jun N-terminal Kinase
KHC: Kinesin heavy chain
KLC: Kinesin light chain
LC8: Dynein light chain
MAPK: Mitogen-activated protein kinase
MAPKK: MAP kinase kinase
MAPKKK: MAP kinase kinase kinase
MEKK1: MEK kinase 1
Miro: Mitochondrial outer membrane Rho GTPase

mitoGFP: Mitochondrial targeted GFP
MLK: Mixed-lineage kinase
Mn: Manganese
MPP: Mitochondrial-processing protease
MPP⁺: 1-methyl-4-phenylpyridinium ion
mTOR: Mechanistic target of rapamycin
NAC: N-acetylcystein
NADPH: Nicotinamide adenine dinucleotide phosphate
NGF: Nerve growth factor
Nox: NADPH oxidase
NOXA1: Nox activator 1
NOXO1: Nox organizer 1
O₂^{-·}: Superoxide anion
OH·: Hydroxyl radical
Opa1: Optic atrophy protein 1
OXPHO: Oxidative phosphorylation
PARL: Presenilin-associated rhomboid-like protease
PDK: Phosphoinositide-dependent protein kinase
PH: Pleckstrin homology
PI3K: Phosphoinositide 3-kinase
PINK1: PTEN-induced putative kinase 1
PIP2: phosphatidylinositol 4,5-biphosphate
PIP3: phosphatidylinositol 3,4,5-biphosphate
PKB/Akt: Protein kinase B
PMCA: Plasma membrane Ca²⁺-ATPase
PTEN: Phosphatase and tensin homolog
puc: *puckered*
QH·: Ubisemiquinone
ROS: Reactive oxygen species
RTK: Receptor tyrosine kinase

RyR: Ryanodine receptors
SCG10: Superior cervical ganglion 10
SERCA: Sarcoplasmic/endoplasmic reticulum Ca^{2+} ATPase
SNARE: Soluble NSF Attachment Protein Receptor
SNpc: Substantia nigra pars compacta
SNs: Segmental nerves
SOC: Store-operated Ca^{2+} channels
SOCE: Store-operated Ca^{2+} entry
SOD: Superoxide dismutase
SR/ER: Sarcoplasmic/endoplasmic reticulum
STIM: Stromal interaction molecule
TAK: TGF β activated kinase
TGF β : Transforming growth factor- β
TIM: Translocase complex of inner membrane
TMRM: Tetramethylrhodamine methyl ester
TOM: Translocase complex of outer membrane
TRAK: Trafficking kinesin protein
TRP: Transient receptor potential
Trx: Thioredoxin
UCP: Uncoupling protein
VALAP: Vaseline, Lanolin and Paraffin
VDAC: Voltage dependent anion channel
VDCC: Voltage dependent Ca^{2+} channel
VG: Ventral ganglion
Zn: Zinc

ABSTRACT

Liao, Pin-Chao. Ph.D., Purdue University, December 2016. ROS Regulation of Axonal Mitochondrial Transport. Major Professor: Peter J. Hollenbeck.

Mitochondria perform critical functions including aerobic ATP production and calcium (Ca^{2+}) homeostasis, but are also a major source of reactive oxygen species (ROS) production. To maintain cellular function and survival in neurons, mitochondria are transported along axons, and accumulate in regions with high demand for their functions. Oxidative stress and abnormal mitochondrial axonal transport are associated with neurodegenerative disorders. However, we know little about the connection between these two. Using primary *Drosophila* neuronal cell culture and the third instar larval nervous system as *in vitro* and *in vivo* models, respectively, we studied mitochondrial transport under oxidative stress conditions. *In vitro*, hydrogen peroxide (H_2O_2) diminished the percentage of moving mitochondria, the mitochondrial length and inner membrane potential. *In vivo*, ROS inhibited specifically mitochondrial axonal transport, primarily due to reduced flux and velocity, but did not affect transport of other organelles. In addition to excess ROS, down-regulation of Nox or Duox expression, which reduces endogenous ROS levels, mitochondrial transport was impaired. To understand the mechanisms underlying these effects, we examined Ca^{2+} levels and the JNK (c-Jun N-terminal Kinase) pathway, which have been shown to regulate mitochondrial transport and general fast axonal transport, respectively. We found that elevated ROS increased Ca^{2+} levels, and that the Ca^{2+} chelator EGTA rescued ROS-induced defects in mitochondrial transport. In addition, activation of the JNK pathway reduced mitochondrial flux and velocities, while JNK knockdown partially rescued ROS-induced defects in the anterograde direction. We conclude that ROS have the capacity to regulate

mitochondrial traffic, and that Ca^{2+} and JNK signaling play roles in mediating these effects.

CHAPTER 1. INTRODUCTION

1.1 Mitochondrial transport in neurons

1.1.1 Importance of mitochondrial transport in neurons

Neurons have an exceptional cellular morphology because of their asymmetry and long length. This somato-dendritic, axonal, and synaptic terminal regions have compartmentalized differences in molecular machinery and signaling. The cell body is the crucial region for synthesis and degradation of proteins or organelles, but axonal regions also have low levels of protein synthesis. Thus, it is a thought that after protein synthesis in the soma, cargoes are transported from the soma to the synaptic terminals (anterograde transport), and accumulate in regions with high demand for their functions. When materials are aged, they could be transported back to the cell body for recycling or degradation (retrograde transport) (Saxton and Hollenbeck, 2012) (Fig. 1.1A).

Among all neuronal cargoes, mitochondria are one of the important organelles. Mitochondria are the source of aerobic ATP production for the cell and also contribute to calcium (Ca^{2+}) homeostasis. Neurons need large amounts of ATP to maintain their high metabolism. Among the different regions of neurons, synapses have among the highest demand for mitochondrial ATP. When a synaptic vesicle releases neurotransmitter, hundreds of postsynaptic channels open and lots of ions enter the cell. To maintain the ion gradients, ATP is required for pumping them back across the plasma membrane (Schwarz, 2013). In addition to the synapse, action potentials also require energy to maintain ion gradients. Two groups have provided evidence that in myelinated nerves, increased electric activity decreases mitochondrial transport in the node of Ranvier or paranodal region. Without stimuli, most stationary mitochondria localize in the internodal or juxtaparanodal region (Zhang et al., 2010; Ohno et al., 2011). The high demand for ATP

and other mitochondrial functions such as Ca^{2+} buffering in this region of the nerve is presented to underlie this localization, and I conclude that correct distribution and transport of mitochondria is crucial for nerves.

1.1.2 Behaviors of mitochondrial transport

Different axonal organelles or cargoes have their preferred dominant direction of transport. For example, fast-moving axonal vesicles containing neuropeptides preferentially move anterogradely (Barkus et al., 2008). On the other hand, the dominant direction of autophagosomes and organelles carrying endocytic cargoes is retrograde (Hollenbeck, 1993; Maday et al., 2012).

Axonal mitochondria exhibit unique transport behaviors, with about 70% of them being stationary and 30% motile (Morris and Hollenbeck, 1993; Pilling et al., 2006; Devireddy et al., 2015). In the motile population, about 2/3 move anterogradely and 1/3 move retrogradely. In the long distance movement, mitochondria usually move with continuous runs intermixed with short pauses or oscillations. They sometimes change direction for a short period but return to movement in their primary direction; completely reversed directions are rare (Morris and Hollenbeck, 1993; Pilling et al., 2006; Devireddy et al., 2015). These unique transport behaviors are regulated by motor proteins, adaptor proteins, and anchor proteins, which are described in the following sections.

1.1.3 Key proteins for mitochondrial transport

1.1.3.1 Microtubule-based motor proteins – kinesin and dynein

The best-known motor proteins for long distance movement of mitochondria are the microtubule-based motor proteins, kinesin and dynein. Kinesin is responsible for anterograde transport, and dynein is responsible for retrograde transport (Pilling et al., 2006; Saxton and Hollenbeck, 2012) (Fig. 1.1B, E).

The main kinesin family that plays a key role in mitochondrial anterograde transport is the kinesin-1 family (also known as KIF5). In mammals, there are three isoforms of KIF5: KIF5A, KIF5B, and KIF5C. All of them have two kinesin heavy chains (KHCs) that dimerize by coiled-coil interactions and two kinesin light chains (KLCs). Each KHC

has a motor domain in the amino-terminal that binds to microtubules and moves toward the microtubule plus ends; in the carboxy-terminal, it contains a cargo-binding domain that is associated with KLCs to bind cargoes or adaptor proteins (Hirokawa et al., 2010). In mitochondrial axonal transport, mutations of *khc* (*Drosophila* KIF5 homologue) produce impaired mitochondrial transport (Pilling et al., 2006). This indicates that kinesin-1 is the primary mitochondrial motor for the anterograde direction. In addition to kinesin-1, KIF1B, one of the kinesin-3 family proteins, has been suggested to transport mitochondria based on an *in vitro* study (Nangaku et al., 1994). KLP6, a newly identified kinesin, may also regulate mitochondrial transport in neuronal cells (Tanaka et al., 2011).

Cytoplasmic dynein contains two dynein heavy chains (DHCs), several light chains (DLCs), light intermediate chains (DLICs), and intermediate chains (DICs). DHCs serve as motors in dynein. Other structures can interact with dynactin, a large complex regulating the interaction between cargoes, microtubules, and dynein, to transport cargoes (Hirokawa et al., 2010). In *Drosophila*, mutations of the dynein heavy chain (*Dhc*) produce reduced velocity and run length of retrograde mitochondrial transport (Pilling et al., 2006). Down-regulation of the dynactin subunit p150^{Glued} also reduces mitochondrial transport (Pilling et al., 2006). These studies indicate that dynein is the primary motor for mitochondrial retrograde transport.

While kinesin and dynein have their dominant directions of movement, their actions can be interdependent. From genetic analysis in *Drosophila*, mutations of kinesin-1 exhibit genetic interactions with mutations of dynein and dynactin (Martin et al., 1999). Mutations of dynein inhibit retrograde mitochondrial transport, whereas mutations of kinesin-1 inhibit mitochondrial transport in both directions (Pilling et al., 2006), indicating there are some interactions between kinesin and dynein. Although Miro possibly interact with both kinesin and dynein (Russo et al., 2009) (More detailed in Section 1.1.3.4), how these proteins cooperate to control mitochondrial transport remains unclear.

1.1.3.2 Actin-based motor protein – myosin

Since axons contain actin filaments with mixed polarity, and mitochondria have been shown to transport on both microtubules and actin filaments (Morris and Hollenbeck,

1995; Bridgman, 2004; Saxton and Hollenbeck, 2012), raising the issue of a role for myosin in mitochondrial transport. In vertebrate neuronal cultures, disruption of actin filaments increases the velocity of mitochondrial transport (Morris and Hollenbeck, 1995). In *Drosophila* neuronal cell culture, down-regulation of myosin V increases mitochondrial transport in both directions. Moreover, down-regulation of myosin VI also increases mitochondrial transport but only in the retrograde direction (Pathak et al., 2010). These suggest that myosin competes with microtubule-based motors and thereby supports mitochondria halting along the axon (Fig. 1.1D).

1.1.3.3 Microtubule-based docking protein -- syntaphilin

Recently, Sheng's group identified a new protein, syntaphilin, that can anchor mitochondria on microtubules (Kang et al., 2008; Chen et al., 2009; Chen and Sheng, 2013) (Fig.1.1C). Syntaphilin was originally reported to regulate fusion or docking of synaptic vesicles by inhibiting SNARE (Soluble NSF Attachment Protein Receptor) formation (Lao et al., 2000). In its carboxyl-terminal domain, syntaphilin has the structure that target to mitochondrial outer membrane. It also contains the microtubule binding domain (Kang et al., 2008). In the stationary mitochondria population, most of mitochondria are co-localized with syntaphilin, whereas moving mitochondria are not. Syntaphilin-tagged mitochondria are highly correlated to the stationary mitochondria. When the syntaphilin gene (*snph*) is deleted, mitochondrial transport dramatically increases; overexpression of syntaphilin produces an almost immobilized population of mitochondria (Kang et al., 2008). Ca^{2+} can regulate the effects of syntaphilin on mitochondrial docking (Chen and Sheng, 2013). Interestingly, dynein light chain LC8 is shown to associate with syntaphilin, facilitating interactions between syntaphilin and microtubules (Chen et al., 2009). However, syntaphilin only exists in mammals and is not found, for example, in *Drosophila* genome. Yet *Drosophila* also shows a similar stationary population of mitochondria, suggesting that other mitochondrial-docking machineries may play an important role in stopping mitochondrial movement. Thus, the mitochondrial docking proteins and mechanisms require further investigation.

1.1.3.4 Motor adaptor proteins – Miro and Milton

Miro and Milton are two important adaptor proteins connecting mitochondria to the kinesin-1 motor for transport (Fig. 1.1 and 1.2A). Miro, a mitochondrial outer membrane Rho GTPase protein, was found and characterized in both humans and *Drosophila* (Fransson et al., 2003; Guo et al., 2005). Miro has two EF-hand Ca^{2+} -binding motifs and GTPase domains. In a *Drosophila* genetic screen, mutations of *Drosophila* Miro impaired mitochondrial axonal transport to the synapses (Guo et al., 2005). Similarly, human Miro-1 and Miro-2 are both essential for mitochondrial traffic in mammals (Fransson et al., 2003; Fransson et al., 2006). Interestingly, mutations in Miro produce a reduction of mitochondrial transport both anterogradely and retrogradely, suggesting a possible interaction between Miro and both kinesin and dynein (Russo et al., 2009). This has not been explored.

Milton is a linker protein between mitochondria and kinesin, first identified from a *Drosophila* genetic screen (Stowers et al., 2002). In homozygous Milton mutants, mitochondria are rare in the terminals of photoreceptors, but are still present in the soma of these cells (Stowers et al., 2002; Górska-Andrzejak et al., 2003). This study suggests that Milton is involved in the mediation of mitochondrial transport. In addition, Milton has been shown to bind directly to the carboxyl-terminal region of KHCs and interacts with Miro, providing the evidence that Miro, Milton, and KHC form an essential protein complex for mitochondrial anterograde transport (Glater et al., 2006).

In mammals, two Milton orthologues TRAK1 and TRAK2 (also known as OIP106 and Grif1, respectively) have been identified and been shown as adaptor proteins physically binding to kinesin motors (Brickley et al., 2005; Smith et al., 2006). Evidence that mammalian TRAK family are involved in the regulation of mitochondrial transport are also provided. Elevated Miro 1 levels recruit TRAK2 to mitochondria and increase mitochondrial transport to the distal ends of neuronal process in hippocampal neurons (MacAskill et al., 2009). In addition, down-regulation of TRAK1 impair mitochondrial transport in axons (Brickley and Stephenson, 2011).

An overall picture of current model of the mitochondrial transport machinery is shown in figure 1.1B – E: For anterograde transport of mitochondria, mitochondria connect to

kinesin-1 using adaptor proteins Miro, Milton, or others (Fig. 1.1E). For retrograde transport, dynein is the primary motor (Fig. 1.1B). For stationary mitochondria, myosin may compete with kinesin or dynein to halt mitochondria (Fig. 1.1D). Syntaphilin is another docking protein in mammals (Fig. 1.1C). Other unknown regulating proteins or factors are also involved in this transport machinery.

1.1.4 Regulation of mitochondrial transport

1.1.4.1 Cytosolic Ca^{2+} in the regulation of mitochondrial transport

Ca^{2+} is one of the most-studied factors regulating mitochondrial transport. In cardiac myoblasts, elevated Ca^{2+} levels in the physiological range inhibit mitochondrial movement (Yi et al., 2004). In primary neuronal culture, synaptic activity or activation of the glutamate receptors increases Ca^{2+} and reduces mitochondrial transport (Rintoul et al., 2003; Chang et al., 2006a). Furthermore, in myelinated nerves, increased Ca^{2+} levels caused by action potentials also reduce mitochondrial motility (Zhang et al., 2010; Ohno et al., 2011). These raise the question: what are the regulators and mechanisms for mitochondrial transport in response to Ca^{2+} ? To date, there are three groups proposing different models of the mechanisms by which mitochondrial halting occurs. (Macaskill et al., 2009; Wang and Schwarz, 2009; Chen and Sheng, 2013) (Fig. 1.2).

MacAskill et. al suggest that Miro is the Ca^{2+} sensor for mitochondrial transport and physically interacts with kinesin. When Ca^{2+} levels increase, Ca^{2+} binds to the EF motifs on Miro, and that releases the mitochondria-Miro-TRAK complex from kinesin. As a result, mitochondrial transport is inhibited (Macaskill et al., 2009) (Fig. 1.2A, B). Wang and Schwarz propose a similar mechanism. Miro physically binds to kinesin, and elevated Ca^{2+} levels inhibit mitochondrial transport. However, when Ca^{2+} levels increase, kinesin remains attached to the mitochondria-Miro-TRAK complex. Ca^{2+} binds to the EF-domain of Miro and induces the attachment of the kinesin motor domain to Miro instead of microtubules, slacking the interaction between kinesin and microtubules (Wang and Schwarz, 2009) (Fig. 1.2C). A recent study from Chen and Sheng included another proposed model of mitochondrial transport inhibition. They suggest that elevated Ca^{2+} levels immobilize mitochondrial transport via docking protein, syntaphilin. They propose

that syntaphilin competes with TRAK and inhibits kinesin motor ATPase activity, such that kinesin cannot move along microtubules. When Ca^{2+} levels increase, it favors the interaction between syntaphilin and kinesin instead of TRAK and kinesin. Thus, mitochondrial movement stops (Chen and Sheng, 2013) (Fig. 1.2D). Overall, although they propose different models, all groups indicate that Ca^{2+} binding to the EF-domain of Miro inhibits mitochondrial transport.

1.1.4.2 Signaling pathways in the regulation of mitochondrial transport

Although Ca^{2+} is the most-studied regulator for mitochondrial transport, many signaling pathways have been shown to play roles in the regulation of general or mitochondrial transport in neurons. In axons, mitochondria are recruited in response to Nerve Growth Factor (NGF), and this recruitment is inhibited by the phosphoinositide 3-kinase (PI3K) inhibitors, suggesting that the PI3K signaling pathway play a role in the regulation. (Chada and Hollenbeck, 2003, 2004).

In addition, Akt/Gsk3 β signaling has been shown to mediate general or mitochondrial axonal transport. Glycogen synthase kinase 3 (Gsk3) can phosphorylate kinesin light chain, which reduces the binding affinity between kinesin-1 and its cargoes, thereby inhibiting axonal organelle transport (Morfini et al., 2002). Other studies show that Gsk3 β can regulate mitochondrial transport, but the results are controversial. Inhibition of Gsk3 β , whose activity is blocked by Akt-mediated phosphorylation, stimulates axonal mitochondrial transport (Chen et al., 2007). However, other studies show that overexpression of Gsk3 β increases mitochondrial transport in both directions, but more robustly in the anterograde direction (Llorens-Martín et al., 2011; Ogawa et al., 2016). This regulation possibly depends on the microtubule associated proteins, Tau, that can be phosphorylated by GSK3 and regulate the bindings of motors to microtubules (Llorens-Martín et al., 2011), or association with TRAK (Ogawa et al., 2016).

Another possible component is the C-Jun N-terminal Kinase (JNK) signaling pathway. Activation of JNK can phosphorylate kinesin heavy chain and reduce its interaction between kinesin and microtubules, thereby causing inhibition of axonal transport (Morfini et al., 2006; Morfini et al., 2009).

1.1.4.3 *PINK1/Parkin in the regulation of mitochondrial transport*

PINK1 and Parkin are two critical genes for a familial early-onset form of Parkinson's disease (Kitada et al., 1998; Valente et al., 2004). PINK1 is PTEN-induced putative kinase 1 and Parkin is an E3 ubiquitin ligase. Both of them are important for mitochondrial function and in the same signaling pathway where Parkin is downstream of PINK1 (Greene et al., 2003; Clark et al., 2006; Park et al., 2006). In healthy mitochondria, PINK1 is imported through the translocases TIM (Translocase complex of inner membrane) and TOM (Translocase complex of outer membrane) and cleaved by mitochondrial-processing protease (MPP) and presenilin-associated rhomboid-like protease (PARL) (Meissner et al., 2011; Greene et al., 2012). However, when mitochondria are depolarized, PINK1 is stabilized on mitochondrial outer membrane, where it recruits Parkin and induces mitophagy (Narendra et al., 2008; Matsuda et al., 2010; Narendra et al., 2010; Lazarou et al., 2012).

The first evidence relating PINK1/Parkin to mitochondrial transport is that PINK1 forms a complex with Miro and Milton (Weihs et al., 2009). Later, Wang et al. provided the evidence that PINK1 and Parkin are involved in the regulation of mitochondrial transport by inhibiting mitochondrial movement (Wang et al., 2011) (Fig. 1.3). They showed that overexpression of PINK1 or Parkin inhibits mitochondrial movement in mammalian hippocampal and *Drosophila* CCAP neurons. In addition, knockdown of PINK1 or Parkin increases mitochondrial movement in *Drosophila*, suggesting that PINK1 and Parkin play a role in the regulation of mitochondrial transport. To induce the PINK1/Parkin pathway, cells are treated with carbonyl cyanide *m*-chlorophenylhydrazone (CCCP). Under these conditions, PINK1 and Parkin are associated with Miro. In addition, PINK1 phosphorylates Miro, which induces degradation of Miro and results in the release of kinesin and Milton from mitochondria (Wang et al., 2011). Another group provide the evidence that Miro is the substrate of Parkin (Liu et al., 2012). Based on these results, Wang et al. proposes this model. When mitochondria are depolarized, they recruit PINK1, which phosphorylates Miro (Fig. 1.3B). This PINK1-phosphorylated Miro may recruit Parkin, which induces Miro

ubiquitination (Fig. 1.3C). Ubiquitinated Miro is then degraded, so mitochondria release from microtubules and stop (Fig. 1.3D).

Although they proposed this model, a recent study shows the opposite results. Devireddy et al. examined mitochondrial transport, morphology, and membrane potential in PINK1 mutation in the *Drosophila* motor neurons. They shows that PINK1 null-mutation inhibits mitochondrial transport by reducing flux in both directions and anterograde duty cycle, whereas overexpression of PINK1 increases retrograde moving mitochondria (Devireddy et al., 2015). Thus, it still remains unclear how PINK1/Parkin regulate mitochondrial transport.

1.1.4.4 Interrelationship of mitochondrial metabolic state, fission-fusion dynamics, and transport

Since motor proteins require ATP for their activity, mitochondrial metabolic state might be associated with mitochondrial transport. In mammalian primary neurons, cells treated by ATPase blocker oligomycin or by an uncoupler (FCCP or CCCP), which inhibits mitochondrial electron transport, show a decrease in mitochondrial transport (Rintoul et al., 2003; Miller and Sheetz, 2004). However, treatment with antimycin, an inhibitor of mitochondrial complex III, increases mitochondrial transport (Miller and Sheetz, 2004). These results suggest that there might be some connections between mitochondrial metabolic state and transport. However, it remains controversial whether mitochondrial membrane potential is different between axonal mitochondria moving in different directions (Miller and Sheetz, 2004; Verburg and Hollenbeck, 2008). Miller and Sheetz suggest that mitochondria with high membrane potential preferentially move anterogradely, and mitochondria with low membrane potential move retrogradely (Miller and Sheetz, 2004). Whereas Verburg and Hollenbeck provide the evidence that anterograde, retrograde, and stationary mitochondria shows no different in mitochondrial membrane potential (Verburg and Hollenbeck, 2008).

In addition to metabolic state, numerous studies provide evidence that mitochondrial fission-fusion dynamics are highly interrelated with mitochondrial transport (Rintoul et al., 2003; Verstreken et al., 2005; Fransson et al., 2006; Baloh et al., 2007; Saotome et al., 2008; Misko et al., 2010; Pathak et al., 2010; Yu et al., 2016). Primary forebrain neurons

treated with glutamate show both reduced mitochondrial movement and mitochondrial length (Rintoul et al., 2003). Overexpression of motor adaptor protein Miro induces mitochondrial fusion (Fransson et al., 2006; Saotome et al., 2008). Knockdown of Myosin V, the motor protein for halting mitochondrial transport, increases mitochondrial length (Pathak et al., 2010)

This connection between fission-fusion and transport might involve mitochondrial fission or fusion proteins, including Drp1 (Dynamin related protein 1), mitofusin 2, or Opa1 (Optic atrophy protein 1) (Verstreken et al., 2005; Baloh et al., 2007; Misko et al., 2010; Yu et al., 2016). In a forward screen in *Drosophila*, mutations of Drp1, one of the mitochondrial fission protein, were found to reduce the number of mitochondria in synaptic terminals (Verstreken et al., 2005). Mitofusin 2, a mitochondrial outer membrane fusion protein, also interacts with Miro/Milton complex and is required for mitochondrial transport (Baloh et al., 2007; Misko et al., 2010). Knockdown of *Drosophila* Opa1, a mitochondrial inner membrane fusion protein, recently has been shown to reduce mitochondrial transport in the third instar larval neurons (Yu et al., 2016), whereas Opa1 has no effect in dorsal root ganglion (DRG) cultures (Misko et al., 2010).

Overall, although the detailed mechanisms remain unclear, these studies indicate that mitochondrial metabolic state, fission-fusion dynamics, and transport are highly interrelated.

1.1.5 Mitochondrial transport and neurodegenerative diseases

Since mitochondrial transport is important for neuronal survival, it is not surprising that defects in mitochondrial transport are associated with a variety of neurodegenerative diseases.

Alzheimer's disease is involved in progressive dementia. Two pathological hallmarks in Alzheimer's disease are neuritic plaques containing Amyloid- β aggregates and neurofibrillary tangles containing hyperphosphorylated Tau proteins. It has been shown that a short period of exposure of cultured hippocampal neurons to Amyloid- β impairs mitochondrial transport (Rui et al., 2006). Moreover, this Amyloid- β induced defects of

mitochondrial transport can be rescued by the reduction of another key pathogenic factor, Tau (Vossel et al., 2010). In addition to Alzheimer's disease, recent studies also provided evidence that factors inducing Parkinson's disease are associated with impaired mitochondrial transport (Kim-Han et al., 2011; Devireddy et al., 2015). Environmental toxin inducing Parkinson's disease, 1-methyl-4-phenylpyridinium ion (MPP⁺), specifically induces defects of mitochondrial transport in dopamine axons (Kim-Han et al., 2011). Mutant PINK1, one of the pathogenic factor inducing familial early-onset Parkinson's disease, also impairs mitochondrial transport by reducing flux and duty cycle (Devireddy et al., 2015).

Other neurodegenerative diseases are also associated with impaired mitochondrial transport. For example, mutations of superoxide dismutase 1 (SOD1) that induce amyotrophic lateral sclerosis (ALS) also produce a decrease in mitochondrial transport (De Vos et al., 2007; Magrané et al., 2009; Magrané et al., 2012; Song et al., 2012). Mutations of huntingtin, which is associated to Huntington's disease, can induce defects in mitochondrial transport, and evidence suggests that this is possibly caused by the interaction between the amino-terminal of mutant huntingtin and mitochondria (Chang et al., 2006b; Orr et al., 2008). In addition, pathogenic huntingtin inhibits axonal transport by the activation of JNK3 and resulting phosphorylation of kinesin (Morfini et al., 2009). Thus, these studies provide strong evidence that impaired mitochondrial transport is one of the important factors inducing neurodegenerative diseases.

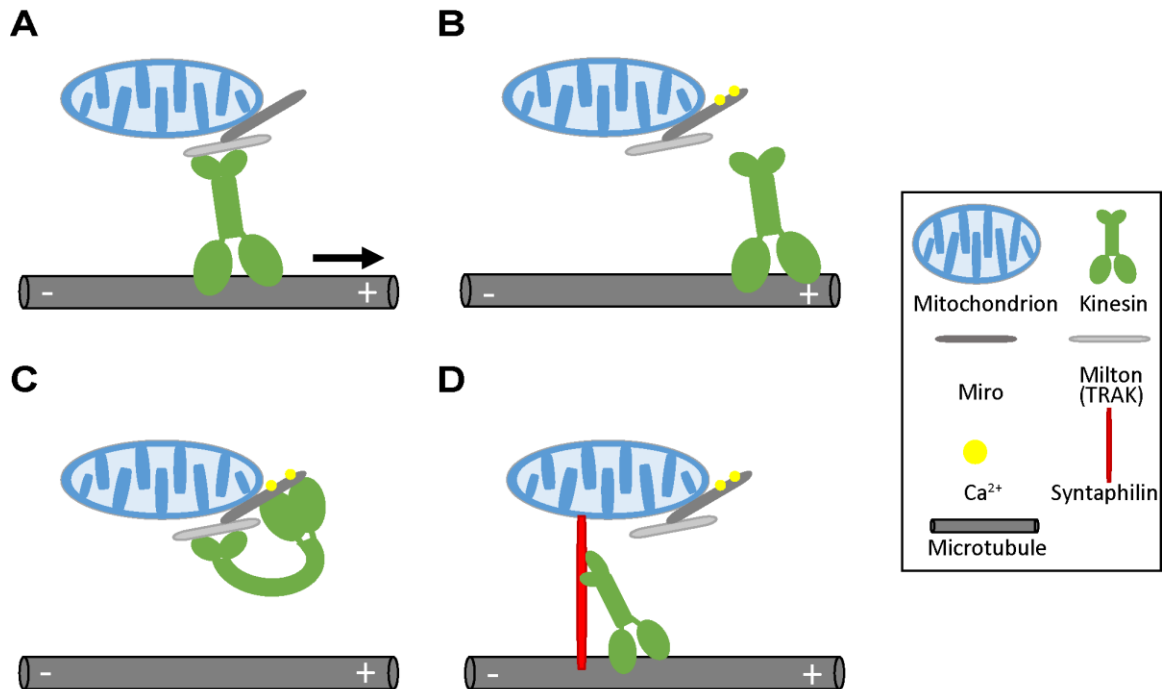


Figure 1.2. Models of Ca^{2+} regulation in mitochondrial transport. **A**, Miro is the mitochondrial outer membrane protein and has two Ca^{2+} binding EF-hand motifs. In the anterograde moving mitochondria, Miro and the adaptor protein Milton form the complex. This Miro-Milton complex interacts with kinesin and drives mitochondrial transport anterogradely. **B**, In the first model, Ca^{2+} binds to Miro and that releases kinesin from mitochondria when Ca^{2+} levels increase. Thus, mitochondrial transport is reduced (Macaskill et al., 2009). **C**, In the second model, Ca^{2+} binding releases the kinesin motor domain from microtubules and induces bindings between the motor domain and Miro (Wang and Schwarz, 2009). **D**, Syntaphilin is involved in the Ca^{2+} regulation of mitochondrial transport. Elevated Ca^{2+} levels switch kinesin binding from Miro-Milton complex to the docking protein, syntaphilin. Syntaphilin can inhibit the activity of kinesin motor ATPase, thereby stopping mitochondrial transport (Chen and Sheng, 2013).

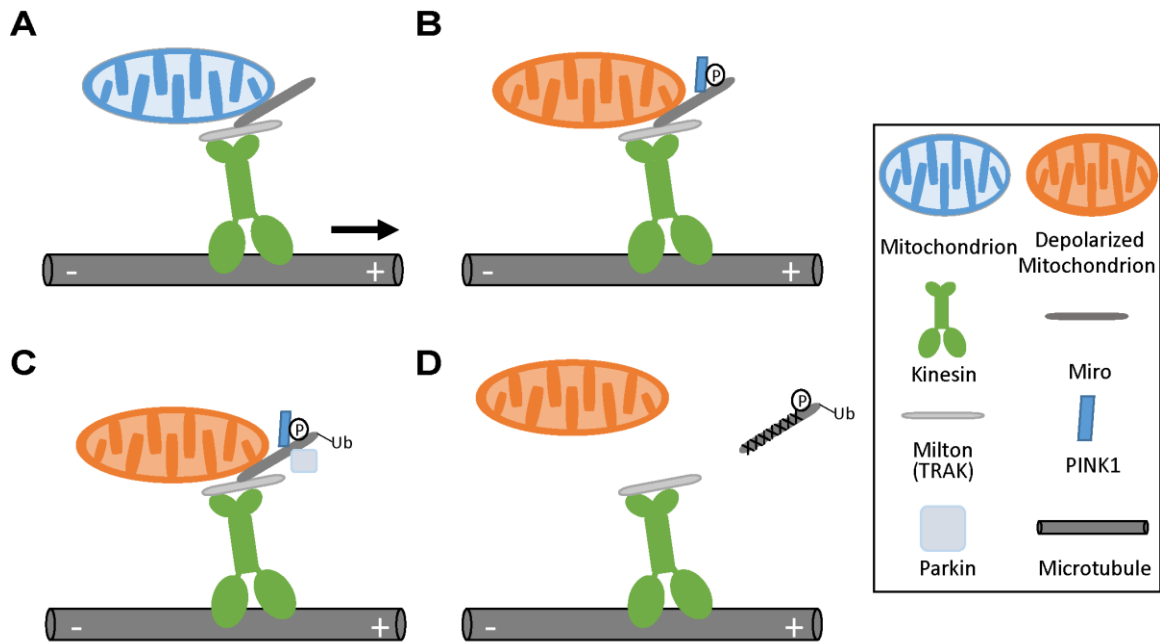


Figure 1.3. Recent model of PINK1/Parkin regulation in mitochondrial transport. **A**, Healthy mitochondria move anterogradely via Miro-Milton-kinesin machinery. **B**, Unhealthy or depolarized mitochondria recruit PINK1, which phosphorylates Miro. **C**, PINK1-phosphorylated Miro may recruit Parkin, which induces Miro ubiquitination. **D**, Miro is degraded, so mitochondria release from microtubules and stop.

1.2 Reactive oxygen species (ROS)

1.2.1 Reactive oxygen species (ROS) and antioxidants

Reactive oxygen species (ROS) are the partially reduced forms of oxygen, which are highly reactive due to their unstable free radicals. There are several varieties of ROS. When oxygen is one-electron reduced, it converts to the superoxide anion ($O_2^{\cdot-}$). Two-electron reduction leads to hydrogen peroxide (H_2O_2) formation. A further one-electron reduction of hydrogen peroxide forms the highly reactive hydroxyl radical ($OH\cdot$) (Brookes et al., 2004; Son et al., 2013; Lambeth and Neish, 2014) (Fig. 1.4). These ROS are harmful for cells because they damage macromolecules or subcellular structures such as proteins, lipids, and DNA (Brookes et al., 2004; D'Autréaux and Toledano, 2007; Son et al., 2013). Although these ROS are highly reactive and potentially destructive, cells use their antioxidant systems to control their levels and maintain the ROS balance.

These antioxidant systems include several antioxidant enzymes as well as non-enzymatic antioxidants (Fig. 1.4). Among antioxidant enzymes, superoxide dismutase (SOD) converts superoxide to hydrogen peroxide. There are three different isoforms of SOD: SOD1, copper-zinc superoxide dismutase (Cu/Zn SOD), is expressed mostly in the cytosol. SOD2, manganese superoxide dismutase (Mn SOD), is expressed primarily in mitochondria. SOD3, extracellular superoxide dismutase (EC SOD), is secreted into the extracellular space (Mruk et al., 2002). Catalase or glutathione peroxidase (GSH Px) reduces hydrogen peroxide to water (H_2O). Catalase mostly resides in peroxisomes, but also exists in the cytoplasm and in mitochondria. Glutathione peroxidase reduces hydrogen peroxide to water using reduced glutathione (GSH) as an electron donor, and these glutathione then forms disulfide bonds (Gandhi and Abramov, 2012). In addition to antioxidant enzymes, there are several non-enzymatic antioxidants, including glutathione, vitamin C and E, thioredoxin (Trx), and others (Gandhi and Abramov, 2012; Son et al., 2013). These non-enzymatic antioxidants also play important roles in the regulation of redox balance.

If the balance of ROS and antioxidants is disrupted, excess ROS production can induce oxidative stress in cells. Oxidative stress has been shown to associate highly with

different neurodegenerative diseases and to activate a variety of signaling pathways (Shen and Liu, 2006; Court and Coleman, 2012; Federico et al., 2012; Fischer et al., 2012; Son et al., 2013; Bhat et al., 2015), as described below.

1.2.2 Major sources of ROS

1.2.2.1 Mitochondria

Mitochondria are one of the major sources of ROS in the cell. In the mitochondrial inner membrane, the electron transport chain is one of the important functional parts of ATP generation, but also is the location of ROS production. ROS are generated in different sites in the electron transport chain, primarily at complex I (NADH-ubiquinone oxidoreductase) and III (ubiquinone-cytochrome c reductase) (Brookes et al., 2004; Bhat et al., 2015; Genova and Lenaz, 2015).

Complex I generates ROS via its iron-sulfur clusters (Genova et al., 2001). These ROS are produced during forward electron transfer in the electron transport chain and stay in the matrix. (Genova et al., 2001; Genova and Lenaz, 2015). ROS formation from complex III depends on the Q-cycle in electron transfer. In the Q-cycle, the ubisemiquinone (QH \cdot) intermediate which normally reduces low-potential cytochrome b (cyt b_L), instead interacts with oxygen and generates superoxide (Brookes et al., 2004; Genova and Lenaz, 2015). ROS generated by complex III are released into the intermembrane space and can be exported to the cytoplasm via the voltage dependent anion channels (VDACs) (Han et al., 2003). In addition to complex I and III, complex II (succinate dehydrogenase) has been suggested to be involved in the generation of ROS by electron transfer back to complex I (Brookes et al., 2004; Genova and Lenaz, 2015). Other enzymes of oxidative phosphorylation (OXPHO) are also involved in the ROS generation, in less defined ways.

Although mitochondria generate significant ROS, they also have some self-defense systems to prevent damage from oxidative stress. For example, in the matrix, mitochondria have Mn-SOD (SOD2) that converts superoxide to H₂O₂ (Son et al., 2013). Mitochondria can use also VDACs or uncoupling proteins UCP2 and 3 to export

superoxide from the matrix to the cytoplasm (Han et al., 2003; Wojtczak et al., 2011), thereby preventing the toxic superoxide accumulation within mitochondria.

1.2.2.2 NADPH oxidase (Nox) family

The NADPH oxidase (Nox) family comprises a group of enzymes that depend on NADPH to reduce oxygen and generate superoxide or hydrogen peroxide. To date, there are seven enzymes known in mammals, including five Nox isoforms (Nox1, Nox2, Nox3, Nox4, and Nox5) and two related enzymes, Duox (Dual oxidase) 1 and Duox 2 (Aguirre and Lambeth, 2010; Katsuyama et al., 2012; Lambeth and Neish, 2014).

Nox2, before called gp91^{phox}, was the first identified Nox enzyme (Royer-Pokora et al., 1986). Activation of Nox2 oxidase requires the assembly of Nox2 and other regulatory factors including p22^{phox}, p47^{phox}, p40^{phox}, p67^{phox}, and a small GTP-binding protein, Rac. Nox1, 3, and 4 also need p22^{phox}. Nox 1 and 3 need additional regulatory subunits NOXO1 (Nox organizer 1) and NOXA1 (Nox activator 1), but Nox4 is constitutively active. Nox5, Duox1, and Duox2 are p22^{phox} independent. These three proteins have EF hand Ca²⁺ binding domains and are activated by Ca²⁺. In addition to EF hand Ca²⁺ binding domains, Duox 1 and 2 contain peroxidase-homology domains and also form complexes with Duox accessory proteins, DuoxA1 and A2, respectively, to localize on the membrane (Aguirre and Lambeth, 2010; Katsuyama et al., 2012; Lambeth and Neish, 2014). The primary species of ROS generated by Nox1, 2, 3, and 5 are superoxide, whereas Nox4, Duox1 and 2 usually produce hydrogen peroxide.

These Nox proteins are involved in the regulation of varied biological processes in mammals. For example, they play physiological roles in growth, development, cell motility, muscle contraction, cytoskeleton reorganization, cell survival/apoptosis, stress adaptation, and inflammation (Lambeth and Neish, 2014). In the nervous system, Nox enzymes are expressed in neurons, microglia, astrocytes, and neuromuscular junctions. There, they play roles in neural development, neural stem cell biology, and overall neural function (Nayernia et al., 2014).

In *Drosophila*, there are just two Nox enzymes. dNox (*Drosophila* Nox) is the homologue of mammalian Nox5, containing EF-hand Ca²⁺ binding domains. dDuox (*Drosophila* Duox) is the homologue of mammalian Duox, containing EF-hand Ca²⁺

binding domains and peroxidase-homology domains (Ha et al., 2005). These Nox enzymes are expressed primarily in gut but also in the central nerve system, at lower levels (Flybase). dNox has been shown to regulate smooth muscle contraction (Ritsick et al., 2007). In addition, symbiotic lactobacilli can stimulate gut epithelial proliferation via dNox (Jones et al., 2013). dDuoX are involved in gut immunity, which is induced by bacterial-derived uracil (Ha et al., 2005; Lee et al., 2013). dDuoX also regulate the wound immunity response and stabilize the cuticle structure of the adult wing (Anh et al., 2011; Razzell et al., 2013).

Thus, ROS are not only toxic for cells, but also play important roles in many biological processes under physiological conditions.

1.2.3 ROS and transport-related cell signaling

Since ROS have highly reactivity and oxidize other molecules such as proteins, it is unsurprising that they have roles in the modulation of signaling pathways. One of the main amino acid residues that can be oxidized is the cysteine residue. When ROS oxidize cysteine residues and lead the formation of disulfide bond ($-SH \rightarrow -S-S-$), it changes protein activity and/or conformation (Son et al., 2013; Genova and Lenaz, 2015). Among these ROS-induced signaling pathways, I will focus on two pathways related to axonal transport (Section 1.1.4.2, above).

1.2.3.1 JNK signaling pathway

c-Jun N-terminal kinase (JNK), also called stress-activated protein kinase, is one of the subgroups of the mitogen-activated protein kinase (MAPK) family. In mammals, there are three isoforms: JNK-1, JNK-2, and JNK-3. JNK-1 and JNK-2 are expressed ubiquitously, but JNK-3 is expressed mainly in neuronal tissue (Shen and Liu, 2006; Son et al., 2013).

Like other MAPK family members, JNK is regulated by MAP kinase kinase kinase (MAPKKK) and MAP kinase kinase (MAPKK). Two MAPKK family members, MKK4 and MKK7 (known as JNKK1/MEK4 and JNKK2/MEK7, respectively) phosphorylate and activate JNK. MKKs are phosphorylated by numerous MAPKKK, including MEK kinase 1 (MEKK1), apoptosis signal-regulating kinase 1(ASK1), mixed-lineage kinase

(MLK), and transforming growth factor- β (TGF β) activated kinase (TAK). (Shen and Liu, 2006; Son et al., 2013). Downstream targets of JNK include members of the transcription factor AP-1 family (for example, c-Jun), p53, and c-Myc (Shen and Liu, 2006).

In *Drosophila*, there are one JNK (Basket, Bsk) and two JNKKs (Hemipterous, Hep, a MKK7 homologue, and dMKK4). These *Drosophila* JNKKs are also activated by different MAPKKs similar to mammals. One of the important downstream genes in the AP-1 family is *puckered* (*puc*), which encodes a JNK-specific phosphatase that inhibits JNK activity (Biteau et al., 2011).

What are the mechanisms involved in the activation of the JNK pathway by ROS? ASK1 plays the major role in this regulation. ASK1 has been shown to be a specific target of ROS since its activation is mediated by two redox-sensitive proteins, thioredoxin and glutaredoxin (Gotoh and Cooper, 1998; Saitoh et al., 1998; Tobiume et al., 2001; Song et al., 2002; Song and Lee, 2003). The reduced form of thioredoxin or glutaredoxin binds to ASK1 and inhibits ASK1 activity. In the presence of ROS, thioredoxin and glutaredoxin are oxidized and released from ASK1, thereby enhancing ASK1 activity (Gotoh and Cooper, 1998; Saitoh et al., 1998; Tobiume et al., 2001; Song et al., 2002; Song and Lee, 2003). Activated ASK1 then initiates the activation of the ASK1-JNKK-JNK signaling pathway and the expression of the downstream genes (Shen and Liu, 2006; Biteau et al., 2011; Son et al., 2013) (Fig. 1.5A).

1.2.3.2 PI3K/Akt/GSK3 β signaling pathway

The PI3K/Akt signaling pathway is involved in many cellular functions including protein synthesis, cell cycle, proliferation, and apoptosis in response to growth factors (Clerkin et al., 2008; Zhang et al., 2016). When growth factors bind and activate receptor tyrosine kinase (RTK), it recruits phosphoinositide-3-kinase (PI3K). After PI3K is recruited, PI3K phosphorylates phosphatidylinositol 4,5-biphosphate (PIP₂) to form phosphatidylinositol 3,4,5-biphosphate (PIP₃). PIP₃ recruits proteins containing pleckstrin homology (PH) domains, such as phosphoinositide-dependent protein kinase (PDK) and protein kinase B (PKB/Akt). These proteins, PDK and Akt, are phosphorylated and activated, and then phosphorylate numerous downstream targets (for

example, GSK3, FOXO, p53, Bad, and mTOR) (Clerkin et al., 2008; Sullivan and Chandel, 2014; Zhang et al., 2016) (Fig. 1.5B).

One of the downstream targets is glycogen synthase kinase 3 β (GSK3 β), a member of a family of conserved serine/threonine kinases (Hardt and Sadoshima, 2002). GSK3 β was originally named because of its function of phosphorylation of glycogen synthase and inhibition of glycogen synthesis, but now it has been shown involved in varied cellular functions (Cohen and Frame, 2001; Hardt and Sadoshima, 2002). GSK3 β is the negative regulator of its downstream targets. Without phosphorylation, GSK3 β is active, but downstream targets are less active. Once GSK3 β is phosphorylated, it becomes inactivated, and thus its downstream targets are active. Thus, activation of PI3K/Akt stimulates downstream targets via inhibition of GSK3 β activity (Cohen and Frame, 2001; Hardt and Sadoshima, 2002) (Fig. 1.5B).

How is the PI3K/Akt/GSK3 β pathway activated by ROS? Since PI3K/Akt/GSK3 β is activated by phosphorylation, this pathway is negatively regulated by phosphatases (Clerkin et al., 2008; Zhang et al., 2016). One of the well-studied phosphatases, Phosphatase and Tensin homologue (PTEN), can dephosphorylate PIP3 to PIP2 and inhibit the PI3K/Akt/GSK3 β pathway. PTEN has cysteine residues in the active site. In the presence of ROS, these cysteine residues are oxidized to form disulfide bonds, thereby inactivating PTEN. Inactivated PTEN loses the ability to dephosphorylate PIP3 to PIP2, and thereby activates the PI3K/Akt/GSK3 β pathway (Clerkin et al., 2008; Zhang et al., 2016) (Fig. 1.5B).

1.2.4 ROS and Ca²⁺ homeostasis

Ca²⁺ is an important second messenger regulating numerous cellular functions such as muscle contraction, gene expression, cell survival and cell death (Berridge, 2012). Ca²⁺ can either flow into the cytoplasm through Ca²⁺ channels or be pumped out of the cytoplasm by Ca²⁺ pumps in the plasma membrane or endoplasmic reticulum (ER). Most of these Ca²⁺ channels and pumps have cysteine residues that are sensitive to redox status (Hidalgo and Donoso, 2008; Görlach et al., 2015). Thus, it is no surprise that ROS can

mediate Ca^{2+} homeostasis. Here I focus on how ROS mediate Ca^{2+} homeostasis via these channels and pumps.

1.2.4.1 Effects of ROS on plasma membrane Ca^{2+} channels and pumps

Ca^{2+} enters cells through numerous Ca^{2+} channels, including voltage-dependent Ca^{2+} channels (VDCC), and receptor-coupled channels, among these are transient receptor potential (TRP) channels and the store-operated Ca^{2+} channels (SOC) mediated by Orai channel proteins (Görlach et al., 2015).

VDCCs can be oxidized by ROS because of the cysteine residues in their pore forming $\alpha 1$ subunits (Hudasek et al., 2004). Depending on the channel type, ROS can either induce or suppress Ca^{2+} influx via VDCCs (Görlach et al., 2015). For example, ROS suppress Ca^{2+} influx in guinea pig ventricular myocytes (Gill et al., 1995), whereas they stimulate Ca^{2+} influx through L-type and T-type VDCCs in smooth muscle cells (Tabet et al., 2004).

TRP channels are a group of Ca^{2+} -permeable cation channels divided into six subfamilies. They are highly expressed in sensory receptor cells, and important for senses such as touch, taste, and smell (Voets et al., 2005). In this TRP family, some members have been shown to be sensitive to redox status (Takahashi and Mori, 2011; Görlach et al., 2015). TRPM2 was the first channel identified for its ROS-sensitivity. H_2O_2 has been shown to activate TRPM2 via the induction of nicotinamide adenine dinucleotide (β -NAD⁺), which directly interacts with TRPM2 (Hara et al., 2002). In addition to TRPM2, some members, including TRPC5, TRV1, TRPA1, are directly mediated by ROS, NO, or oxidants via their cysteine residues (Yoshida et al., 2006; Xu et al., 2008; Görlach et al., 2015).

Store-operated Ca^{2+} entry (SOCE) is the mechanism by which Ca^{2+} depletion of the ER lumen induces Ca^{2+} influx by activating Ca^{2+} -permeable channels on the plasma membrane (Shen et al., 2011). When Ca^{2+} is depleted in the ER, an ER Ca^{2+} sensor, STIMs (stromal interaction molecules) move near the plasma membrane and activate Orai Ca^{2+} channels on the membrane, thereby inducing Ca^{2+} influx (Shen et al., 2011). ROS have been suggested to deplete Ca^{2+} of ER and activate SOCE (Grupe et al., 2010).

However, other groups have suggested that ROS inhibit Orai via their cysteine residues and reduce Ca^{2+} influx (Bogeski et al., 2010; Bogeski et al., 2012).

The plasma membrane Ca^{2+} pump, or plasma membrane Ca^{2+} -ATPase (PMCA), is important for maintaining resting cytoplasmic free Ca^{2+} concentration, and requires ATP hydrolysis to actively transport Ca^{2+} . PMCA is activated by the dissociation of its autoinhibitory domain through the binding of calmodulin (CaM) and PMCA (Hidalgo and Donoso, 2008). While it remains unclear which residues are sensitive to redox, both PMCA and CaM have been shown to be sensitive to ROS, which inhibits PMCA activity (Hidalgo and Donoso, 2008; Zaidi, 2010; Görlach et al., 2015).

1.2.4.2 Effects of ROS on intracellular Ca^{2+} channels and pumps

Intracellular Ca^{2+} is released from sarcoplasmic/endoplasmic reticulum (SR/ER) through two main Ca^{2+} channels: ryanodine receptors (RyR) in excitable cells; and inositol 1,4,5-trisphosphate receptors (IP₃R) in non-excitable cells (Görlach et al., 2015).

RyR channels play important roles in cellular functions, including muscle contraction, synaptic activity, secretion, and cell death (Hidalgo and Donoso, 2008). They form homotetramers in the SR and ER membrane and contain numerous cysteine residues, rendering them sensitive to redox status (Hidalgo and Donoso, 2008; Görlach et al., 2015). Oxidation of RyR has been shown to enhance RyR activity and thereby increase cytoplasmic Ca^{2+} levels (Hidalgo and Donoso, 2008; Görlach et al., 2015). For example, oxidation of RyR thiols increases SR Ca^{2+} leakage (Terentyev et al., 2008) and spark frequency (Yan et al., 2008).

IP₃Rs are important for the regulation of development and fertilization mainly in the non-excitable cells, but also contribute to in cardiac and neuronal cells (Hidalgo and Donoso, 2008; Görlach et al., 2015). They are localized in the ER, and are activated by the binding of the ligand, inositol 1,4,5-trisphosphate (IP₃). When the IP₃ binds to the IP₃R, these channels open and release Ca^{2+} from the ER to the cytoplasm (Hidalgo and Donoso, 2008; Görlach et al., 2015). Several oxidants have been shown to activate IP₃Rs by increasing the sensitivity of receptors to the ligands. For example, thimerosal oxidizes cysteine residues and stabilizes the active form of the IP₃Rs (Bootman et al., 1992; Khan, 2013). Diamide also induces S-glutathionylation of the receptors and increases

intracellular Ca^{2+} levels (Lock et al., 2011). Thus, IP_3Rs can be activated even IP_3 levels are low.

The primary intracellular Ca^{2+} pumps are the sarcoplasmic/endoplasmic reticulum Ca^{2+} ATPase (SERCA). SERCA contains many cysteine residues (from 22 to 28 cysteines, depending on different isoforms), so it is sensitive to redox (Hidalgo and Donoso, 2008; Görlach et al., 2015). Several studies indicate that ROS inhibit SERCA activity via cysteine or tyrosine residues (Xu et al., 1997; Barnes et al., 2000; Brookes et al., 2004). In addition, since SERCA pumps require ATP for their activity, it is notable that ROS-oxidized SERCAs reduce their ability to bind ATP and thus lose activity (Sharov et al., 2006; Cook et al., 2012). Thus, in the presence of ROS, active Ca^{2+} transport by SERCAs is inhibited.

1.2.5 ROS and neurodegenerative diseases

ROS have been shown to be associated with several neurodegenerative diseases. Most studies and reviews in this area focus on Alzheimer's disease and Parkinson's disease (Zhao and Zhao, 2013; Bhat et al., 2015; Blesa et al., 2015; Kim et al., 2015).

As mentioned in section 1.1.5, neuritic plaques containing Amyloid- β aggregates and neurofibrillary tangles containing hyperphosphorylated Tau proteins are two pathological hallmarks of Alzheimer's disease. Amyloid- β has been shown to increase H_2O_2 levels (Behl et al., 1994). In transgenic mouse models with overexpression of mutant amyloid precursor protein (APP), accumulated Amyloid- β evokes oxidative stress (Smith et al., 1998; Matsuoka et al., 2001). On the other hand, oxidative stress apparently increases the production of Amyloid- β oligomerization or plaque. In the transgenic mouse models, deletion of antioxidant enzymes, SOD1 or 2, increases Amyloid- β oligomerization or plaque formation (Li et al., 2004; Murakami et al., 2011), and overexpression of SOD2 reduces oxidative stress and also decreases Amyloid- β plaque (Dumont et al., 2009). In addition to Amyloid- β , tau proteins are associated with oxidative stress. Tau has been shown to both block vesicle traffic and to enhance oxidative stress (Stamer et al., 2002), and oxidative stress enhances tau-induced neurodegeneration in a *Drosophila* model

(Dias-Santagata et al., 2007). Overall, these studies provide evidence that oxidative stress is highly interrelated with Alzheimer's disease.

Parkinson's disease is characterized by the selective loss of dopaminergic (DA) neurons in the substantia nigra pars compacta (SNpc). One class of factors inducing Parkinson's disease is environmental toxins. Some toxins, such as MPTP (or its derivative MPP⁺) and rotenone that are the inhibitors of mitochondrial complex I, are preferentially toxic to the DA neurons (Blesa and Przedborski, 2014). They inhibit the normal activity of complex I, disrupt the electron transport chain, and produce ROS mainly in the DA neurons, thereby inducing Parkinson's disease (Mizuno et al., 1987; Betarbet et al., 2000). Paraquat is also preferentially toxic to DA neurons by activating NOX in microglia cells. In both *in vitro* and *in vivo* systems, paraquat neurotoxic actions to DA neurons in microglia cells is inhibited if NOX is deficient (Wu et al., 2005; Purisai et al., 2007). The pathological hallmark of both familial and sporadic Parkinson's disease is the accumulation of the protein α -synuclein. It has been shown that this accumulation increases oxidative stress in DA neurons (Martin et al., 2006). Furthermore, oxidative stress also induces accumulation and oligomerization of α -synuclein in oligodendrocytes or brain slice cultures (Xu et al., 2013; Pukass and Richter-Landsberg, 2014), suggesting that oxidative stress and Parkinson's disease are highly associated in a feed-forward manner. Mutations linked to the familial Parkinson's disease are also linked to ROS. For example, PINK1 mutations have been shown to induce abnormal mitochondrial morphology and enhance vulnerability to ROS (Clark et al., 2006; Gautier et al., 2008), and that is rescued by downstream Parkin expression (Yang et al., 2006; Exner et al., 2007).

Overall these numerous studies show that one of the factors inducing neurodegenerative disease is ROS, while the detailed mechanism remains unclear. Thus, it is important to find the fundamental connections between these two.

1.2.6 ROS and mitochondrial axonal transport

As mentioned above (Sections 1.1.5 and 1.2.5), ROS and impaired axonal transport of mitochondria are both implicated in neurodegenerative diseases. However, it is still not

clear whether or how ROS directly affect mitochondrial transport. Recent studies have shown that the H₂O₂ donor, tert-butyl hydroperoxide, or H₂O₂ treatment itself in cell culture systems leads to the reduction of organelle transport (Isonaka et al., 2011; Fang et al., 2012). In addition, an SOD1 mutant has been shown to reduce mitochondrial transport *in vitro* (Song et al., 2012). Whether these effects occur in the more complex, homeostatic, and normoxic *in vivo* environment remains unknown. Moreover, the mechanisms involved in the regulation of mitochondrial transport in the presence of ROS are still unclear.

Thus, in this study I used primary *Drosophila* neuronal cell culture and the third instar larval nervous system as *in vitro* and *in vivo* models, respectively, to elucidate the mechanistic connections between ROS and mitochondrial transport.

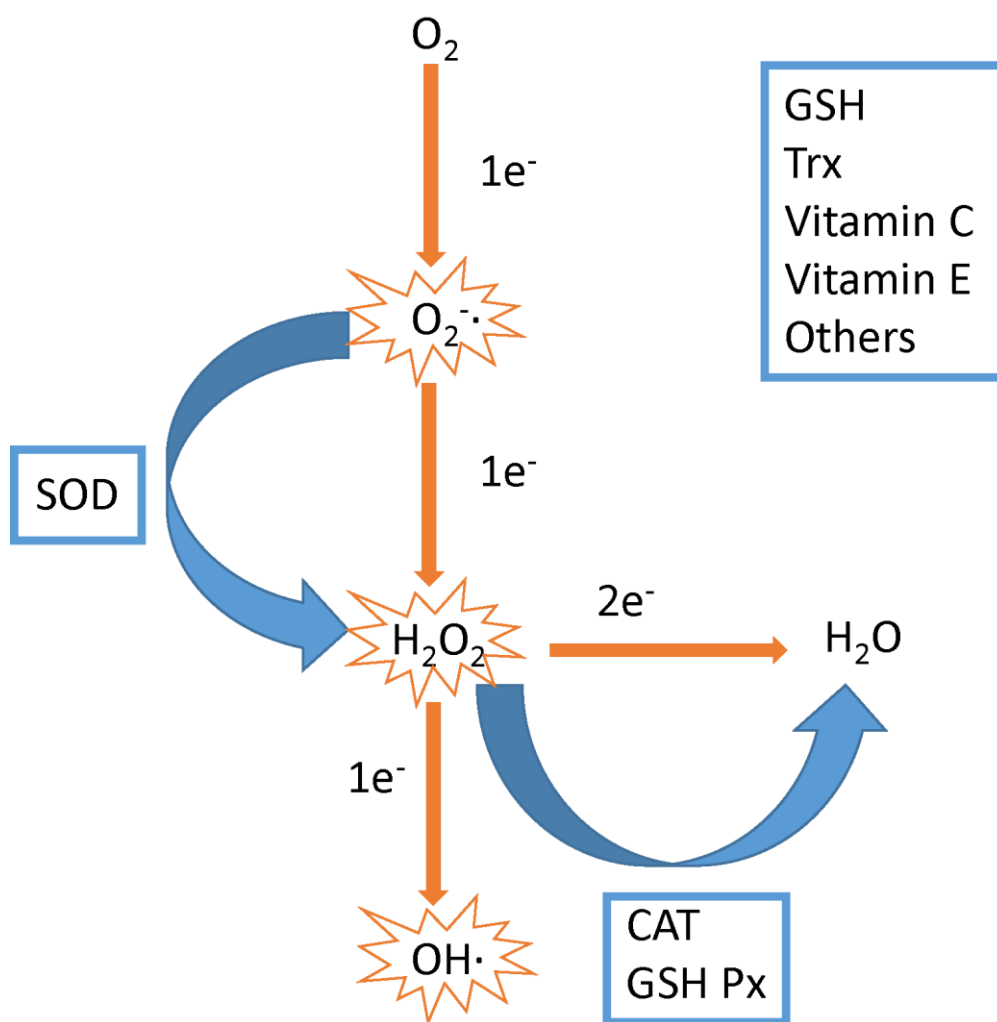


Figure 1.4. ROS and antioxidant systems. When oxygen is one-electron reduced, oxygen converts to superoxide anion ($O_2^{\cdot-}$). Two-electron reduction leads to hydrogen peroxide (H_2O_2) formation. A further one-electron reduction of hydrogen peroxide forms the highly reactive hydroxyl radical (OH^{\cdot}). Cells have antioxidant enzymes. SOD converts $O_2^{\cdot-}$ to H_2O_2 ; CAT and GSH Px convert H_2O_2 to H_2O . Other antioxidants (some shown in the box) are also involved in the regulation of redox balance (Song et al., 2013).

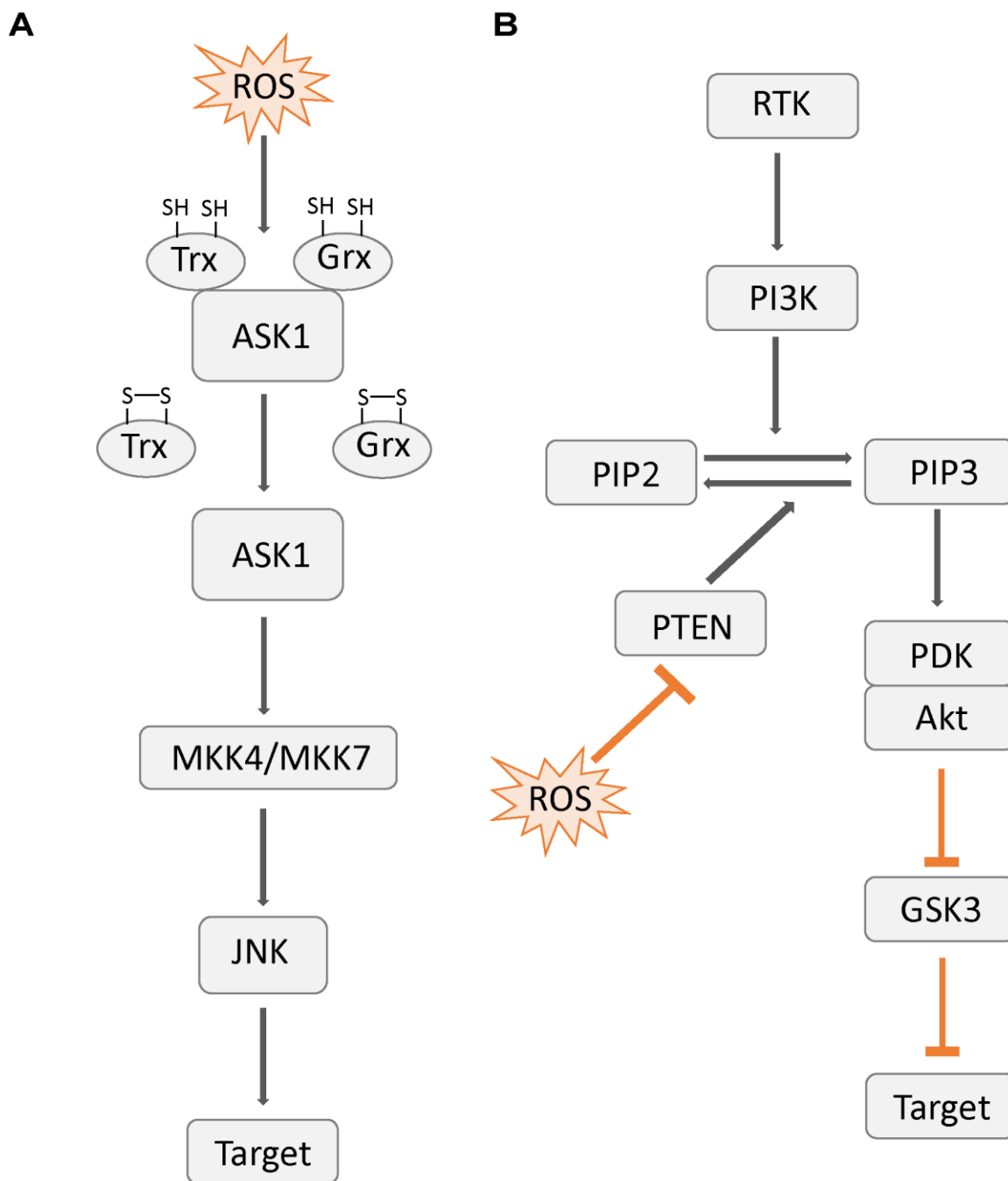


Figure 1.5 ROS regulation of the JNK and the PI3K/Akt/GSK3 β pathway. A, ROS oxidize the cysteine residues of Trx or Grx, which activates ASK1 because of the dissociation of Trx or Grx. Activated ASK1 then phosphorylates downstream proteins and thereby activates the JNK pathway. **B,** ROS activate the PI3K/Akt/GSK3 β pathway via the inhibition of the phosphatase PTEN. GSK3 is the negative regulator of the downstream targets. Activation of the Akt phosphorylates and inhibits GSK3 activity, and thereby activates the downstream targets.

CHAPTER 2. MATERIALS AND METHODS

2.1 Materials and chemicals

2.1.1 Materials for *in vivo* studies

Dissecting microscope (Nikon SMZ645), Scissors (Fine Science Tools- FST # 15000-00 straight), two pairs of forceps (FST, Dumont #5 Dumonstar # 11295-00), Sylgard plate (Sylgard 182 Silicone Elastomer Kit), Minutien insect pins (FST # 26002-10), glass slides (Rite-On microslides Cat # 3050, size 25mm X 75mm), coverslips (24 X 40 mm No.1, VWR Cat #16004-306) , double sided permanent tape (Scotch Cat # 137DM-2 or 3M with 0.5 inch thickness), VALAP (Vaseline, Lanolin and Paraffin wax in equal parts) heated to 75°C, and small art paint brush.

2.1.2 Materials for *in vitro* studies

Dissecting microscope (ZEISS STEMI SR), two pairs of forceps (FST, Dumont #5 Dumonstar # 11295-00), Sylgard plate (Sylgard 182 Silicone Elastomer Kit), glass slides (Rite-On microslides Cat # 3050, size 25mm X 75mm), coverslips (VWR micro cover glass), double sided permanent tape (Scotch Cat # 137DM-2 or 3M with 0.5 inch thickness), VALAP (Vaseline, Lanolin and Paraffin wax in equal parts) heated to 75°C, and small paint brush.

2.1.3 Chemicals for *in vivo* studies

HL6 buffer (Hemolymph-Like buffer): 23.7 mM NaCl (Mallinckrodt chemicals), 24.8 mM KCl (Sigma), 15 mM MgCl₂·6H₂O (Mallinckrodt chemicals), 10 mM NaHCO₃ (Sigma), 20 mM Isothionic acid sodium salt (Sigma), 5 mM BES (Sigma), 80 mM Trehalose dehydrate (Sigma), 5.7 mM L-Alanine (Sigma), 2 mM L-Arginine

monohydrochloride (Sigma), 14.5 mM Glycine (Sigma), 11 mM L-Histidine (Sigma), 1.7 mM L-Methionine (Sigma), 13 mM L-Proline (Sigma), 2.3 mM L-Serine (Sigma), 2.5 mM L-Threonine (Sigma), 1.4mM L-Tyrosine (Sigma), 1 mM L-Valine (Sigma), 0.6 mM CaCl₂ Dihydrate (Sigma;), 4 mM L-Glutamate monosodium salt hydrate (Sigma) Paraquat (Sigma)

2.1.4 Chemicals for *in vitro* studies

Schneider's medium (Gibco), 10% heat-inactivated Fetal bovine serum (FBS, Atlanta Biologicals), Pen-Strep (50 U/mL penicillin with 50 µg/mL streptomycin, Gibco), collagenase (Sigma), concanavalin A (Sigma), tetramethylrhodamine methyl ester (TMRM, Life Technologies, Molecular Probes) , hydrogen peroxide 30% solution (H₂O₂, Macron Fine Chemicals), ethylene glycol tetraacetic acid (EGTA, Sigma), BAPTA-AM (Sigma)

Ca²⁺/Mg²⁺ free saline: 137 mM NaCl, 2.7 mM KCl, 0.36 mM NaH₂PO₄·H₂O, 11.9 mM NaHCO₃, 5.6 mM glucose

S2 saline: 120 mM NaCl, 5 mM KCl, 8 mM MgCl₂, 2 mM CaCl₂, 10 mM HEPES

2.2 *Drosophila* lines and maintenance

All *Drosophila* Stocks were maintained on normal fly food at 25°C with 40%-60% humidity and a 12 hr light/dark cycle. Fly genotypes used in this study are shown in the table (Table 2.1).

Table 2.1 Genotypes of flies in this study

Number	Fly genotypes	Source
1	<i>+</i> ; <i>D42-Gal4, UAS-mitoGFP</i>	Leo J. Pallanck (University of Washington)
2	<i>sp/Cyo; D42-Gal4, UAS-ANF-GFP</i>	William M. Saxton (UC Santa Cruz)
3	<i>+</i> ; <i>D42-Gal4</i>	Leo J. Pallanck (University of Washington)
4	<i>UAS-SOD1;+</i>	Bloomington stock center
5	<i>UAS-SOD2;+</i>	Bloomington stock center
6	<i>UAS-SOD1; D42-Gal4, UAS-mitoGFP</i>	Generated from #1 and #4
7	<i>UAS-SOD2; D42-Gal4, UAS-mitoGFP</i>	Generated from #1 and #5
8	<i>UAS-GCaMP6m;+</i>	Bloomington stock center
9	<i>UAS-GCaMP6m/+; D42-Gal4/+</i>	Generated from #3 and #8
10	<i>UAS-Hep^{B2};+</i>	Bloomington stock center
11	<i>UAS-Bsk RNAi;+</i>	Vienna Drosophila RNAi Center (VDRC)
12	<i>UAS-Hep^{B2}; D42-Gal4, UAS-mitoGFP</i>	Generated from #1 and #10
13	<i>UAS-Bsk RNAi; D42-Gal4, UAS-mitoGFP</i>	Generated from #1 and #11
14	<i>UAS-Hep^{B2}/UAS-GCaMP6m; D42-Gal4/+</i>	Generated from #9 and #10
15	<i>UAS-Bsk RNAi /UAS-GCaMP6m; D42-Gal4/+</i>	Generated from #9 and #11
16	<i>UAS-Nox RNAi/+</i>	Vienna Drosophila RNAi Center (VDRC)
17	<i>UAS-Duox RNAi/+</i>	Vienna Drosophila RNAi Center (VDRC)
18	<i>UAS-Nox RNAi; D42-Gal4, UAS-mitoGFP</i>	Generated from #1 and #18
19	<i>UAS-Duox RNAi; D42-Gal4, UAS-mitoGFP</i>	Generated from #1 and #19

2.3 Preparation of primary neuronal cell culture and dissected larvae for live imaging

2.3.1 Preparation of *Drosophila* larval primary neuronal culture

Prior to dissection, 4 third-instar larvae were washed with 70% ethanol once and endotoxin-free water for three times. Larvae were dissected in Schneider's medium by pulling the mouth hook, which opened the animal's body and exposed the brains and ventral ganglia. After cleaning away debris, the brains and ventral ganglia were incubated in $\text{Ca}^{2+}/\text{Mg}^{2+}$ free saline with 0.7 mg/ml collagenase for 1 hr at room temperature. Samples were centrifuged at 300 g for 3 min and washed once with Schneider's medium. Tissue was then triturated with siliconized pipette tips to disperse it into individual cells, which were then plated on coverslips coated with 15 $\mu\text{g}/\text{ml}$ concanavalin A and incubated in Schneider's medium containing 1% FBS in a humidified chamber at 25°C for 72 hrs. Before imaging, 50 μl of Schneider's medium was placed on a glass slide with a single layer of double-sided tape as a spacer. The coverslip with cells was flipped onto the glass slide. The sample was then sealed with VALAP and ready for imaging.

2.3.2 *Drosophila* larval dissection for live imaging

Third instar larvae were prepared using methods described previously (Pilling et al., 2006; Devireddy et al., 2014; Devireddy et al., 2015). First, third instar larvae were washed with distilled water and pinned at posterior and anterior ends with the dorsal side up on a slygard plate (Fig. 2.1A), and moistened with HL6 buffer. A small hole was cut at the posterior end of the body (Fig. 2.1B) and the larva was opened by snipping through the cuticle with dissecting scissors (Fig. 2.1C). Muscles and fat bodies were removed exposing the brain, ventral ganglion, and the intact segmental nerves (Fig. 2.1D), which retained their connections to the muscles of the body wall. To make the larva lie flat, 4 small lateral cuts (2 close to the anterior end and 2 close to the posterior end) were made in the body wall (Fig. 2.1E). The dissected larva was then moved and opened gently onto a glass slide containing two layers of double-sided tape as spacers (Fig. 2.1F), and the ventral ganglion and the segmental nerves were stretched by gently holding the mouth

hook (Fig. 2.1G, H). This sample was then covered by a coverslip, incubated in HL6 buffer, and the resulting chamber was sealed with VALAP. The whole procedure was done in 10 minutes.

2.3.3 ROS induction *in vitro* and *in vivo*

To induce oxidative stress *in vitro*, cells were treated with 100 μM H_2O_2 for 1 hr, followed by imaging (Fang et al., 2012). To induce oxidative stress *in vivo*, second to third instar larvae were starved for 3 hr and then maintained on the standard fly food containing 20 mM paraquat for 24 hrs (Lee et al., 2009), followed by dissection and imaging.

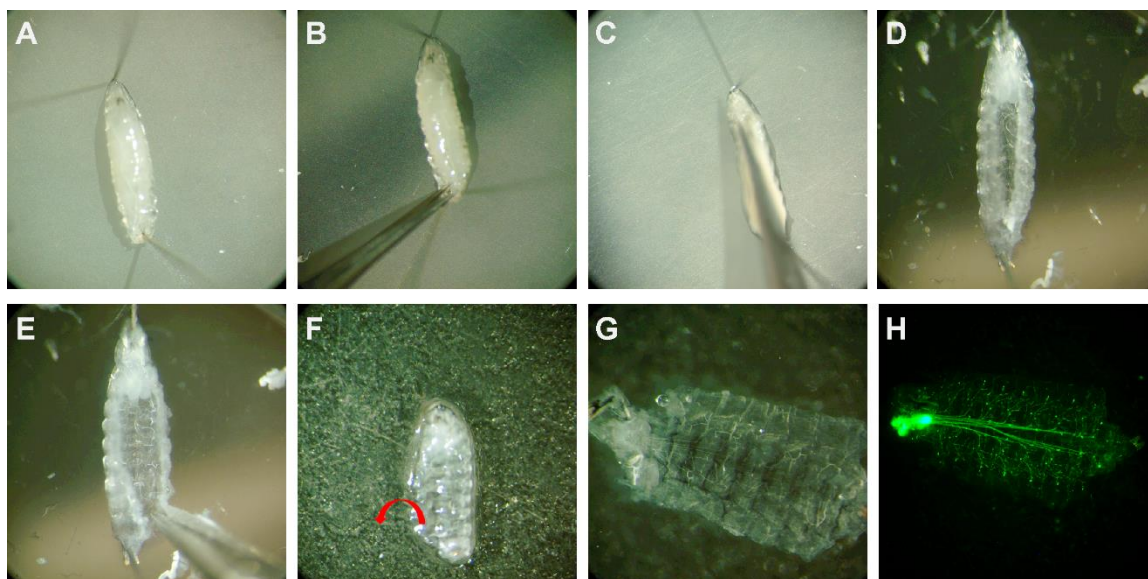


Figure 2.1. Steps of *in vivo* larval dissection. A, Larva is pinned on a slygard plate at anterior and posterior positions. B, An incision is made at the posterior end. C, Larva is opened by cutting through the cuticle on the dorsal side. D, Fat bodies and muscles are cleaned to expose intact nervous system. E, Small lateral incisions are made to flatten the larva (4 positions at anterior and posterior ends, only shown one position here). F, Larva is transferred to a glass slide and body walls are opened (red arrow). G and H, Bright field and fluorescence images of dissected larva are shown. (Figure is adapted and modified from Devireddy et al., 2014)

2.4 Analysis of mitochondrial and dense core vesicle (DCV) transport

2.4.1 Acquisition of time lapse confocal images

In vitro, mitochondria or DCVs were imaged using 60x oil-immersion objective lens and 3x zoom of the upright, time-lapse laser confocal microscope (LSCM, Nikon Eclipse 90i) with a 488 nm laser (5%; 150mW laser power). The time resolution was 1 frame/s for a duration of 120 s. Transport of DCVs was also visualized using spinning disk confocal microscopy (Olympus IX-71 microscope equipped with a 60X 1.45 NA TIRFM PlanApo objective and Disk Scanning Unit). The time resolution in this case was 5 frames/s for a duration of 120 s (Fig. 2.2A, B).

In vivo, time lapse confocal images of mitochondrial or DCV transport were acquired in the middle segment (A4 region) of the longest larval segmental nerves using LSCM with a 488 nm laser. The time resolution was 1 frame/s for a duration of 200 s (Fig. 2.2C – E).

2.4.2 *In vitro* analysis of mitochondrial and DCV transport

For mitochondrial transport, the percentage of moving mitochondria was analyzed. The number of the moving or stationary mitochondria was counted using the *Cell Counter* plug-in in Image J software.

For DCV transport, due to the fast transport behavior, flux and velocity were analyzed from kymographs created by MetaMorph software. Flux is the number of vesicles passing an assigned point in a 60 sec period. Velocity is the average of the instantaneous velocity. I analyzed the flux by counting the number of the moving organelle tracks passing through the vertical midline of the kymograph. Velocity was calculated from the slope of the lines in kymographs. Anterograde transport is defined as the transport toward synaptic terminals; retrograde transport is defined as the transport toward to cell bodies.

2.4.3 *In vivo* analysis of mitochondrial and DCV transport

Kymographs of mitochondrial or DCV transport *in vivo* were prepared using Nikon NIS-Elements software. *Manual Tracking* plug-in in Image J software was used to track

individual mitochondria or DCVs by marking the x-y positions of every vesicle in every frame. A stationary vesicle was also “tracked” as a reference point to eliminate the effects of larval moving or stage drift. These positional data were used to analyze different parameters of transport behavior described as follows (Devireddy et al., 2014; Devireddy et al., 2015):

1. **Run** is the motion sustained in at least three frames with the velocity larger than $0.1 \mu\text{m/s}$ or smaller than $-0.1 \mu\text{m/s}$.
2. **Flux** is defined as the number of vesicles that cross an assigned point in one-minute interval. In a 200 s period, I recorded how many mitochondria moved anterogradely and retrogradely across a line drawn in the center of the movie frame.
3. **Velocity** is the average of velocity of each run. Velocity was considered as run velocity only rather than average velocity including pauses. This run velocity was determined by the total length/total time of all runs.
4. The **percentage of moving vesicles** is the fraction of vesicles that move either anterogradely or retrogradely. *Cell Counter* plug-in was used to count the number of moving or stationary mitochondria.
5. **Duty cycle** is the percentage of time spent moving in a particular direction, anterograde, retrograde, or paused.
6. **Run length** is the average moving distance per run. Typically I used total distance of total runs/the number of runs to get average run length.

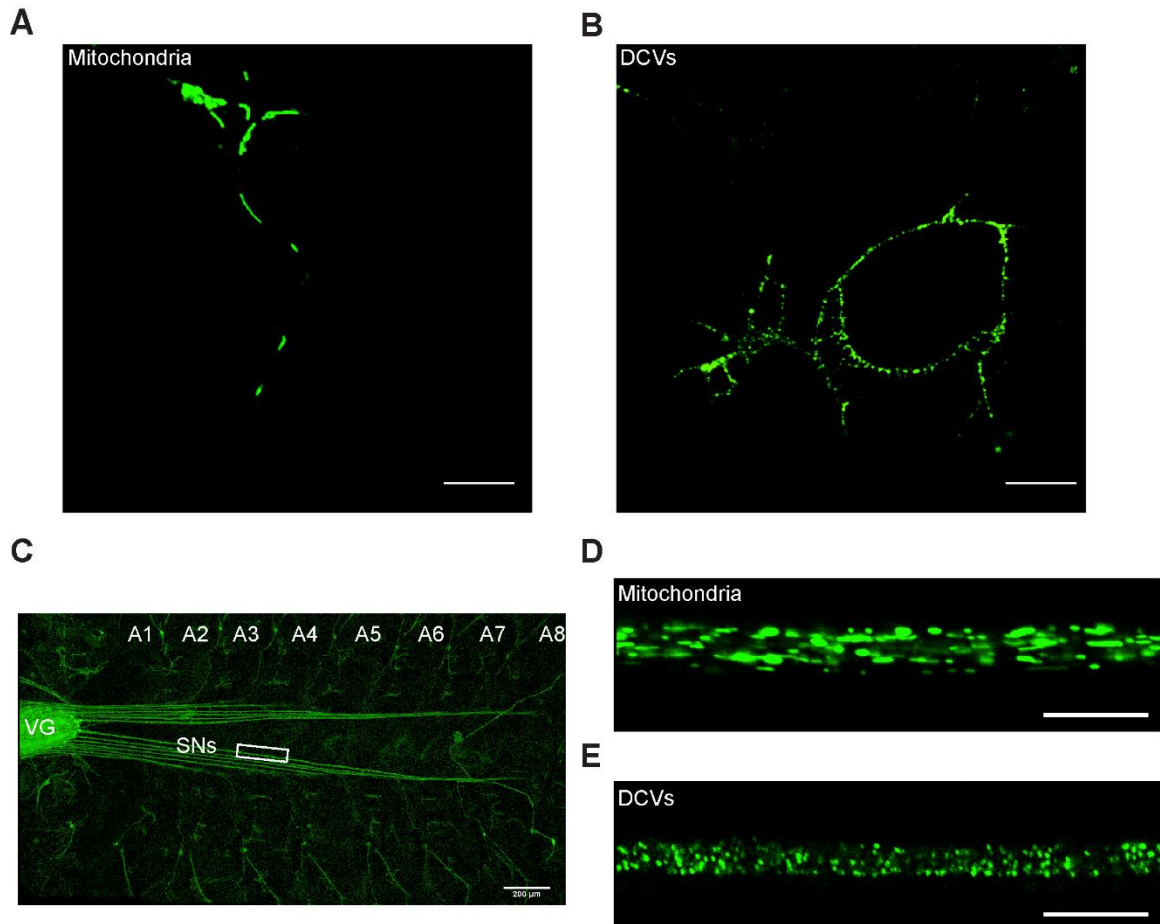


Figure 2.2. GFP expression of mitochondria or DCVs *in vivo* and *in vitro*. A and B, Mitochondria (A) and DCVs (B) are shown in primary neuronal cell culture. C, all 8 segments, segmental nerves (SNs), and ventral ganglion (VG) are shown. The white box shows the A4 (Abdominal segment 4) region of the longest segmental nerves, used for visualizing transport. D and E, Mitochondria (D) and DCVs (E) are shown in the A4 region of the longest segmental nerves. Scale bars in (A,B,D,E) indicates 10 μm . (Figure is adapted and modified from Devireddy et al., 2014)

2.5 Measurement of mitochondrial membrane potential

2.5.1 TMRM treatment in cell culture

A 20 mM tetramethylrhodamine methyl ester (TMRM) stock was prepared in DMSO. A 25 μ M TMRM working stock was prepared freshly for each experiment by diluting the first stock with DMSO. Cells were incubated in Schneider's medium containing 25 nM TMRM for 10 minutes, and washed once with 6.25 nM TMRM washing solution. The treated samples were imaged in washing solution to maintain dye equilibrium. All procedures were performed avoiding light exposure (Shidara and Hollenbeck, 2010; Devireddy et al., 2014; Devireddy et al., 2015).

2.5.2 Imaging and quantification of TMRM intensity

Cells were imaged using 60x oil-immersed objective lens with 3x zoom of confocal microscope (Nikon Eclipse 90i) with 5% 488 nm and 561 nm laser. To image motor neurons specifically, cells containing green signals due to the expression of mitoGFP driven by *D42-Gal4* were selected. The laser power of the 561 nm channel was sometimes adjusted to prevent saturated exposure in the images.

To quantify the TMRM intensity, images were thresholded in the intensity range between 350 and 4095 units (highest intensity: 4095) and the intensity of mitochondrial fluorescence (Fm) was measured using Nikon NIS-Elements software. The fluorescence intensity in cytosol (Fc) was determined as the average intensity of two 5 pixel x 5 pixel regions next to the mitochondria. The mitochondrial membrane potential was then expressed as the intensity ratio of mitochondrial fluorescence to cytosolic fluorescence (Fm/Fc) which is logarithmically related to mitochondrial membrane potential.

2.6 Quantification of mitochondrial density and lengths

2.6.1 Quantification of mitochondrial density

Mitochondrial density was determined by finding the total mitochondrial pixels in fields imaged in the center of segmental nerves (A4) using MetaMorph software. The

second frame of the time lapse images was used to reduce background noise and sharpen the image by low-pass Laplace filters in the software. Then the image was thresholded at 350 intensity units and binarized. From this binary image, integrated mitochondrial pixels (number of mitochondrial pixels divided by total pixels in the nerve field) were measured as mitochondrial density.

2.6.2 Quantification of mitochondrial length

In cell culture, only mitochondria in the processes were selected for length measurement. Mitochondrial length was measured using *Annotations* and *Measurements/Length/2 Points* or *Polyline* function in Nikon NIS-Elements software.

2.7 Measurement of Ca^{2+} levels and analysis of transport affected by Ca^{2+}

2.7.1 Ca^{2+} chelation and release in cell culture

Neuronal cells expressing GCaMP6 in motor neurons (*UAS-GCaMP6m/+; D42-Gal4/+*) were used to visualize Ca^{2+} levels. Before treatment, cells were washed three times with sterile S2 saline. To chelate extracellular Ca^{2+} , cells were incubated in Ca^{2+} -free saline (S2 saline without CaCl_2) containing 0.1 mM EGTA for 30 minutes. To remove both extracellular and intracellular Ca^{2+} , cells were incubated in Ca^{2+} -free saline containing 0.1 mM EGTA and 10 μM BAPTA-AM for 30 minutes (Kim and Sharma, 2004; Yeromin et al., 2004; Huang et al., 2014). To induce ROS in Ca^{2+} chelation conditions, cells were incubated in above-described solutions containing 100 μM H_2O_2 for 1 hr. After incubation, cells were prepared for imaging.

To artificially increase intracellular Ca^{2+} levels dramatically, cells were treated with S2 saline containing 10 μM ionomycin, an ionophore. To induce intracellular Ca^{2+} levels from the intracellular Ca^{2+} pool, cells were treated with S2 saline containing 2 μM thapsigargin, an ER Ca^{2+} -ATPase inhibitor (Yeromin et al., 2004). After treatment, cells were imaged immediately.

2.7.2 Imaging and quantification of Ca²⁺ levels

Cells were imaged using a 60x oil-immersion objective lens with 3x zoom on the confocal microscope (Nikon Eclipse 90i) using 10% power from the 488 nm laser. To image motor neurons specifically, cells containing green signals due to the expression of GCaMP6 driven by *D42-Gal4* were selected.

To quantify the Ca²⁺ levels, images were thresholded in the intensity range between 30 and 4095 units (highest intensity: 4095) and the intensity of Ca²⁺ was measured in whole cells using Nikon NIS-Elements software. Total intensity/total area was used to get the average intensity of Ca²⁺ in a cell.

2.7.3 Imaging the effects of Ca²⁺ on transport

To determine the effects of elevated Ca²⁺ on mitochondrial or DCV transport, 10 μM ionomycin or 2 μM thapsigargin was used as in section 2.7.1, above. Before treatment, cells were washed with S2 saline for three times and imaged using the *in vitro* settings as in section 2.4.1, above. The same sample was then treated with S2 saline containing 10 μM ionomycin or 2 μM thapsigargin. After treatment, the same cell was imaged again immediately. To analyze transport, the percentage of mitochondria transport or velocity of DCV of the same cell before and after treatment was analyzed using the methods described in section 2.4.2, above.

To determine the effects of Ca²⁺ chelation on mitochondrial transport, conditions of treatment were the same as in section 2.7.1, above. The settings for the acquisition and analysis were the same as in sections 2.4.1 and 2.4.2, respectively.

2.8 Statistics

All statistical analysis was performed using GraphPad Prism 5 software. All error bars in graphs indicate mean ± SEM. In the *in vivo* studies, the experimental unit is an individual larva. In the *in vitro* studies, the experimental unit is a cell. Data were analyzed using a one-way ANOVA with Bonferroni's post-test for multiple group comparisons, paired or unpaired Student's t-test for two group comparisons. In all cases, at least three

independent experiments were performed. The specific type of statistical analysis was shown in figure legends.

CHAPTER 3. RESULTS

3.1 Mitochondrial transport in axons is reduced in response to oxidative stress

3.1.1 Mitochondrial transport is reduced *in vitro* in response to oxidative stress

Impairment of the axonal transport of mitochondria has been shown to correlate with neurodegenerative diseases (Saxton and Hollenbeck, 2012; Sheng and Cai, 2012). However, how ROS production might circle back to regulate mitochondrial transport, an issue that may be important in the pathophysiology of neurodegeneration, is still unknown. Diminished overall mitochondrial transport under oxidative stress conditions has been shown in cultured neurons (Fang et al., 2012). Thus, I first examined whether oxidative stress affected mitochondrial transport in *Drosophila* primary neuron cell cultures obtained from brains and ventral ganglia of third instar larvae expressing mtiochondrially-targeted GFP in motor neurons.

To induce oxidative stress, I treated cells with 100 μM H_2O_2 for 1 hr and found that the percentage of moving mitochondria in axons decreased significantly (Fig. 3.1A, B). Longer periods of treatment (up to 3 hrs) did not produce any further reduction in mitochondrial motility (Fig. 3.1C). These results indicate that in *Drosophila* primary neuronal cell cultures, mitochondrial transport is diminished under conditions of oxidative stress, consistent with previous *in vitro* studies (Fang et al., 2012).

3.1.2 Mitochondrial transport is reduced *in vivo* in response to oxidative stress

Although the results showed that oxidative stress reduced mitochondrial transport in cultured neurons, it remained unknown whether or not ROS affect mitochondrial transport in axons of the nervous system *in vivo*. In the more complex *in vivo* environment, homeostatic control of ROS is probably more robust, and physiological

pO₂ is lower than *in vitro*. Thus, I quantified different parameters of mitochondrial transport under oxidative stress conditions *in vivo* in 3rd instar larvae expressing mito-GFP in their motor neurons and prepared as previously described (Shidara et al, 2010; Devireddy et al, 2014). I expected that, as *in vitro*, an *in vivo* ROS increase would affect mitochondrial transport. To induce oxidative stress in the larval nervous system, I treated larvae with 20 mM paraquat for 24 hrs (Lee et al., 2009), and quantified mitochondrial movements in axons in the central region of the longest segmental nerves (Devireddy et al., 2014).

In axons, moving mitochondria are categorized into anterograde and retrograde populations by their dominant and net direction of movement, which is easily distinguishable despite pauses and brief reversals of direction. I first quantified flux, which is a gross indicator of movement representing how many mitochondria pass a fixed point per unit time. I found reduced mitochondrial flux in both the anterograde and retrograde populations after paraquat treatment *in vivo* (Fig. 3.2A, B). To perform a more detailed analysis and determine the possible mechanisms decreasing flux, I examined more specific parameters of mitochondrial transport: velocity, duty cycle, run length, percentage of moving mitochondria, and density (Devireddy et al., 2014). Under oxidative stress conditions, I found reduced run velocities in both directions (Fig. 3.2C), of a magnitude nearly large enough to explain the reduction in flux. In addition, duty cycle was modestly-reduced in the retrograde direction (Fig. 3.3A). Due to the reduction of velocity and duty cycle, retrograde run length was also modestly reduced (Fig. 3.3B). Moreover, reduced flux was caused by an increased percentage of stationary mitochondria (Fig. 3.3C). Mitochondrial density is not directly linked to motility, but reduced density can definitely contribute to reduced flux. However, there was no significant difference in mitochondrial density of segmental nerve axons under oxidative stress conditions (Fig. 3.3D), indicating that mitochondrial motility is directly reduced under these conditions *in vivo*.

3.2 Overexpression of SOD attenuates defects of mitochondrial transport under oxidative stress conditions

3.2.1 Overexpression of SOD rescues ROS-induced defects of mitochondrial transport *in vitro*

Superoxide dismutase (SOD), a well-characterized anti-oxidant enzyme, converts superoxide to H₂O₂ (Matés et al., 1999; Fischer et al., 2012). Overexpression of SOD has been shown to relieve oxidative stress in *Drosophila* (Parkes et al., 1998; Elia et al., 1999). To ensure that the reduced mitochondrial transport observed above was specifically caused by oxidative stress, I overexpressed cytosolic SOD (SOD1) or mitochondrial SOD (SOD2) under oxidative stress conditions, with the expectation that ROS-induced defects in mitochondrial transport would be rescued. As expected, the defects in the percentage of moving mitochondria *in vitro* were fully rescued by overexpression of either SOD1 or SOD2 (Fig. 3.1A, B), indicating that the defects of mitochondrial transport were specifically caused by oxidative stress *in vitro*.

3.2.2 Overexpression of SOD rescues ROS-induced defects of mitochondrial transport *in vivo*

In vivo, both the reduced flux and velocity produced by paraquat were rescued by SOD1 or 2 overexpression (Fig. 3.2). In the retrograde direction, both the modestly-reduced duty cycle and run length were also rescued (Fig. 3.3A, B). For the percentage of moving mitochondria *in vivo*, the increase in stationary mitochondria was rescued (Fig. 3.3C). Interestingly, SOD2 overexpression alone produced an increase in the percentage of anterograde moving mitochondria. In addition, under oxidative stress conditions, SOD2 overexpression produced an increased percentage of retrograde moving mitochondria (Fig. 3.3C), suggesting that mitochondrial SOD overexpression could play a role in recycling mitochondria back to cell bodies. These results indicate that inducing a reduction of excess ROS levels can diminish the defects in mitochondrial transport *in vivo*. On the other hand, there is no significant difference in axonal mitochondrial density compared to controls with SOD1 or 2 overexpression alone (Fig. 3.3D), suggesting that mitochondrial biogenesis, turnover,

and/or the traffic steady state were not affected by the overexpression. In sum, these results indicate that excess ROS do produce defects of mitochondrial transport both *in vitro* and *in vivo*.

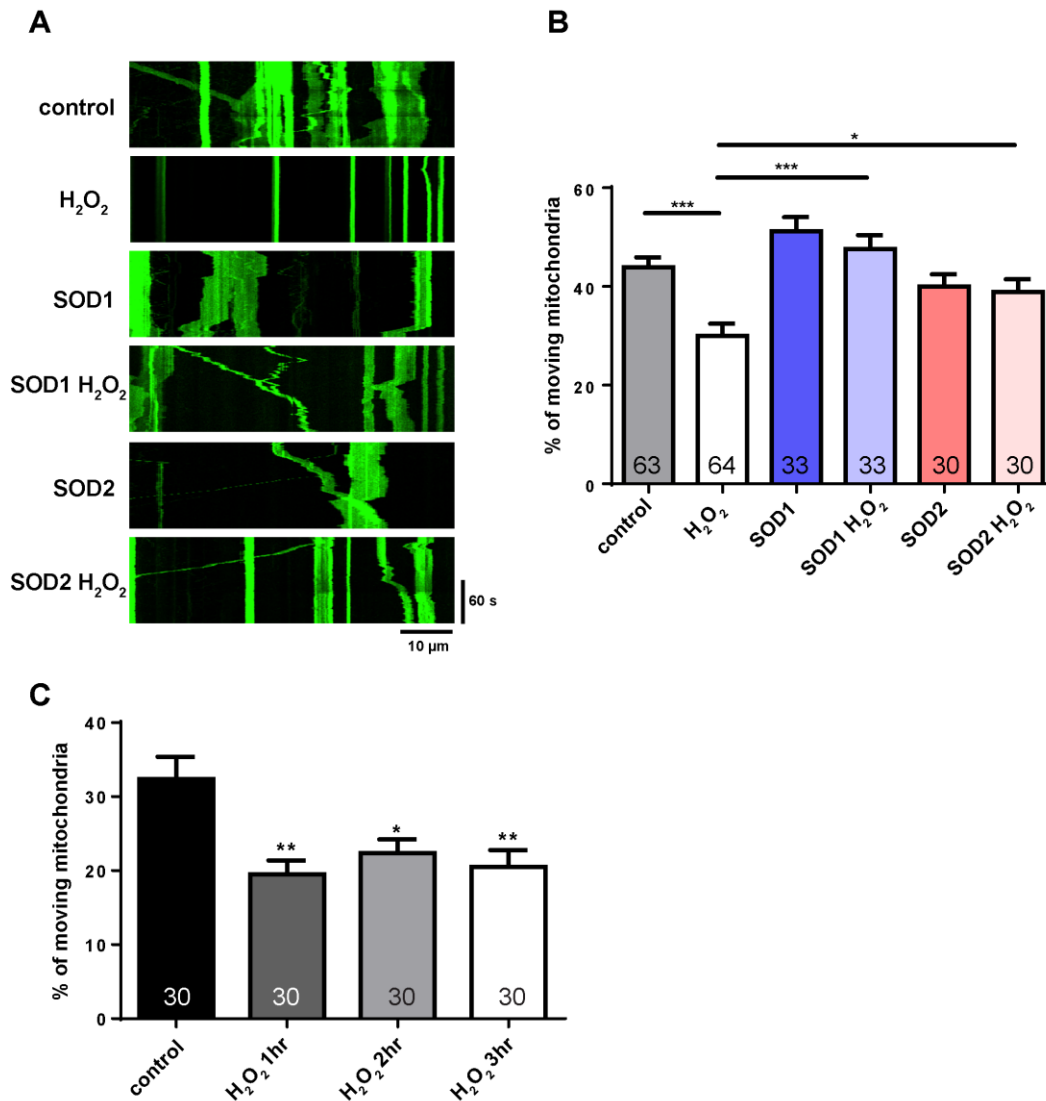


Figure 3.1. The percentage of moving mitochondria is reduced in response to ROS and rescued by SOD overexpression *in vitro*. **A**, Representative kymographs of mitochondrial transport under H₂O₂ treatment. Anterograde transport is toward the right; retrograde transport is toward the left. **B**, The percentage of moving mitochondria is reduced with H₂O₂ treatment. SOD1 or SOD2 overexpression can rescue the defect. **C**, The percentage of moving mitochondria decreases with the same levels after H₂O₂ treatment for 1 to 3 hrs. Number of cells is shown on bars. Error bars indicate mean \pm SEM. Significance is determined by one-way ANOVA with Bonferroni's post-test. * $p < 0.05$, ** $p < 0.01$, and *** $p < 0.001$.

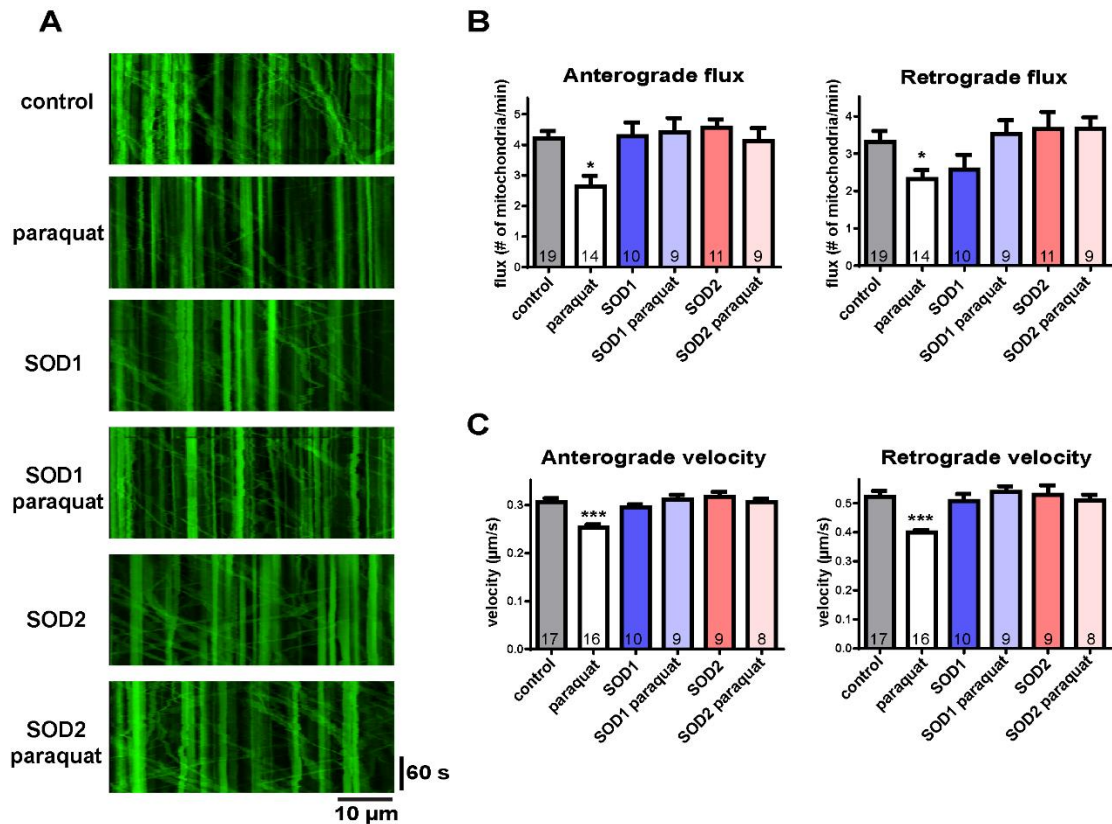


Figure 3.2. ROS change mitochondrial motility mainly by reducing flux and velocity *in vivo*. **A**, Representative kymographs of mitochondrial transport under paraquat treatment. Anterograde transport is toward the right; retrograde transport is toward the left. **B**, Paraquat treatment produces a decrease in mitochondrial flux, which is rescued by overexpression of SOD1 or SOD2 in both directions. **C**, Velocity is reduced with paraquat treatment, which is rescued by SOD1 or SOD2 overexpression in both directions. Number of larvae is shown on bars. Error bars indicate mean \pm SEM. Significance is determined by one-way ANOVA with Bonferroni's post-test. * $p < 0.05$, and *** $p < 0.001$.

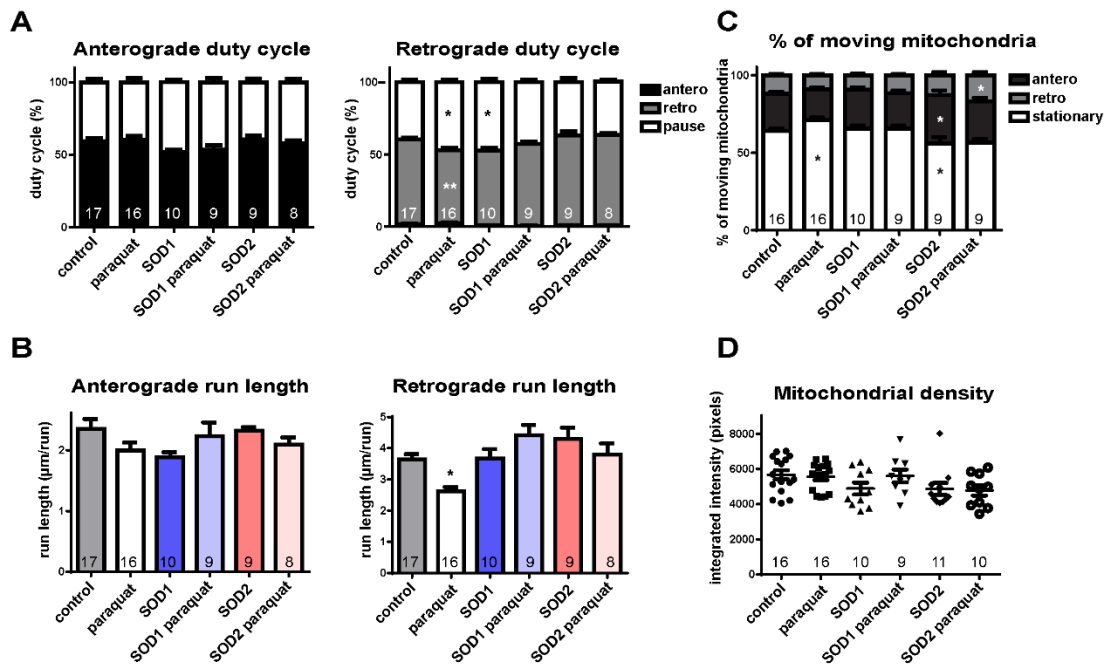


Figure 3.3. ROS modestly affect mitochondrial duty cycle, run length, and percentage of moving mitochondria *in vivo*. **A**, Paraquat treatment gives a small reduction in retrograde duty cycle with an increase of pause time and a decrease of moving time; overexpression of SOD1 shows a small increase of pause time. **B**, Retrograde run length is modestly reduced with paraquat treatment. **C**, Paraquat treatment shows an increase of the percentage of stationary mitochondria, which is rescued by SOD overexpression. The percentage of anterograde moving mitochondria increases with SOD2 overexpression. **D**, Mitochondrial density is comparable to control with paraquat treatment or SOD overexpression. Number of larvae is shown on bars. Error bars indicate mean \pm SEM. Significance is determined by one-way ANOVA with Bonferroni's post-test. * $p < 0.05$, and ** $p < 0.01$.

3.3 Transport of neuropeptide-bearing large DCVs is barely affected in the presence of ROS

3.3.1 DCV transport is barely affected in response to oxidative stress *in vitro*

To test whether the defects of transport in response to oxidative stress are specific to mitochondria, I further investigated fast axonal transport of other cargoes. To examine this, ANF (atrial natriuretic peptide)-GFP, a GFP fusion targeted to the lumen of neuropeptide-bearing DCVs, was expressed in motor neurons using the *D42-Gal4* driver (Barkus et al., 2008).

In vitro, time lapse images were taken using a spinning disk confocal microscope with 5 frames/s time resolution. Then images were converted to kymographs for analysis of flux and velocity (Fig. 3.4A). Under oxidative stress conditions, the flux of DCV transport was not affected in either direction (Fig. 3.4B). Velocity analysis showed that only retrograde, but not anterograde, velocity was modestly affected (Fig. 3.4C). These results indicate that DCV transport is barely affected under oxidative stress conditions *in vitro*.

3.3.2 DCV transport is not affected in response to oxidative stress *in vivo*

In vivo, detailed parameters of DCV transport in response to ROS -- including velocity, duty cycle, run length, and density -- were analyzed (Fig 3.5). As with the *in vitro* results, all of parameters under paraquat treatment were comparable to controls, indicating that DCV transport is not affected by oxidative stress conditions (Fig 3.5B-D). In addition, since the DCV density is unchanged (Fig. 3.5E), DCV biogenesis and degradation appear to be maintained in their normal steady state. Thus, based upon both *in vitro* and *in vivo* results, I conclude that oxidative stress impedes mitochondrial transport specifically, rather than the general axonal transport of organelles.

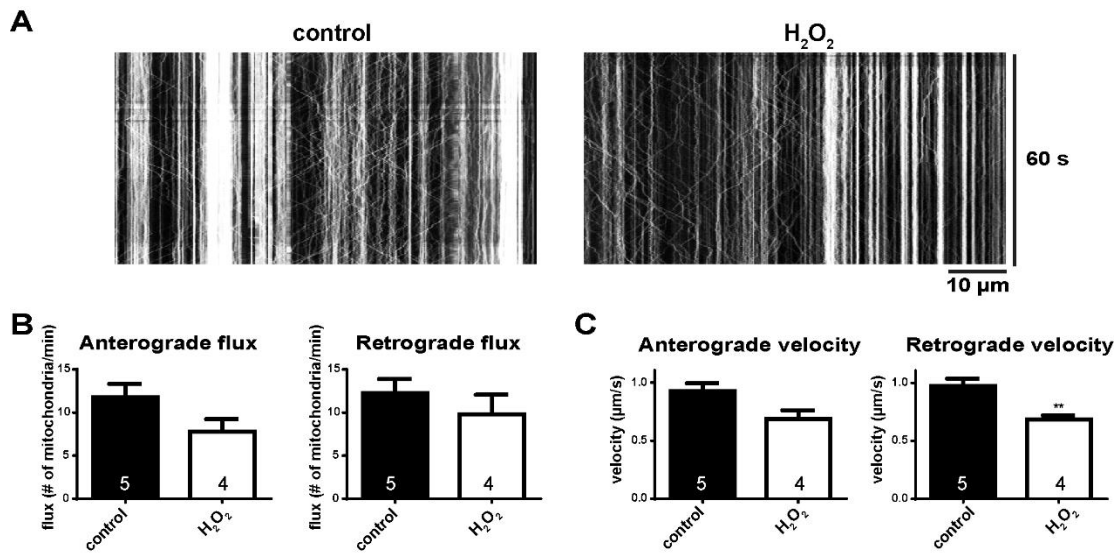


Figure 3.4. DCV transport is nearly unaffected by ROS treatment *in vitro*. **A**, Representative kymographs of DCV transport *in vitro*. Anterograde transport is toward the right; retrograde transport is toward the left. **B**, There is no significant difference in both anterograde and retrograde flux of DCV transport with H₂O₂ treatment. **C**, Retrograde velocity of DCV transport is reduced with H₂O₂ treatment. Number of plates is shown on bars. Each plate contains at least 5 cells. Error bars indicate mean \pm SEM. Significance is determined by Mann Whitney test. **p < 0.01.

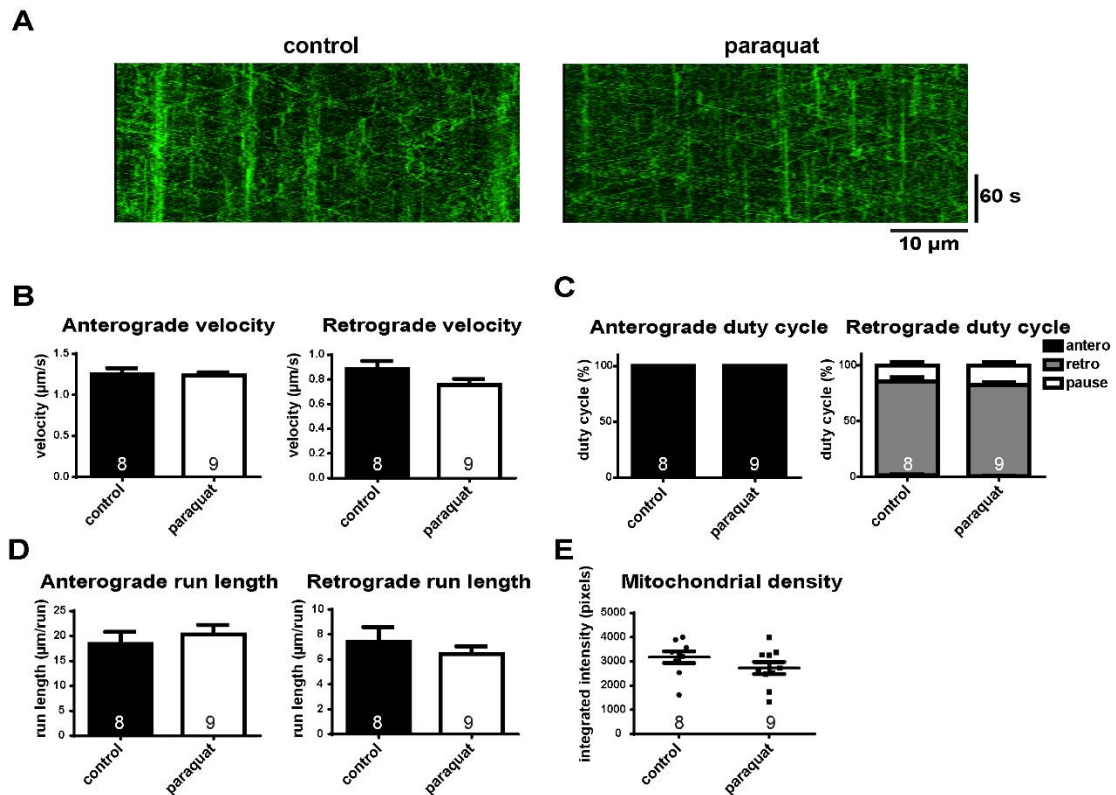


Figure 3.5. DCV transport is unaffected by ROS treatment *in vivo*. **A**, Representative kymographs of DCV transport *in vivo*. Anterograde transport is toward the right; retrograde transport is toward the left. **B-E**, Parameters in DCV transport with paraquat treatment including velocity (**B**), duty cycle (**C**), run length (**D**), and density (**E**) are comparable to controls. Number larvae is shown on bars. Error bars indicate mean \pm SEM. Significance is determined by Student's t-test.

3.4 Endogenous Nox and Duox play roles in the regulation of mitochondrial transport

It has been shown that excessive ROS induce oxidative stress and cellular damage. However, recent evidence makes it clear that endogenous ROS are important signaling molecules required for different functions such as wound response, muscle contraction, and neurite outgrowth, among other roles. (Ritsick et al., 2007; Razzell et al., 2013; Munnamalai et al., 2014; Nayernia et al., 2014). So aside from excessive ROS, it is unclear whether endogenous ROS levels also affect mitochondrial transport in axons. To examine this, NADPH oxidase (Nox) and Dual oxidase (Duox) were down-regulated by RNAi in motor neurons and mitochondrial transport was examined *in vivo*.

I examined different parameters including flux, velocity, duty cycle, run length, percentage of moving mitochondria and density in both directions under Nox or Duox down-regulation (Fig. 3.6 and 3.7). Interestingly, all transport parameters were reduced in both directions with Nox down-regulation (Fig. 3.6 and 3.7), indicating that endogenous ROS are required for mitochondrial transport. On the other hand, only retrograde mitochondrial transport showed a general reduction with Duox down-regulation (Fig. 3.6 and 3.7), suggesting a directional difference of influence between Duox and Nox. Furthermore, only run length decreased in the anterograde direction (Fig. 3.7B), suggesting that the specific motility pattern is affected by Duox knockdown. Mitochondrial density under down-regulation of Nox or Duox was comparable to controls, indicating the observed defects were due to transport behavior. These data suggest that either abnormally high or low levels of ROS affect mitochondrial movement in axons, implying that physiological ROS levels are crucial for mitochondrial transport. This also raises the possibility that the defects of mitochondrial transport observed under conditions of excessive ROS are caused not only by oxidative damage but also by the subversion of ROS-induced signaling pathways.

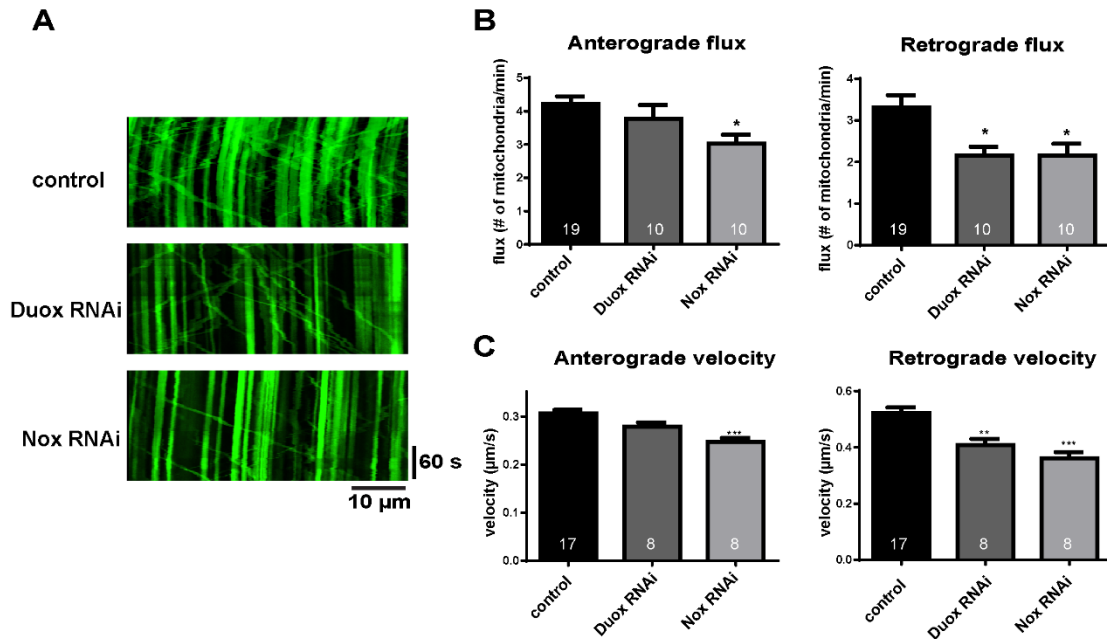


Figure 3.6. Endogenous ROS affect mitochondrial flux and velocity *in vivo*. **A**, Representative kymographs of mitochondrial transport with knockdown of Duox or Nox. Anterograde transport is toward the right; retrograde transport is toward the left. **B**, Knockdown of Duox produces a decrease in mitochondrial flux retrogradely, but knockdown of Nox reduces flux in both directions. **C**, Velocity is reduced in both directions by down-regulation of Nox, but is reduced only in the retrograde direction by down-regulation of Duox. Number of larvae is shown on bars. Error bars indicate mean \pm SEM. Significance is determined by one-way ANOVA with Bonferroni's post-test. * $p < 0.05$, ** $p < 0.01$, and *** $p < 0.001$.

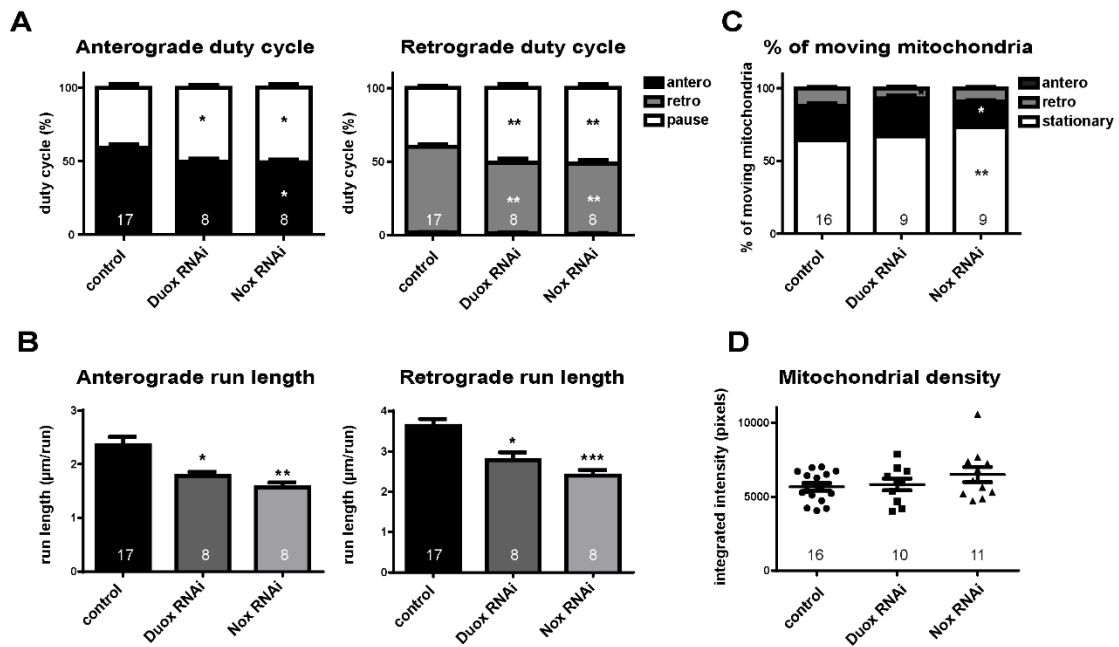


Figure 3.7. Endogenous ROS affect mitochondrial duty cycle, run length, and the percentage of moving mitochondria *in vivo*. **A**, Knockdown of Nox gives a reduction in duty cycle with an increase of pause time and a decrease of moving time in both directions. Knockdown of Duox decreases retrograde duty cycle and increases pause time in anterograde direction. **B**, Run length is reduced by knockdown of Duox or Nox in both directions. **C**, Knockdown of Duox shows a decrease of the percentage of retrograde moving mitochondria. Knockdown of Nox shows an increase of the percentage of paused mitochondria and a decrease of the percentage of anterograde moving mitochondria. **D**, Mitochondrial density is comparable to control with knockdown of Duox or Nox. Number of larvae is shown on bars. Error bars indicate mean \pm SEM. Significance is determined by one-way ANOVA with Bonferroni's post-test. * $p < 0.05$, ** $p < 0.01$, and *** $p < 0.001$.

3.5 Mitochondrial fission-fusion balance and inner membrane potential are both diminished by ROS treatment

3.5.1 Mitochondrial length is reduced under oxidative stress conditions

Different elements of the mitochondrial life cycle including mitochondrial length, membrane potential, transport, and mitophagy are highly interrelated. For example, mutation of mitochondrial fusion protein, mitofusin 2, both induces mitochondrial fragmentation and reduces mitochondrial transport (Verstreken et al., 2005; Baloh et al., 2007; Misko et al., 2010; Misko et al., 2012).

To determine whether disrupted mitochondrial transport caused by ROS is accompanied by changes in fission-fusion steady state, mitochondrial length was examined after H₂O₂ treatment for 1 hr. After treatment, mitochondrial shapes became more rounded and length was reduced (Fig. 3.8A, B), indicating that excess ROS affect the mitochondrial fission-fusion steady state by reducing mitochondrial length. In addition, overexpression of SOD1 or SOD2 fully rescued the reduced mitochondrial length (Fig. 3.8A, B), further confirming that these morphological defects are produced by oxidative stress.

3.5.2 Mitochondrial membrane potential is reduced under oxidative stress conditions

Mitochondrial membrane potential and mitochondrial transport may be correlated (Miller and Sheetz, 2004; Saxton and Hollenbeck, 2012). Thus, I also examined whether ROS-induced inhibition of mitochondrial transport was accompanied by diminished membrane potential. To test this, mitochondria were stained with TMRM and mitochondrial membrane potential was expressed as the intensity ratio of mitochondrial and cytosolic TMRM fluorescence.

Under oxidative stress conditions, mitochondrial membrane potential was reduced, indicating that the mitochondrial metabolic state is disrupted (Fig. 3.8A, C). However, SOD1 or SOD2 overexpression did not rescue the diminished mitochondrial membrane potential caused by ROS (Fig. 3.8A, C), suggesting that SOD overexpression is not sufficient to rescue these defects. It is possible that other ROS

scavengers, including glutathione peroxidase or catalase, might be required to restore the normal metabolic state. Altogether, these data indicate that oxidative stress produces imbalances in mitochondrial fission-fusion and metabolic state, and suggest that mitochondrial transport, fission-fusion, and membrane potential are closely interrelated in the response to ROS.

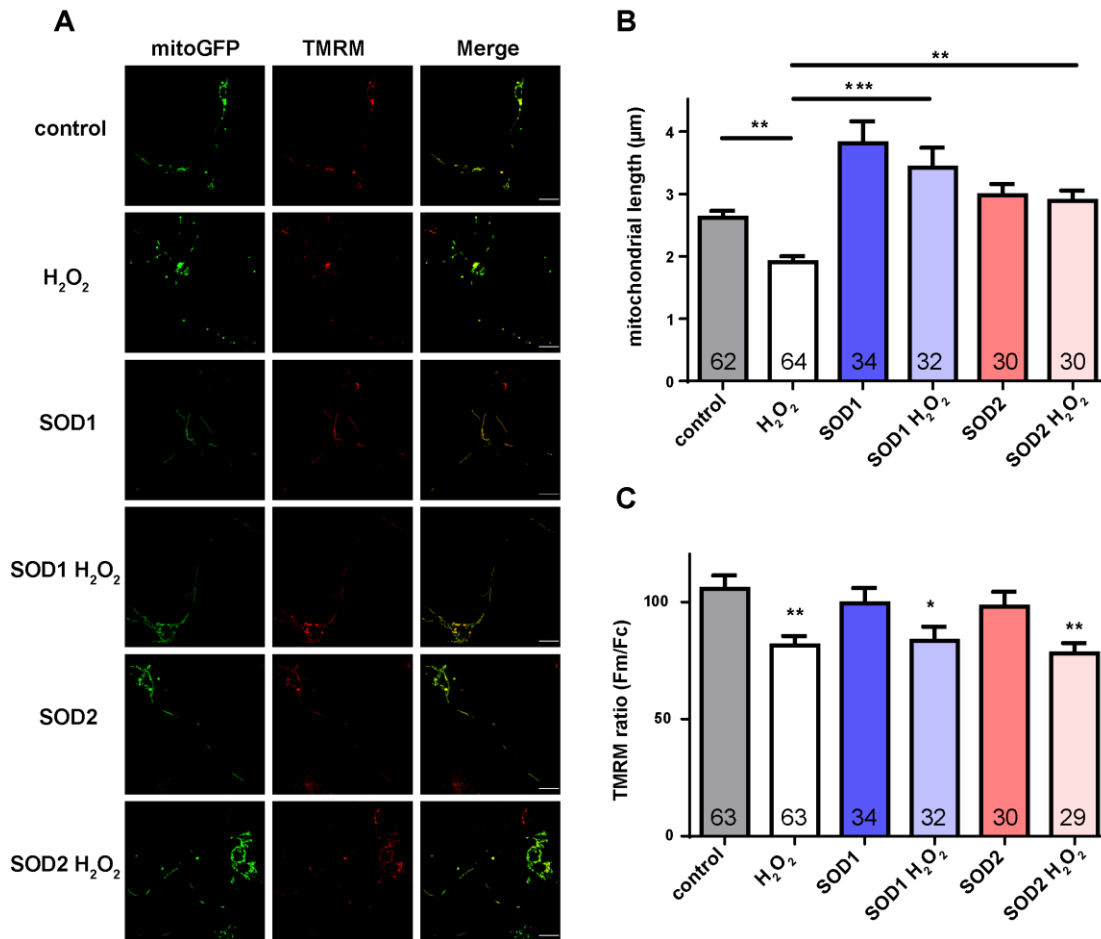


Figure 3.8. Mitochondrial length and membrane potential are reduced in response to ROS. **A**, Representative images of mitochondrial length and membrane potential. Mitochondrial lengths are measured using mitoGFP signals and mitochondrial membrane potential is measured using TMRM staining by the intensity ratio of mitochondrial fluorescence and cytosolic fluorescence. Scale bars indicate 10 µm. **B**, Quantitative results of mitochondrial length. ROS treatment shows a decrease of mitochondrial length, which is rescued by SOD1 or SOD2 overexpression. **C**, Quantitative results of mitochondrial membrane potential. Mitochondrial membrane potential is reduced under oxidative stress conditions. SOD1 or SOD2 overexpression does not rescue these defects. Number of cells is shown on bars. Error bars indicate mean ± SEM. Significance is determined by one-way ANOVA with Bonferroni's post-test. * $p < 0.05$, and *** $p < 0.001$.

3.6 ROS-induced defects of mitochondrial transport are caused by Ca²⁺ levels

3.6.1 ROS elevate intracellular Ca²⁺ levels

Mitochondrial transport is inhibited by Ca²⁺ levels. Mitochondria have Miro proteins that contain Ca²⁺ binding EF-domain. When Ca²⁺ levels increase, Ca²⁺ binds the EF-domain on Miro and mitochondrial transport is inhibited (Macaskill et al., 2009; Wang and Schwarz, 2009; Chen and Sheng, 2013). In addition, it has been shown that Ca²⁺ and redox signaling have significant interactions. ROS could stimulate Ca²⁺ influx via different Ca²⁺ channels including voltage-dependent Ca²⁺ channels or channels involved in receptor-induced Ca²⁺ signals (Hidalgo and Donoso, 2008; Gleichmann and Mattson, 2011; Görlach et al., 2015). Thus, the defects of mitochondrial transport caused by oxidative stress might be regulated by elevated Ca²⁺ levels.

To determine whether the defects in mitochondrial transport in response to ROS are related to intracellular Ca²⁺ levels, Ca²⁺ levels were measured using the genetically-encoded calcium indicator GCaMP6 which I expressed in motor neurons using the D42-Gal4 driver (Chen et al., 2013). After 1 hr H₂O₂ treatment, cells showed about 50% higher GCaMP6 intensity compared to controls (Fig. 3.9), indicating that ROS do indeed induce increased intracellular Ca²⁺ levels. I also treated cells for a longer period with ROS and found no further increase in GCaMP intensity, consistent with the result that longer ROS treatment did not produce further reduced mitochondrial transport (Fig. 3.1C, above).

3.6.2 Elevated Ca²⁺ levels inhibit mitochondrial transport specifically

While Ca²⁺ has been shown to inhibit mitochondrial transport in different systems (Macaskill et al., 2009; Wang and Schwarz, 2009; Chen and Sheng, 2013), whether Ca²⁺ inhibits mitochondrial transport in our system is still unknown. I first artificially induced Ca²⁺ levels dramatically by treating cells with the Ca²⁺ ionophore, ionomycin (Fig. 3.9A, B), and examined both mitochondrial transport and DCV transport (Fig. 3.10A). Notably, this treatment reduced transport of mitochondria only

(Fig. 3.10B). Compared to controls, the velocity of DCV transport in ionomycin-treated cells did not show a significant difference (Fig. 3.10C).

Although mitochondrial transport was reduced in ionomycin-treated cells, Ca^{2+} levels were much higher than physiological or ROS-treated levels. To confirm that the reduction did not require a dramatic increase of Ca^{2+} levels, I treated cells with thapsigargin, an ER Ca^{2+} ATPase inhibitor that increases only intracellular Ca^{2+} levels, to mimic Ca^{2+} levels under oxidative stress (Fig. 3.9A, B). Under these conditions, the percentage of moving mitochondria was reduced to a similar level to that seen in H_2O_2 -treated cells (Fig. 3.1, 3.10D, E). In addition, the velocity of DCV transport was similar to controls (Fig. 3.10D, F), further confirming that elevated Ca^{2+} levels reduced mitochondrial transport specifically.

3.6.3 ROS-induced defects of mitochondrial transport is mediated by Ca^{2+} levels

The results reported in sections 3.6.1 and 3.6.2 indicate that ROS increase intracellular Ca^{2+} , and that artificially increased Ca^{2+} levels reduce mitochondrial transport, supporting the hypothesis that ROS produce defects of mitochondrial transport through the elevation of Ca^{2+} levels. To test further the hypothesis, the ROS-induced increase in Ca^{2+} levels was stymied by incubating cells in Ca^{2+} -free medium containing EGTA. Under these conditions, I examined whether ROS-induced defects of mitochondrial transport were rescued.

Before examining transport, I first confirmed that EGTA treatment did reduce Ca^{2+} levels, using the GCaMP6 indicator (Fig. 3.11A, B). EGTA treatment alone did not decrease intracellular Ca^{2+} levels, but it rescued the ROS-induced Ca^{2+} levels to physiological levels (Fig. 3.11A, B). Next, I examined mitochondrial transport under these conditions. Under ROS treatment with Ca^{2+} levels held to control levels, the percentage of moving mitochondria was similar to controls (Fig. 3.11C, D). In addition, the ROS-reduced percentage of moving mitochondria was partially rescued, indicating that ROS-induced defects of mitochondrial transport are mediated in large part by the elevation of Ca^{2+} levels.

3.6.4 Ca^{2+} homeostasis is required for mitochondrial transport

Since EGTA treatment, rescuing Ca^{2+} to physiological levels, rescued ROS-induced defects of mitochondrial transport, I wondered whether further reduction of Ca^{2+} levels could increase mitochondrial transport. To examine this, cells were treated with both EGTA and BAPTA-AM, a Ca^{2+} chelator that can cross the cell membrane, to further reduce intracellular Ca^{2+} levels (Fig. 3.11E, F). First, I showed that cells incubated with H_2O_2 , EGTA, and BAPTA-AM also showed reduced Ca^{2+} levels compared to controls (Fig. 3.11E, F), indicating that combined intracellular and extracellular Ca^{2+} chelation indeed reduces Ca^{2+} levels lower than physiological levels.

Surprisingly, cells with Ca^{2+} levels lower than physiological levels also showed unexpected defects in mitochondrial transport. The percentage of moving mitochondria was reduced under these conditions (Fig. 3.11G, H), indicating that lower Ca^{2+} levels also inhibit mitochondrial transport.

Altogether, these data suggest that Ca^{2+} homeostasis is required for mitochondrial transport, and that modulation of Ca^{2+} levels mediates the effect of ROS on mitochondria.

3.6.5 Ca^{2+} homeostasis is required for mitochondrial transport

Mitochondrial fission-fusion steady state has been shown to correlate to mitochondrial transport. Disruption of the fission-fusion steady state by mutation of mitochondrial fusion protein, Mitofusin, produces mitochondrial fragment and reduced mitochondrial movement (Verstreken et al., 2005; Baloh et al., 2007; Misko et al., 2010; Misko et al., 2012). I have shown that oxidative stress reduced both mitochondrial transport and length (Fig. 3.8A, B). To examine whether the Ca^{2+} -induced defects of mitochondrial transport are also related to mitochondrial length control, I measured the mitochondrial length under the conditions described in section 3.6.4.

I found that the mitochondrial length reduction caused by oxidative stress was rescued by EGTA treatment but was not rescued by combined BAPTA-AM and EGTA treatment (Fig. 3.12), which was consistent with the transport data (Fig. 3.11D,

H). These results indicate that either higher or lower Ca^{2+} levels affect mitochondrial length. All together, these data indicate that Ca^{2+} homeostasis is important for both mitochondrial transport and mitochondrial fission-fusion steady state.

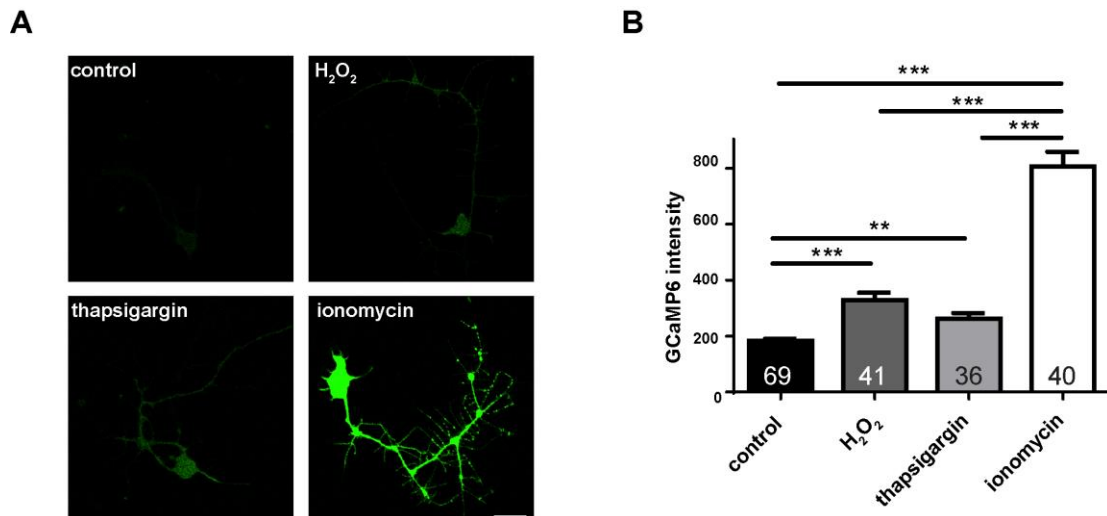


Figure 3.9. Elevated Ca^{2+} levels are induced by H_2O_2 . **A**, Representative Ca^{2+} imaging with H_2O_2 , thapsigargin, or ionomycin treatment are measured by the intensity of GCaMP6 indicator. Scale bars indicate $10\ \mu\text{m}$. **B**, Quantitative results from **(A)**. H_2O_2 or thapsigargin treatment produces an increase of Ca^{2+} levels of similar extent. Ionomycin treatment produces a large increase compared to controls. Number of cells is shown on bars. Each plate contains at least 5 cells. Error bars indicate mean \pm SEM. Significance is determined by one-way ANOVA with Bonferroni's post-test. ** $p < 0.01$, and *** $p < 0.001$.

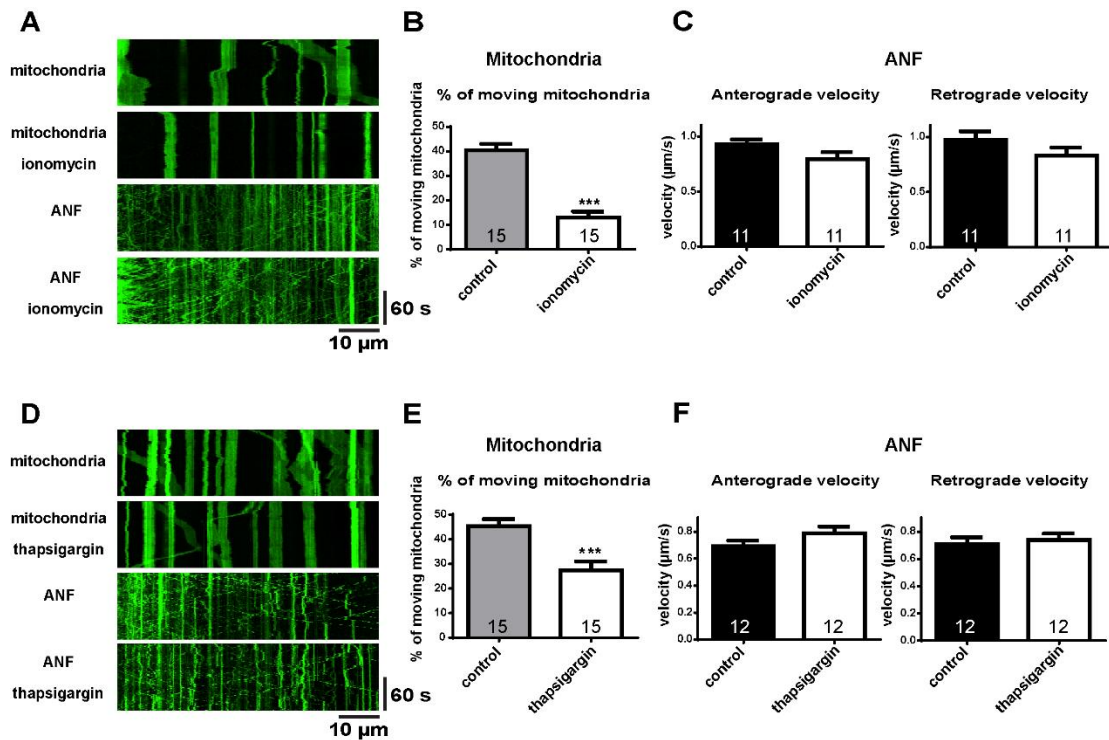


Figure 3.10. Elevated Ca^{2+} levels inhibit mitochondrial transport. **A**, Representative kymographs of axonal transport of mitochondria or DCVs under ionomycin treatment. Anterograde transport is toward the right; retrograde transport is toward the left. **B**, The percentage of moving mitochondria is dramatically reduced by ionomycin treatment. **C**, Velocity of DCV transport is not affected by ionomycin. **D**, Representative kymographs of axonal transport of mitochondria or DCVs with thapsigargin treatment. **E**, The percentage of moving mitochondria is reduced by thapsigargin treatment, but the effect is not as large as ionomycin treatment. **F**, Velocity of DCV transport is not affected by thapsigargin. Number of cells is shown on bars. Error bars indicate mean \pm SEM. Significance is determined by paired Student's t-test. *** $p < 0.001$.

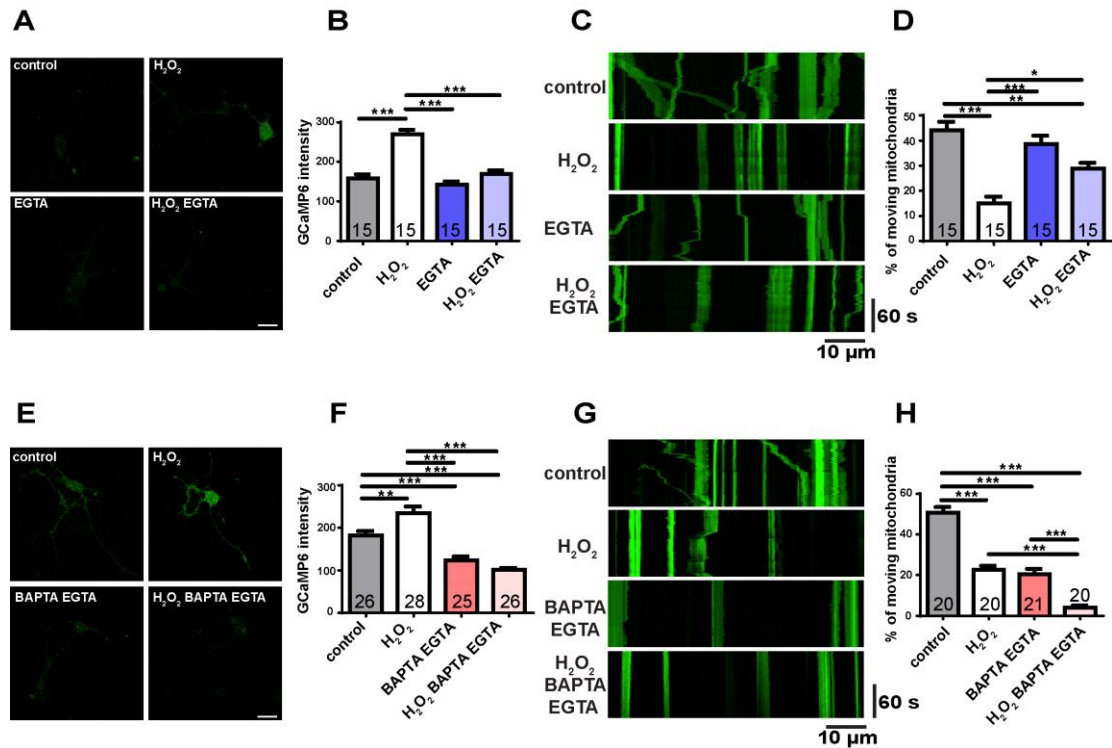


Figure 3.11. Ca²⁺ homeostasis is required for normal mitochondrial transport. **A**, Representative Ca²⁺ imaging with H₂O₂ or EGTA treatment are measured by the intensity of GCaMP6 indicator. Scale bars indicate 10 μ m. **B**, Quantitative results from (A). Elevated Ca²⁺ levels induced by H₂O₂ are rescued by EGTA treatment. EGTA alone does not affect intracellular Ca²⁺ levels. **C**, Representative kymographs of mitochondrial transport under H₂O₂ or EGTA treatment. Anterograde transport is toward the right; retrograde transport is toward the left. **D**, The reduced percentage of moving mitochondria by H₂O₂ is partially rescued by EGTA. EGTA alone does not affect mitochondrial transport. **E**, Representative Ca²⁺ imaging with H₂O₂ or EGTA/BAPTA treatment are measured by the intensity of GCaMP6 indicator. Scale bars indicate 10 μ m. **F**, Quantitative results from (E). Ca²⁺ levels are increased by H₂O₂ but reduced with EGTA/BAPTA treatment. **G**, Representative kymographs of mitochondrial transport with H₂O₂ or EGTA/BAPTA treatment. Anterograde transport is toward the right; retrograde transport is toward the left. **H**, EGTA/BAPTA treatment produces a decrease of mitochondrial transport. The reduced percentage of moving mitochondria by H₂O₂ is further reduced by EGTA/BAPTA treatment. Error bars indicate mean \pm SEM. Number of cells is shown on bars. Significance is determined by one-way ANOVA with Bonferroni's post-test. * $p < 0.05$, ** $p < 0.01$, and *** $p < 0.001$.

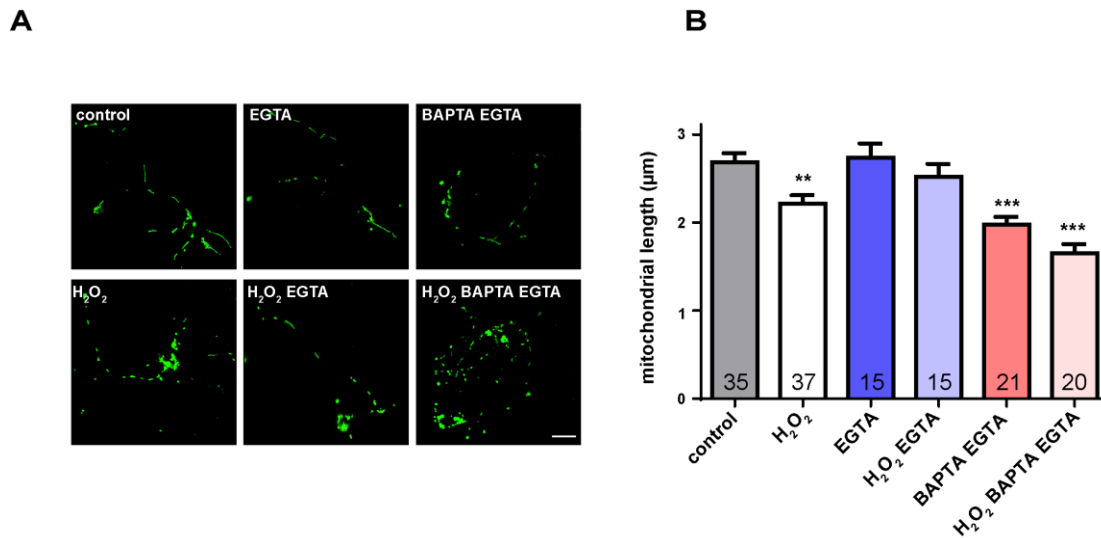


Figure 3.12. Ca²⁺ homeostasis is required for normal mitochondrial morphology. **A**, Representative images of mitochondrial length measured using the mitoGFP signal. Scale bars indicate 10 μm. **B**, H₂O₂ and/or EGTA/BAPTA reduce mitochondrial length, which is consistent with the results of mitochondrial transport (**Fig. 3.11D, H**). Error bars indicate mean ± SEM. Number of cells is shown on bars. Significance is determined by one-way ANOVA with Bonferroni's post-test. **p < 0.01, and ***p < 0.001, compared to the control group.

3.7 The JNK pathway plays a role in the regulation of mitochondrial transport in axons by oxidative stress

It seems clear so far that the effects of ROS exposure on mitochondrial transport are probably not due simply to generalized oxidative damage, but probably involve an imbalance of normal ROS-based signaling. To investigate this further, I examined the JNK pathway, which is activated under oxidative stress conditions (Shen and Liu, 2006; Son et al., 2013) and involved in regulating axonal transport (Morfini et al., 2006; Morfini et al., 2009). Previous studies have shown that activated JNK pathway reduces axonal transport in squid axoplasm via the phosphorylation of kinesin heavy chain (Morfini et al., 2006). Thus, I hypothesized that ROS induced defects of mitochondrial transport involve the activation of the JNK pathway.

3.7.1 Mitochondrial transport is not affected by JNK signaling *in vitro*

To test this hypothesis, I activated the JNK pathway by overexpressing Hep^{B2} (JNK kinase in *Drosophila*), or down-regulated it by RNAi knockdown of Bsk (JNK in *Drosophila*). I expected that mitochondrial transport would increase with the down-regulation of the JNK pathway and decrease with the activation of the JNK pathway.

However, when I examined the percentage of moving vs. persistently stationary mitochondria in *Drosophila* neurons *in vitro*, I did not find significant differences between control and JNK activation/down-regulation under basal conditions. In addition, under oxidative stress, the percentage of moving mitochondria was reduced in both overexpression and knockdown animals (Fig. 3.13), suggesting that JNK signaling is not involved in the regulation of mitochondrial transport in response to ROS *in vitro*.

3.7.2 The JNK signaling pathway plays a role in the regulation of mitochondrial transport under oxidative stress *in vivo*

Previous studies have shown that the JNK pathway affected axonal transport mainly in anterograde direction (Morfini et al., 2006; Morfini et al., 2009). It is possible that the percentage of moving mitochondria *in vitro* is not high enough to

reveal directional defects. To determine more accurately whether the JNK pathway affected mitochondrial transport only in one direction, I examined more detailed parameters *in vivo*.

First, I examined the gross transport indicator, flux. In the anterograde direction, flux was reduced by JNK activation. In addition, under oxidative stress conditions, flux was not further reduced by JNK activation (Fig. 3.14A, B), implying that the JNK pathway is downstream of the effects of oxidative stress on anterograde mitochondrial flux. Furthermore, the ROS-induced defects in anterograde flux were partially rescued by JNK knockdown (Fig. 3.14A, B), also suggesting that the JNK pathway plays a role in mediating the inhibition of mitochondrial anterograde transport by oxidative stress. To analyze which parameters resulted in the reduced flux, velocity, duty cycle, run length, and the percentage of mitochondria were examined. Similar to the flux results, activation of the JNK pathway reduced mitochondrial velocity (Fig. 3.14A, C), and down-regulation of JNK partially rescued the reduced velocity caused by ROS treatment in the anterograde direction (Fig. 3.14A, C), indicating that the velocity is one of the factors contributing to the difference in flux.

However, for retrograde movement, either activation or down-regulation of the JNK pathway produced a decrease of mitochondrial flux and velocity under oxidative stress conditions (Fig. 3.14A-C), suggesting that other mechanisms might be responsible for the regulation of the effects of oxidative stress on retrograde mitochondrial transport. Thus, although the regulatory systems are directionally differentiated, optimal levels of activity in the JNK pathway are important for mitochondrial transport in both directions. Other parameters of mitochondrial motility such as duty cycles, run length, and the percentage of moving mitochondria were only modestly affected by either overexpression or knockdown of the JNK pathway (Fig. 3.15), indicating that JNK signaling mediates mitochondrial flux in response to ROS mainly via effects on velocity.

3.7.3 Activation of the JNK pathway shows a decrease of mitochondrial density

In addition to transport parameters, mitochondrial density was examined under these conditions (Fig. 3.16). Surprisingly, activation of the JNK pathway produced a decrease in axonal mitochondrial density (Fig. 3.16). This reduced density did not further decrease under oxidative stress conditions (Fig. 3.16), suggesting that the activation of the JNK pathway might reduce mitochondrial biogenesis and/or increase mitochondrial degradation. In addition, the reduced density also implicates another component of the mitochondrial life cycle that could contribute to the difference in the flux.

In sum, these results demonstrated that the JNK pathway, activated by oxidative stress, plays a role in the regulation of mitochondrial transport in the anterograde direction, consistent with the role of JNK in the regulation of anterograde-specific axonal transport. In addition to mitochondrial transport, the JNK pathway also plays a role in the regulation of mitochondrial density, suggesting the important role of JNK signaling on mitochondrial quality control.

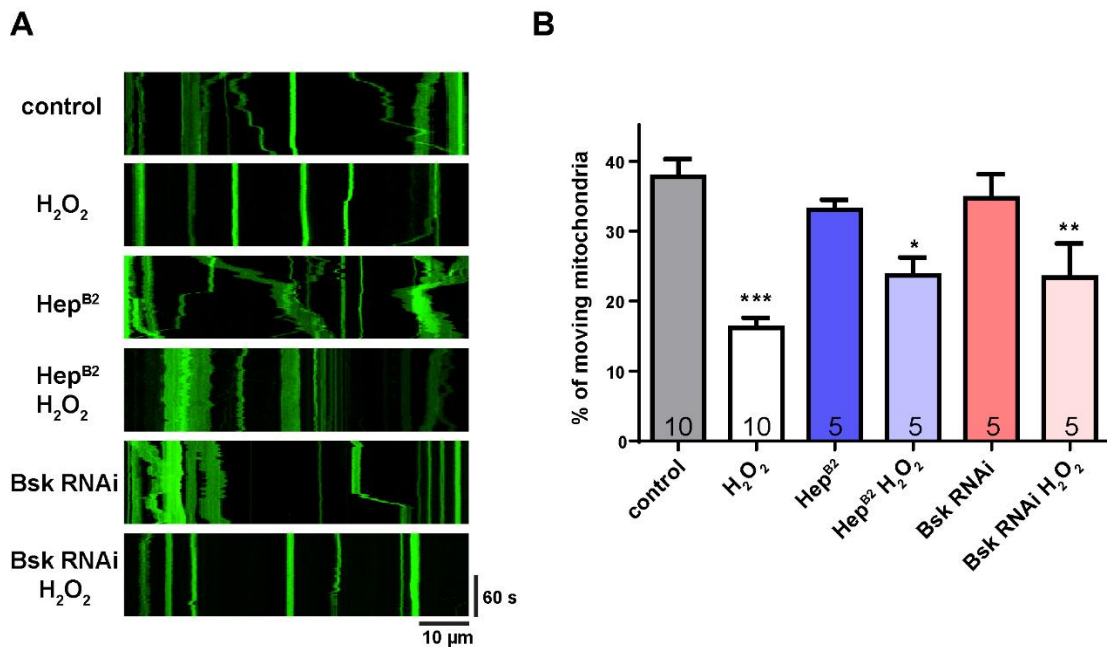


Figure 3.13. The percentage of moving mitochondria is not affected by the JNK pathway under oxidative stress conditions *in vitro*. **A**, Representative kymographs of mitochondrial transport with overexpression of JNK kinase (Hep^{B2}) or knockdown of JNK (Bsk RNAi) in response to H₂O₂. Anterograde transport is toward the right; retrograde transport is toward the left. **B**, The percentage of moving mitochondria is reduced with H₂O₂ treatment. Either overexpression of JNK kinase (Hep^{B2}) or knockdown of JNK (Bsk RNAi) does not rescue the defects. Number of plates is shown on bars. Each plate contains at least 5 cells. Error bars indicate mean \pm SEM. Significance is determined by one-way ANOVA with Bonferroni's post-test. * $p < 0.05$, ** $p < 0.01$, and *** $p < 0.001$, compared to the control group.

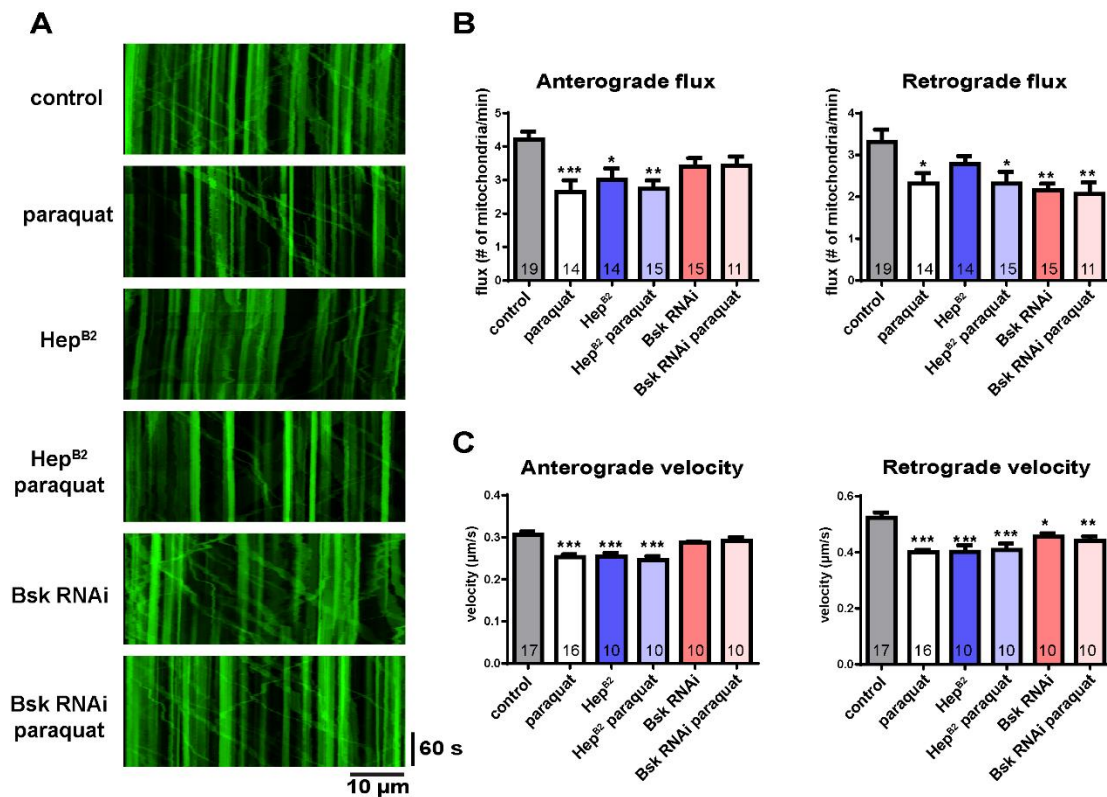


Figure 3.14. The JNK pathway plays a role in the regulation of mitochondrial transport *in vivo*. **A**, Representative kymographs of mitochondrial transport with overexpression of JNK kinase (Hep^{B2}) or knockdown of JNK (Bsk RNAi) in response to paraquat. Anterograde transport is toward the right; retrograde transport is toward the left. **B**, Paraquat and/or overexpression of Hep^{B2} produce a decrease in mitochondrial flux anterogradely. Knockdown of Bsk partially rescues the effect of paraquat. Both overexpression of Hep^{B2} and knockdown of Bsk reduce retrograde flux. **C**, Anterograde velocity is reduced by paraquat or overexpression of Hep^{B2}, and knockdown of Bsk partially rescues the effect of paraquat. Retrograde velocity is reduced in both overexpression of Hep^{B2} and knockdown of Bsk. Number of larvae is shown on bars. Error bars indicate mean \pm SEM. Significance is determined by one-way ANOVA with Bonferroni's post-test. * $p < 0.05$, ** $p < 0.01$, and *** $p < 0.001$.

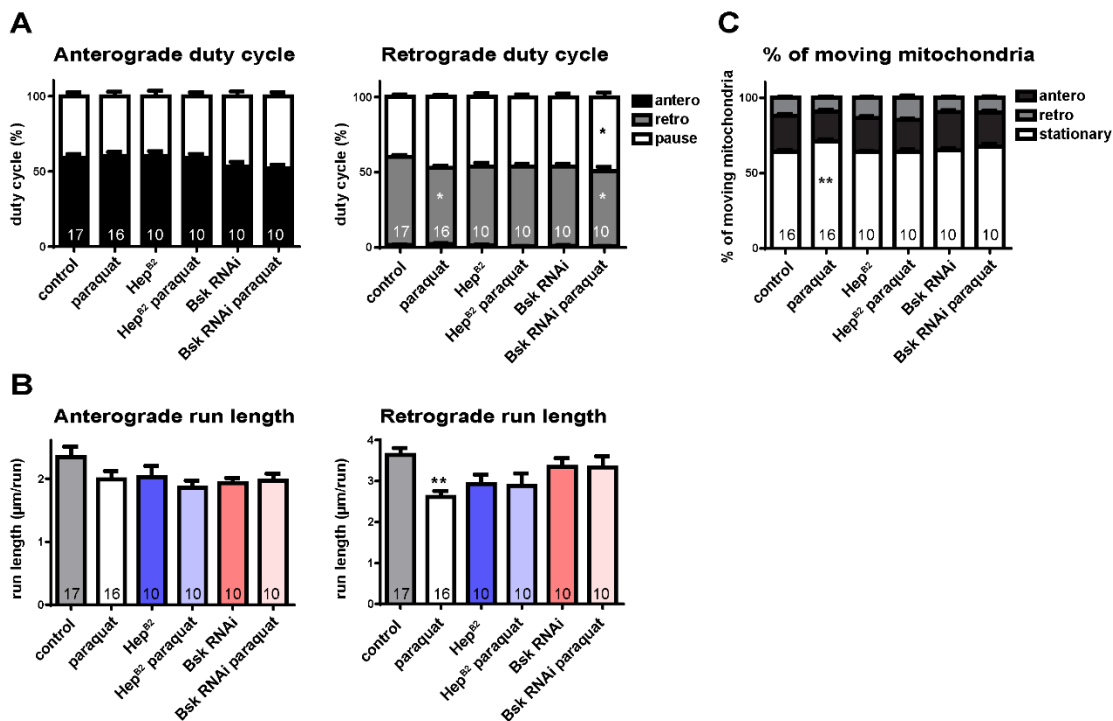


Figure 3.15. Mitochondrial duty cycle, run length, and percentage of moving are not affected by the JNK pathway *in vivo*. **A**, Paraquat treatment shows slightly reduction in retrograde duty cycle with a decrease of moving time; Knockdown of Bsk in response to paraquat shows a slightly increase of pause and a decrease of moving time. **B**, Retrograde run length is modestly reduced by paraquat treatment. Either overexpression of Hep^{B2} or knockdown of Bsk does not show significant difference compared to controls. **C**, Paraquat treatment shows an increase of the percentage of stationary mitochondria, while either overexpression of Hep^{B2} or knockdown of Bsk does not show significant difference. Number of larvae is shown on bars. Error bars indicate mean \pm SEM. Significance is determined by one-way ANOVA with Bonferroni's post-test. * $p < 0.05$ and ** $p < 0.01$.

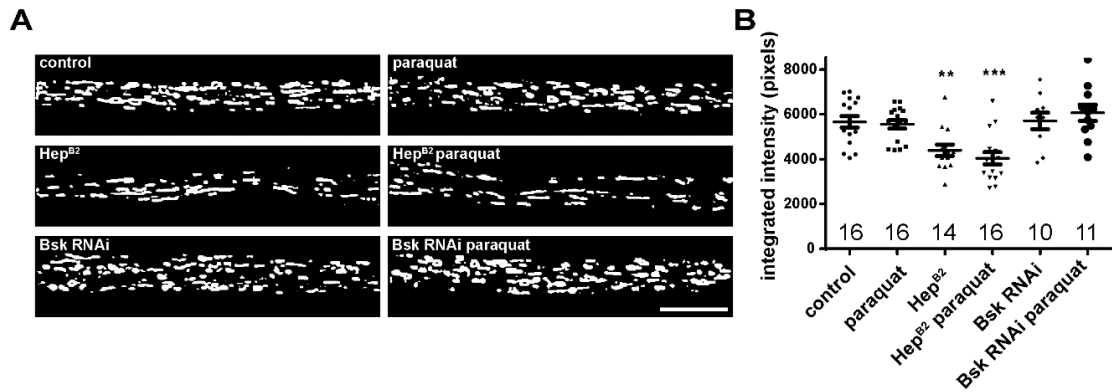


Figure 3.16. Activation of the JNK pathway shows a decrease of mitochondrial density. **A**, Representative binary images of mitochondrial density with overexpression of Hep^{B2} or knockdown of Bsk in response to paraquat treatment. **B**, Overexpression of Hep^{B2} shows reduced integrated mitochondrial density compared to the control. Number of larvae is shown on bars. Error bars indicate mean \pm SEM. Significance is determined by one-way ANOVA with Bonferroni's post-test. ** $p < 0.01$ and *** $p < 0.001$.

3.8 Activation or down-regulation of the JNK pathway does not affect intracellular Ca²⁺ levels

Previous results provide evidence that ROS-induced defects of mitochondrial transport are mediated by Ca²⁺ and the JNK pathway (Section 3.6 and 3.7, above). However, it is not clear how Ca²⁺ and the JNK pathway might interact in the ROS regulation of mitochondrial transport. To determine whether the JNK pathway is upstream of Ca²⁺ signaling, I examined intracellular Ca²⁺ levels in primary neurons expressing GCaMP6 with either genetic activation or down-regulation of the JNK pathway in motor neurons.

Similar to previous results, these neurons showed about 50% higher GCaMP6 intensity compared to controls after H₂O₂ treatment (Fig. 3.9 and 3.17). However, neither activation nor down-regulation of the JNK pathway affects intracellular Ca²⁺ levels (Fig. 3.17B), indicating that the JNK pathway is not upstream of the Ca²⁺ signaling. This suggests that the defects of mitochondrial transport caused by ROS-induced Ca²⁺ levels are not mediated by the JNK pathway, and also raises the possibility that Ca²⁺ and JNK signaling regulate mitochondrial transport in parallel.

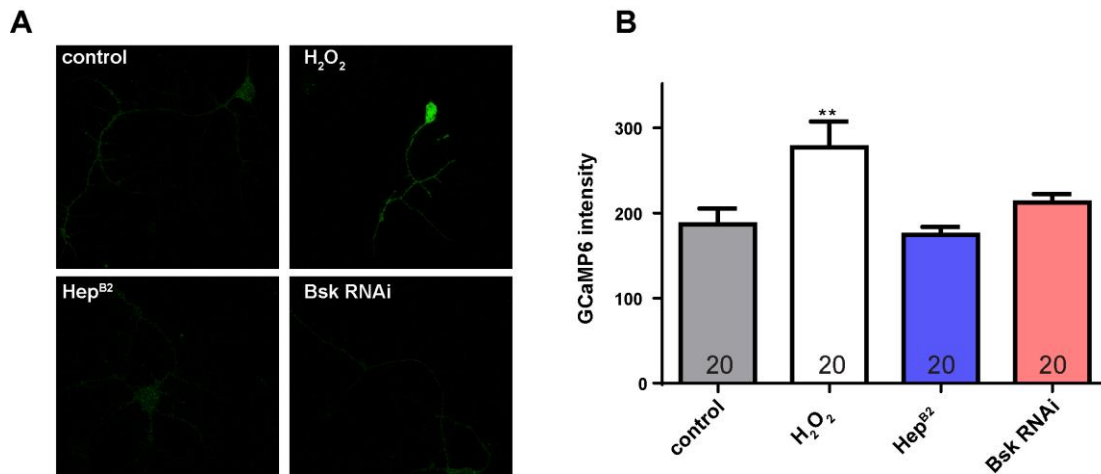


Figure 3.17 Activation or down-regulation of the JNK pathway does not affect intracellular Ca^{2+} levels. **A**, Representative Ca^{2+} imaging with overexpression of Hep^{B2} or down-regulation of Bsk; Ca^{2+} is measured by the intensity of GCaMP6 fluorescence. Scale bars indicate 10 μm . **B**, Quantitative results from (A). H_2O_2 treatment produces an increase of Ca^{2+} levels, but neither overexpression of Hep^{B2} nor down-regulation of Bsk produces a significant difference in the result. Number of plates is shown on bars. Each plate contains at least 5 cells. Error bars indicate mean \pm SEM. Significance is determined by one-way ANOVA with Bonferroni's post-test. ** $p < 0.01$.

CHAPTER 4. DISCUSSION

Although excess ROS produce varied damage to macromolecules, organelles and cells (Brookes et al., 2004; Court and Coleman, 2012), they are probably more in their important roles as signaling molecules at physiological levels (Lambeth and Neish, 2014; Nayernia et al., 2014). Mitochondria are the major source of ROS (Brookes et al., 2004; Bhat et al., 2015; Genova and Lenaz, 2015) and also are damaged by them: since ROS have been shown to affect mitochondrial transport, fission-fusion, and mitophagy *in vitro* (Jendrach et al., 2008; Fan et al., 2010; Fang et al., 2012; Frank et al., 2012), it is important to elucidate the underlying mechanisms linking these effects. In this study, I have focused on the relationship between ROS and mitochondrial transport, and have demonstrated fundamental mechanistic connections between these two. I find that: 1) ROS specifically reduce mitochondrial transport both *in vitro* and *in vivo*, and produce a decrease of mitochondrial length and membrane potential; 2) In addition to excess ROS, the reduction of physiological ROS levels by knockdown of the Nox family also induces defects in mitochondrial transport. 3) Excess ROS disturb neuronal Ca^{2+} homeostasis, increasing Ca^{2+} levels, which in turn inhibit mitochondrial transport and reduce mitochondrial length; 4) ROS-induced defects of mitochondrial transport are mediated by a signaling pathway. The JNK pathway in particular plays a role in the regulation of anterograde transport in the presence of excess ROS.

4.1 Mitochondrial transport is preferentially affected by ROS

Mitochondrial axonal transport is reduced in the presence of excess ROS both *in vitro* and *in vivo*, primarily via reduced organelle flux and velocity (Fig. 3.1 – 3.3). More important, ROS preferentially affect mitochondria, since the transport of DCVs is barely affected under oxidative stress conditions (Fig. 3.4 and 3.5). This is

consistent with a previous *in vitro* study that though mitochondria and Golgi-derived vesicles show reduced mobility by ROS, mitochondrial transport is preferentially affected (Fang et al., 2012). Based on these studies, I propose that among the axonal transport cargoes, mitochondria are a prime target of ROS.

What possible mechanism could explain the specific sensitivity of mitochondrial transport to ROS? Unlike other axonal vesicles and organelles, mitochondria are linked to kinesin motor proteins via a complex of a mitochondrial Rho GTPase, Miro, and the adapter protein, Milton. When the intracellular Ca^{2+} levels increase, Ca^{2+} binds to the two EF-domains of Miro, causing a conformational change that disrupts the ability of kinesin to move the mitochondria but, interestingly, inhibiting both directions of mitochondrial transport (Macaskill et al., 2009; Wang and Schwarz, 2009; Chen and Sheng, 2013). This regulation by Ca^{2+} is a major difference in the axonal transport of mitochondria versus other organelles, and prompted one of my areas of experimentation.

The JNK pathway might also affect mitochondrial transport more specifically. While several studies suggest that the JNK pathway affects general axonal transport via phosphorylation of kinesin or superior cervical ganglion 10 (SCG10), a microtubule binding protein in axons (Morfini et al., 2006; Shin et al., 2012), other studies suggest that there is a regulatory difference in transport between mitochondria and other cargoes. For example, mutants in APLIP1, the *Drosophila* homologue of a JNK-interacting protein (JIP), reduce general transport of cargoes in both directions, but reduce mitochondrial transport only in the retrograde direction, suggesting a unique regulatory feature of mitochondrial transport (Horiuchi et al., 2005). In addition, the alpha subunit of the heterotrimeric G protein G12 ($\text{G}\alpha 12$) has been shown to stimulate JNK activity (Nagao et al., 1999); this is notable because $\text{G}\alpha 12$ is targeted to mitochondria and itself affects mitochondrial motility (Andreeva et al., 2008). These studies suggest the possibility that the JNK pathway has some specific effects on axonal transport of mitochondria.

4.2 ROS homeostasis is required for mitochondrial transport

In addition to elucidating the effects of excess ROS on mitochondrial transport, I have also provided evidence that ROS levels reduced below physiological conditions by knockdown of the Nox family also impaired mitochondrial transport (Fig. 3.6 and 3.7). Interestingly, though knockdown of Nox and Duox reduces mitochondrial transport, the detailed motility phenotypes are different. Knockdown of Nox produces the general reduction in different parameters of transport in both directions, whereas knockdown of Duox affects general retrograde transport but only anterograde run length (Fig. 3.6 and 3.7). This suggests unique different regulatory features of mitochondrial transport. More specifically, Nox and Duox are both required for retrograde transport. However, Nox might play more important roles in the anterograde transport, since knockdown of Nox affects all parameters of anterograde transport. Knockdown of Duox only affect run length, suggesting that mitochondria spend more runs to reach the destination. Thus, it is possible that the role of Duox in the anterograde transport is to maintain efficient, continuous movement. It has been shown that myosin motors compete with microtubule-based motors and halt mitochondrial movement (Pathak et al., 2010). Whether Duox prevents competition between myosin and microtubule-based motors remains for further investigation.

What could explain the effects of Nox and Duox downregulation on mitochondrial transport? Since their main function is ROS production, knockdown of these enzymes reduces ROS levels below physiological levels. Under normal physiological conditions, ROS serve as important signaling molecules and regulate numerous cellular functions (Lambeth and Neish, 2014; Nayernia et al., 2014) (Section 1.2.2.2, above). Thus, it should not be surprising that knockdown of Nox and Duox impairs mitochondrial transport. Are there any signaling pathways or mechanisms that can be related to the impairment of mitochondrial transport by low ROS? One candidate is the PI3K/Akt/GSK3 β pathway. This pathway has been shown to be activated by Nox-released ROS (Nakanishi et al., 2014) and to stimulate mitochondrial transport (Chen et al., 2007). Thus, knockdown of Nox family, which reduces ROS levels, may be impairing mitochondrial transport possibly through the inactivation of PI3K/Akt/GSK3 β pathway.

4.3 The ROS-induced effects on mitochondrial transport is mediated via changes of Ca²⁺ levels

As mentioned above (Section 1.1.4.1 and 4.1), cytosolic Ca²⁺ regulates mitochondrial transport. Here I have shown that excess ROS do increase Ca²⁺ levels (Fig. 3.9) and that Ca²⁺ chelation by EGTA rescues the defects of mitochondrial transport (Fig. 3.11A - D), consistent with Ca²⁺ inhibition of mitochondrial transport (Macaskill et al., 2009; Wang and Schwarz, 2009; Chen and Sheng, 2013).

It is notable that H₂O₂-induced high Ca²⁺ levels are rescued to physiological levels by the extracellular Ca²⁺ chelator EGTA (Fig. 3.11A and B), suggesting that the ROS-induced Ca²⁺ increase is caused by the Ca²⁺ influx from the extracellular environment. A likely explanation involves several Ca²⁺ channels on the plasma membrane that are regulated by redox balance (Görlach et al., 2015). For example, H₂O₂ treatment has been shown to induce Ca²⁺ influx through L-type or T-type voltage-dependent Ca²⁺ channels (VDCC) (Hudasek et al., 2004; Tabet et al., 2004) (Section 1.2.4.1). In addition to VDCC, ROS are known to stimulate Ca²⁺ influx through channels involved in receptor-induced Ca²⁺ signals such as transient receptor potential (TRP) channels and store-operated Ca²⁺ channels (SOC) mediated by Orai channel proteins (Hara et al., 2002; Grupe et al., 2010) (Section 1.2.4.1). Thus, I propose that elevated Ca²⁺ levels are induced by ROS through stimulating one or more Ca²⁺ channels on the plasma membrane.

While most studies have focused on the effects of elevated Ca²⁺ levels on mitochondrial transport (Macaskill et al., 2009; Wang and Schwarz, 2009; Chen and Sheng, 2013; Nguyen et al., 2014; Stephen et al., 2015), I found that experimentally decreased intracellular Ca²⁺ levels also produce a decrease of mitochondrial transport (Fig. 3.11E - H), indicating that normal Ca²⁺ homeostasis is important for mitochondrial transport. This might explain a previous study showing that the defects of mitochondrial transport induced by MPP⁺ are rescued by thio-antioxidant N-acetylcystein (NAC; precursor of glutathione), whereas they are not rescued by a high concentration of EGTA (2.5 mM). The latter probably reduced Ca²⁺ levels below physiological conditions (Kim-Han et al., 2011).

4.4 The ROS-induced defects of mitochondrial transport is mediated by the signaling pathway

Although Ca^{2+} levels regulate mitochondrial transport, I found that the defects of mitochondrial transport was not fully rescued by Ca^{2+} chelation (Fig. 3.11A - D), suggesting that other factors might be involved in ROS regulation of mitochondrial transport. Indeed, several signaling pathways have been shown to regulate axonal transport. Axonal mitochondria are recruited in response to Nerve Growth Factor (NGF), and this recruitment is regulated in part via the phosphoinositide 3-kinase (PI3K) (Chada and Hollenbeck, 2004). Glycogen synthase kinase 3 (GSK3) can phosphorylate kinesin light chain (Klc) to inhibit axonal transport, whereas activation of Akt, which inhibits GSK3 β , stimulates axonal mitochondrial transport (Morfini et al., 2002; Chen et al., 2007). In addition, activation of the JNK pathway phosphorylates kinesin heavy chain (Khc), reducing the interaction between kinesins and microtubules and thus inhibiting anterograde axonal transport (Morfini et al., 2006) (Section 1.1.4.2).

Here I have shown that activation of the JNK pathway reduces anterograde mitochondrial transport, and that ROS-induced defects are rescued by knockdown of the JNK pathway (Fig. 3.14). This anterograde direction-specific regulation might be caused by the phosphorylation of kinesin by JNK (Morfini et al., 2006). In the retrograde direction, knockdown of the JNK pathway decreases mitochondrial transport (Fig. 3.14). It has been shown that JIPs are required for the stress-induced JNK activation (Yasuda et al., 1999; Whitmarsh et al., 2001; Taru et al., 2002), and the mutation of the *Drosophila* JIP homologue reduces mitochondrial transport only in the retrograde direction (Horiuchi et al., 2005). Thus, disruption of the JNK pathway either by knockdown of JNK or by mutation of a *Drosophila* JIP homologue is suggested to produce retrograde-specific defects of mitochondrial transport although the mechanism remains unknown.

Although I found that the JNK pathway plays a role in the regulation of ROS-induced defects of mitochondrial transport, I have not excluded other signaling pathways from the regulation. Since ROS activate the PI3/Akt/GSK3 β pathway (Clerkin et al., 2008; Zhang et al., 2016), and activation of the PI3/Akt/GSK3 β

pathway stimulates mitochondrial transport (Chen et al., 2007), I initially did not consider this pathway as a candidate. However, two recent studies have provided evidence that overexpression of GSK3 β promotes mitochondrial transport (Llorens-Martín et al., 2011; Ogawa et al., 2016), raising the possibility that ROS might also inhibit mitochondrial transport via the PI3/Akt/GSK3 β pathway.

In addition to the effects on mitochondrial transport, activation of the JNK pathway reduces mitochondrial density (Fig. 8). This density reduction might involve upregulation of the mitophagic process. JNK has been shown to increase the expression of the mitophagy marker Bcl-2 E1B 19-KDa interacting protein 3 (BNIP3) in stressed cardiomyocytes (Chaanine et al., 2012), and to stabilize PINK1 on the mitochondrial outer membrane and subsequently activate mitophagy in stressed neuroblastoma cells (Park et al., 2016). These two results suggest that the reduced density might result from increased mitophagy produced by activated JNK.

4.5 How might Ca²⁺ and the JNK pathway interact in the ROS regulation of mitochondrial transport?

Several studies have shown that elevated intracellular Ca²⁺ levels activate the JNK pathway, and subsequently induce apoptosis or neurodegeneration (Kim and Sharma, 2004; Sato et al., 2015; Zhang et al., 2015). However, it is possible that the JNK pathway is not simply downstream of Ca²⁺ signaling in the ROS regulation of mitochondrial transport. ROS could increase Ca²⁺ influx from extracellular environment by activating Ca²⁺ channels on the plasma membrane (Hara et al., 2002; Hudasek et al., 2004; Tabet et al., 2004; Grupe et al., 2010), and activate the JNK pathway via the mediation of ASK1 (Tobiome et al., 2001; Shen and Liu, 2006; Son et al., 2013), suggesting parallel, independent pathways of ROS-activated Ca²⁺ influx and JNK signaling. Activation or down-regulation of JNK signaling does not affect Ca²⁺ levels (Fig. 3.17), supporting the parallel hypothesis. In addition, Ca²⁺ inhibits mitochondrial transport in both directions (Macaskill et al., 2009; Wang and Schwarz, 2009; Chen and Sheng, 2013), but activation of the JNK pathway inhibits mitochondrial transport in anterograde direction (Fig. 3.14). Since Ca²⁺ influx and the JNK pathway are likely activated by ROS via different mechanisms, and produce

different effects on mitochondrial transport, it is likely that they regulate mitochondrial transport in parallel.

4.6 Mitochondrial fission-fusion, metabolic state, and transport are interrelated in response to ROS

In addition to elucidating the mechanistic connection between ROS and mitochondrial transport, I have provided evidence that mitochondrial quality control is correlated with transport. I found that excess ROS and abnormal Ca^{2+} homeostasis impair mitochondrial transport (Fig. 3.1, 3.2, 3.3, 3.10, and 3.11A - D) and reduce mitochondrial length (Fig. 3.8A, B and 3.11E - J). Moreover, when mitochondrial transport is rescued either by SOD overexpression (Fig. 3.1 and 3.2) or by EGTA treatment (Fig. 3.11C, D), mitochondrial length is also rescued (Fig. 4A, B, and 6I, J). Previous studies have shown that the mutation of the mitochondrial fusion protein, Mitofusin, reduces mitochondrial length, impairs mitochondrial transport and increases Ca^{2+} levels in axons (Baloh et al., 2007; Misko et al., 2010; Misko et al., 2012), consistent with our findings. These studies together reinforce the idea that mitochondrial fission-fusion and transport are highly interrelated. This interrelationship between fission-fusion and transport is possibly related to Miro/Milton complex since Mitofusin can interact with Miro/Milton complex, and the transport defects produced by knockdown of Miro is similar to the defects caused by knockout of Mitofusin (Misko et al., 2010).

This study also provides evidence that both mitochondrial membrane potential and transport are reduced in response to ROS (Fig. 3.1 - 3.3), suggesting an association between these two. This idea is supported by other studies in neurodegenerative disease models. For example, in a *Drosophila* model of Friedreich Ataxia, reduced frataxin expression produce defects in mitochondrial transport and membrane potential; PINK1 mutation also reduces both mitochondrial transport and membrane potential. (Shidara and Hollenbeck, 2010; Devireddy et al., 2015). In addition, in mammalian primary neurons, cells treated by ATPase blocker oligomycin or by an uncoupler (FCCP or CCCP), which inhibits mitochondrial electron transport, produce a decrease in mitochondrial transport (Rintoul et al., 2003; Miller and Sheetz, 2004).

These studies show that defects in mitochondrial membrane potential are accompanied with defects in mitochondrial transport, suggesting the interplay between them.

In conclusion, I have provided evidence that oxidative stress not only affects mitochondrial morphology and membrane potential, but also reduces mitochondrial axonal transport both *in vitro* and *in vivo*. These defects in mitochondrial transport are caused by an imbalance of Ca^{2+} homeostasis and activation of the JNK pathway. Furthermore, under physiological conditions, ROS homeostasis is important for mitochondrial transport. Thus, our study establishes the mechanistic links between ROS and mitochondrial transport, and suggests a possible new and more subtle role for ROS in the induction of neurodegeneration, which will suggest new strategies to ameliorate neurodegenerative diseases.

LIST OF REFERENCES

LIST OF REFERENCES

- Aguirre J, Lambeth JD (2010) Nox enzymes from fungus to fly to fish and what they tell us about Nox function in mammals. *Free Radic Biol Med* 49:1342-1353.
- Andreeva AV, Kutuzov MA, Voyno-Yasenetskaya TA (2008) G alpha12 is targeted to the mitochondria and affects mitochondrial morphology and motility. *FASEB J* 22:2821-2831.
- Anh NT, Nishitani M, Harada S, Yamaguchi M, Kamei K (2011) Essential role of Duox in stabilization of Drosophila wing. *J Biol Chem* 286:33244-33251.
- Baloh RH, Schmidt RE, Pestronk A, Milbrandt J (2007) Altered axonal mitochondrial transport in the pathogenesis of Charcot-Marie-Tooth disease from mitofusin 2 mutations. *J Neurosci* 27:422-430.
- Barkus RV, Klyachko O, Horiuchi D, Dickson BJ, Saxton WM (2008) Identification of an axonal kinesin-3 motor for fast anterograde vesicle transport that facilitates retrograde transport of neuropeptides. *Mol Biol Cell* 19:274-283.
- Barnes KA, Samson SE, Grover AK (2000) Sarco/endoplasmic reticulum Ca²⁺-pump isoform SERCA3a is more resistant to superoxide damage than SERCA2b. *Mol Cell Biochem* 203:17-21.
- Behl C, Davis JB, Lesley R, Schubert D (1994) Hydrogen peroxide mediates amyloid beta protein toxicity. *Cell* 77:817-827.
- Berridge MJ (2012) Calcium signalling remodelling and disease. *Biochem Soc Trans* 40:297-309.
- Betarbet R, Sherer TB, MacKenzie G, Garcia-Osuna M, Panov AV, Greenamyre JT (2000) Chronic systemic pesticide exposure reproduces features of Parkinson's disease. *Nat Neurosci* 3:1301-1306.

- Bhat AH, Dar KB, Anees S, Zargar MA, Masood A, Sofi MA, Ganie SA (2015) Oxidative stress, mitochondrial dysfunction and neurodegenerative diseases; a mechanistic insight. *Biomed Pharmacother* 74:101-110.
- Biteau B, Karpac J, Hwangbo D, Jasper H (2011) Regulation of *Drosophila* lifespan by JNK signaling. *Exp Gerontol* 46:349-354.
- Blesa J, Przedborski S (2014) Parkinson's disease: animal models and dopaminergic cell vulnerability. *Front Neuroanat* 8:155.
- Blesa J, Trigo-Damas I, Quiroga-Varela A, Jackson-Lewis VR (2015) Oxidative stress and Parkinson's disease. *Front Neuroanat* 9:91.
- Bogeski I, Kilch T, Niemeyer BA (2012) ROS and SOCE: recent advances and controversies in the regulation of STIM and Orai. *J Physiol* 590:4193-4200.
- Bogeski I, Kummerow C, Al-Ansary D, Schwarz EC, Koehler R, Kozai D, Takahashi N, Peinelt C, Griesemer D, Bozem M, Mori Y, Hoth M, Niemeyer BA (2010) Differential redox regulation of ORAI ion channels: a mechanism to tune cellular calcium signaling. *Sci Signal* 3:ra24.
- Bootman MD, Taylor CW, Berridge MJ (1992) The thiol reagent, thimerosal, evokes Ca²⁺ spikes in HeLa cells by sensitizing the inositol 1,4,5-trisphosphate receptor. *J Biol Chem* 267:25113-25119.
- Brickley K, Stephenson FA (2011) Trafficking kinesin protein (TRAK)-mediated transport of mitochondria in axons of hippocampal neurons. *J Biol Chem* 286:18079-18092.
- Brickley K, Smith MJ, Beck M, Stephenson FA (2005) GRIF-1 and OIP106, members of a novel gene family of coiled-coil domain proteins: association in vivo and in vitro with kinesin. *J Biol Chem* 280:14723-14732.
- Bridgman PC (2004) Myosin-dependent transport in neurons. *J Neurobiol* 58:164-174.
- Brookes PS, Yoon Y, Robotham JL, Anders MW, Sheu SS (2004) Calcium, ATP, and ROS: a mitochondrial love-hate triangle. *Am J Physiol Cell Physiol* 287:C817-833.

- Chaanine AH, Jeong D, Liang L, Chemaly ER, Fish K, Gordon RE, Hajjar RJ (2012) JNK modulates FOXO3a for the expression of the mitochondrial death and mitophagy marker BNIP3 in pathological hypertrophy and in heart failure. *Cell Death Dis* 3:265.
- Chada SR, Hollenbeck PJ (2003) Mitochondrial movement and positioning in axons: the role of growth factor signaling. *J Exp Biol* 206:1985-1992.
- Chada SR, Hollenbeck PJ (2004) Nerve growth factor signaling regulates motility and docking of axonal mitochondria. *Curr Biol* 14:1272-1276.
- Chang DT, Honick AS, Reynolds IJ (2006a) Mitochondrial trafficking to synapses in cultured primary cortical neurons. *J Neurosci* 26:7035-7045.
- Chang DT, Rintoul GL, Pandipati S, Reynolds IJ (2006b) Mutant huntingtin aggregates impair mitochondrial movement and trafficking in cortical neurons. *Neurobiol Dis* 22:388-400.
- Chen S, Owens GC, Crossin KL, Edelman DB (2007) Serotonin stimulates mitochondrial transport in hippocampal neurons. *Mol Cell Neurosci* 36:472-483.
- Chen TW, Wardill TJ, Sun Y, Pulver SR, Renninger SL, Baohan A, Schreiter ER, Kerr RA, Orger MB, Jayaraman V, Looger LL, Svoboda K, Kim DS (2013) Ultrasensitive fluorescent proteins for imaging neuronal activity. *Nature* 499:295-300.
- Chen Y, Sheng ZH (2013) Kinesin-1-syntaphilin coupling mediates activity-dependent regulation of axonal mitochondrial transport. *J Cell Biol* 202:351-364.
- Chen YM, Gerwin C, Sheng ZH (2009) Dynein light chain LC8 regulates syntaphilin-mediated mitochondrial docking in axons. *J Neurosci* 29:9429-9438.
- Clark IE, Dodson MW, Jiang C, Cao JH, Huh JR, Seol JH, Yoo SJ, Hay BA, Guo M (2006) *Drosophila pink1* is required for mitochondrial function and interacts genetically with parkin. *Nature* 441:1162-1166.
- Clerkin JS, Naughton R, Quiney C, Cotter TG (2008) Mechanisms of ROS modulated cell survival during carcinogenesis. *Cancer Lett* 266:30-36.
- Cohen P, Frame S (2001) The renaissance of GSK3. *Nat Rev Mol Cell Biol* 2:769-776.

- Cook NL, Viola HM, Sharov VS, Hool LC, Schöneich C, Davies MJ (2012) Myeloperoxidase-derived oxidants inhibit sarco/endoplasmic reticulum Ca²⁺-ATPase activity and perturb Ca²⁺ homeostasis in human coronary artery endothelial cells. *Free Radic Biol Med* 52:951-961.
- Court FA, Coleman MP (2012) Mitochondria as a central sensor for axonal degenerative stimuli. *Trends Neurosci* 35:364-372.
- D'Autréaux B, Toledano MB (2007) ROS as signalling molecules: mechanisms that generate specificity in ROS homeostasis. *Nat Rev Mol Cell Biol* 8:813-824.
- De Vos KJ, Chapman AL, Tennant ME, Manser C, Tudor EL, Lau KF, Brownlee J, Ackerley S, Shaw PJ, McLoughlin DM, Shaw CE, Leigh PN, Miller CC, Grierson AJ (2007) Familial amyotrophic lateral sclerosis-linked SOD1 mutants perturb fast axonal transport to reduce axonal mitochondria content. *Hum Mol Genet* 16:2720-2728.
- Devireddy S, Liu A, Lampe T, Hollenbeck PJ (2015) The Organization of Mitochondrial Quality Control and Life Cycle in the Nervous System In Vivo in the Absence of PINK1. *J Neurosci* 35:9391-9401.
- Devireddy S, Sung H, Liao PC, Garland-Kuntz E, Hollenbeck PJ (2014) Analysis of mitochondrial traffic in *Drosophila*. *Methods Enzymol* 547:131-150.
- Dias-Santagata D, Fulga TA, Duttaroy A, Feany MB (2007) Oxidative stress mediates tau-induced neurodegeneration in *Drosophila*. *J Clin Invest* 117:236-245.
- Dumont M, Wille E, Stack C, Calingasan NY, Beal MF, Lin MT (2009) Reduction of oxidative stress, amyloid deposition, and memory deficit by manganese superoxide dismutase overexpression in a transgenic mouse model of Alzheimer's disease. *FASEB J* 23:2459-2466.
- Elia AJ, Parkes TL, Kirby K, St George-Hyslop P, Boulianne GL, Phillips JP, Hilliker AJ (1999) Expression of human FALS SOD in motorneurons of *Drosophila*. *Free Radic Biol Med* 26:1332-1338.

- Exner N, Treske B, Paquet D, Holmström K, Schiesling C, Gispert S, Carballo-Carbajal I, Berg D, Hoepken HH, Gasser T, Krüger R, Winklhofer KF, Vogel F, Reichert AS, Auburger G, Kahle PJ, Schmid B, Haass C (2007) Loss-of-function of human PINK1 results in mitochondrial pathology and can be rescued by parkin. *J Neurosci* 27:12413-12418.
- Fan X, Hussien R, Brooks GA (2010) H₂O₂-induced mitochondrial fragmentation in C2C12 myocytes. *Free Radic Biol Med* 49:1646-1654.
- Fang C, Bourdette D, Banker G (2012) Oxidative stress inhibits axonal transport: implications for neurodegenerative diseases. *Mol Neurodegener* 7:29.
- Federico A, Cardaioli E, Da Pozzo P, Formichi P, Gallus GN, Radi E (2012) Mitochondria, oxidative stress and neurodegeneration. *J Neurol Sci* 322:254-262.
- Fischer F, Hamann A, Osiewacz HD (2012) Mitochondrial quality control: an integrated network of pathways. *Trends Biochem Sci* 37:284-292.
- Frank M, Duvezin-Caubet S, Koob S, Occhipinti A, Jagasia R, Petcherski A, Ruonala MO, Priault M, Salin B, Reichert AS (2012) Mitophagy is triggered by mild oxidative stress in a mitochondrial fission dependent manner. *Biochim Biophys Acta* 1823:2297-2310.
- Fransson A, Ruusala A, Aspenström P (2003) Atypical Rho GTPases have roles in mitochondrial homeostasis and apoptosis. *J Biol Chem* 278:6495-6502.
- Fransson S, Ruusala A, Aspenström P (2006) The atypical Rho GTPases Miro-1 and Miro-2 have essential roles in mitochondrial trafficking. *Biochem Biophys Res Commun* 344:500-510.
- Gandhi S, Abramov AY (2012) Mechanism of oxidative stress in neurodegeneration. *Oxid Med Cell Longev* 2012:428010.
- Gautier CA, Kitada T, Shen J (2008) Loss of PINK1 causes mitochondrial functional defects and increased sensitivity to oxidative stress. *Proc Natl Acad Sci U S A* 105:11364-11369.
- Genova ML, Lenaz G (2015) The Interplay Between Respiratory Supercomplexes and ROS in Aging. *Antioxid Redox Signal* 23:208-238.

- Genova ML, Ventura B, Giuliano G, Bovina C, Formiggini G, Parenti Castelli G, Lenaz G (2001) The site of production of superoxide radical in mitochondrial Complex I is not a bound ubiquinone but presumably iron-sulfur cluster N2. *FEBS Lett* 505:364-368.
- Gill JS, McKenna WJ, Camm AJ (1995) Free radicals irreversibly decrease Ca²⁺ currents in isolated guinea-pig ventricular myocytes. *Eur J Pharmacol* 292:337-340.
- Glater EE, Megeath LJ, Stowers RS, Schwarz TL (2006) Axonal transport of mitochondria requires milton to recruit kinesin heavy chain and is light chain independent. *J Cell Biol* 173:545-557.
- Gleichmann M, Mattson MP (2011) Neuronal calcium homeostasis and dysregulation. *Antioxid Redox Signal* 14:1261-1273.
- Gotoh Y, Cooper JA (1998) Reactive oxygen species- and dimerization-induced activation of apoptosis signal-regulating kinase 1 in tumor necrosis factor- α signal transduction. *J Biol Chem* 273:17477-17482.
- Greene AW, Grenier K, Aguilera MA, Muise S, Farazifard R, Haque ME, McBride HM, Park DS, Fon EA (2012) Mitochondrial processing peptidase regulates PINK1 processing, import and Parkin recruitment. *EMBO Rep* 13:378-385.
- Greene JC, Whitworth AJ, Kuo I, Andrews LA, Feany MB, Pallanck LJ (2003) Mitochondrial pathology and apoptotic muscle degeneration in *Drosophila parkin* mutants. *Proc Natl Acad Sci U S A* 100:4078-4083.
- Grupe M, Myers G, Penner R, Fleig A (2010) Activation of store-operated I(CRAC) by hydrogen peroxide. *Cell Calcium* 48:1-9.
- Guo X, Macleod GT, Wellington A, Hu F, Panchumarthi S, Schoenfield M, Marin L, Charlton MP, Atwood HL, Zinsmaier KE (2005) The GTPase dMiro is required for axonal transport of mitochondria to *Drosophila* synapses. *Neuron* 47:379-393.
- Górska-Andrzejak J, Stowers RS, Borycz J, Kostyleva R, Schwarz TL, Meinertzhagen IA (2003) Mitochondria are redistributed in *Drosophila* photoreceptors lacking milton, a kinesin-associated protein. *J Comp Neurol* 463:372-388.

- Görlach A, Bertram K, Hudecova S, Krizanova O (2015) Calcium and ROS: A mutual interplay. *Redox Biol* 6:260-271.
- Ha EM, Oh CT, Bae YS, Lee WJ (2005) A direct role for dual oxidase in *Drosophila* gut immunity. *Science* 310:847-850.
- Han D, Antunes F, Canali R, Rettori D, Cadenas E (2003) Voltage-dependent anion channels control the release of the superoxide anion from mitochondria to cytosol. *J Biol Chem* 278:5557-5563.
- Hara Y, Wakamori M, Ishii M, Maeno E, Nishida M, Yoshida T, Yamada H, Shimizu S, Mori E, Kudoh J, Shimizu N, Kurose H, Okada Y, Imoto K, Mori Y (2002) LTRPC2 Ca²⁺-permeable channel activated by changes in redox status confers susceptibility to cell death. *Mol Cell* 9:163-173.
- Hardt SE, Sadoshima J (2002) Glycogen synthase kinase-3 β : a novel regulator of cardiac hypertrophy and development. *Circ Res* 90:1055-1063.
- Hidalgo C, Donoso P (2008) Crosstalk between calcium and redox signaling: from molecular mechanisms to health implications. *Antioxid Redox Signal* 10:1275-1312.
- Hirokawa N, Niwa S, Tanaka Y (2010) Molecular motors in neurons: transport mechanisms and roles in brain function, development, and disease. *Neuron* 68:610-638.
- Hollenbeck PJ (1993) Products of endocytosis and autophagy are retrieved from axons by regulated retrograde organelle transport. *J Cell Biol* 121:305-315.
- Horiuchi D, Barkus RV, Pilling AD, Gassman A, Saxton WM (2005) APLIP1, a kinesin binding JIP-1/JNK scaffold protein, influences the axonal transport of both vesicles and mitochondria in *Drosophila*. *Curr Biol* 15:2137-2141.
- Huang Y, Li X, Wang Y, Wang H, Huang C, Li J (2014) Endoplasmic reticulum stress-induced hepatic stellate cell apoptosis through calcium-mediated JNK/P38 MAPK and Calpain/Caspase-12 pathways. *Mol Cell Biochem* 394:1-12.
- Hudasek K, Brown ST, Fearon IM (2004) H₂O₂ regulates recombinant Ca²⁺ channel α 1C subunits but does not mediate their sensitivity to acute hypoxia. *Biochem Biophys Res Commun* 318:135-141.

- Isonaka R, Hiruma H, Kawakami T (2011) Inhibition of axonal transport caused by tert-butyl hydroperoxide in cultured mouse dorsal root ganglion neurons. *J Mol Neurosci* 45:194-201.
- Jendrach M, Mai S, Pohl S, Vöth M, Bereiter-Hahn J (2008) Short- and long-term alterations of mitochondrial morphology, dynamics and mtDNA after transient oxidative stress. *Mitochondrion* 8:293-304.
- Jones RM, Luo L, Ardita CS, Richardson AN, Kwon YM, Mercante JW, Alam A, Gates CL, Wu H, Swanson PA, Lambeth JD, Denning PW, Neish AS (2013) Symbiotic lactobacilli stimulate gut epithelial proliferation via Nox-mediated generation of reactive oxygen species. *EMBO J* 32:3017-3028.
- Kang JS, Tian JH, Pan PY, Zald P, Li C, Deng C, Sheng ZH (2008) Docking of axonal mitochondria by syntaphilin controls their mobility and affects short-term facilitation. *Cell* 132:137-148.
- Katsuyama M, Matsuno K, Yabe-Nishimura C (2012) Physiological roles of NOX/NADPH oxidase, the superoxide-generating enzyme. *J Clin Biochem Nutr* 50:9-22.
- Khan SR (2013) Reactive oxygen species as the molecular modulators of calcium oxalate kidney stone formation: evidence from clinical and experimental investigations. *J Urol* 189:803-811.
- Kim GH, Kim JE, Rhie SJ, Yoon S (2015) The Role of Oxidative Stress in Neurodegenerative Diseases. *Exp Neurobiol* 24:325-340.
- Kim J, Sharma RP (2004) Calcium-mediated activation of c-Jun NH₂-terminal kinase (JNK) and apoptosis in response to cadmium in murine macrophages. *Toxicol Sci* 81:518-527.
- Kim-Han JS, Antenor-Dorsey JA, O'Malley KL (2011) The parkinsonian mimetic, MPP⁺, specifically impairs mitochondrial transport in dopamine axons. *J Neurosci* 31:7212-7221.
- Kitada T, Asakawa S, Hattori N, Matsumine H, Yamamura Y, Minoshima S, Yokochi M, Mizuno Y, Shimizu N (1998) Mutations in the parkin gene cause autosomal recessive juvenile parkinsonism. *Nature* 392:605-608.

- Lambeth JD, Neish AS (2014) Nox enzymes and new thinking on reactive oxygen: a double-edged sword revisited. *Annu Rev Pathol* 9:119-145.
- Lao G, Scheuss V, Gerwin CM, Su Q, Mochida S, Rettig J, Sheng ZH (2000) Syntaphilin: a syntaxin-1 clamp that controls SNARE assembly. *Neuron* 25:191-201.
- Lazarou M, Jin SM, Kane LA, Youle RJ (2012) Role of PINK1 binding to the TOM complex and alternate intracellular membranes in recruitment and activation of the E3 ligase Parkin. *Dev Cell* 22:320-333.
- Lee KA, Kim SH, Kim EK, Ha EM, You H, Kim B, Kim MJ, Kwon Y, Ryu JH, Lee WJ (2013) Bacterial-derived uracil as a modulator of mucosal immunity and gut-microbe homeostasis in *Drosophila*. *Cell* 153:797-811.
- Lee KS, Iijima-Ando K, Iijima K, Lee WJ, Lee JH, Yu K, Lee DS (2009) JNK/FOXO-mediated neuronal expression of fly homologue of peroxiredoxin II reduces oxidative stress and extends life span. *J Biol Chem* 284:29454-29461.
- Li F, Calingasan NY, Yu F, Mauck WM, Toidze M, Almeida CG, Takahashi RH, Carlson GA, Flint Beal M, Lin MT, Gouras GK (2004) Increased plaque burden in brains of APP mutant MnSOD heterozygous knockout mice. *J Neurochem* 89:1308-1312.
- Liu S, Sawada T, Lee S, Yu W, Silverio G, Alapatt P, Millan I, Shen A, Saxton W, Kanao T, Takahashi R, Hattori N, Imai Y, Lu B (2012) Parkinson's disease-associated kinase PINK1 regulates Miro protein level and axonal transport of mitochondria. *PLoS Genet* 8:e1002537.
- Llorens-Martín M, López-Doménech G, Soriano E, Avila J (2011) GSK3 β is involved in the relief of mitochondria pausing in a Tau-dependent manner. *PLoS One* 6:e27686.
- Lock JT, Sinkins WG, Schilling WP (2011) Effect of protein S-glutathionylation on Ca²⁺ homeostasis in cultured aortic endothelial cells. *Am J Physiol Heart Circ Physiol* 300:H493-506.
- MacAskill AF, Brickley K, Stephenson FA, Kittler JT (2009) GTPase dependent recruitment of Grif-1 by Miro1 regulates mitochondrial trafficking in hippocampal neurons. *Mol Cell Neurosci* 40:301-312.

- Macaskill AF, Rinholm JE, Twelvetrees AE, Arancibia-Carcamo IL, Muir J, Fransson A, Aspenstrom P, Attwell D, Kittler JT (2009) Miro1 is a calcium sensor for glutamate receptor-dependent localization of mitochondria at synapses. *Neuron* 61:541-555.
- Maday S, Wallace KE, Holzbaur EL (2012) Autophagosomes initiate distally and mature during transport toward the cell soma in primary neurons. *J Cell Biol* 196:407-417.
- Magrané J, Sahawneh MA, Przedborski S, Estévez Á, Manfredi G (2012) Mitochondrial dynamics and bioenergetic dysfunction is associated with synaptic alterations in mutant SOD1 motor neurons. *J Neurosci* 32:229-242.
- Magrané J, Hervias I, Henning MS, Damiano M, Kawamata H, Manfredi G (2009) Mutant SOD1 in neuronal mitochondria causes toxicity and mitochondrial dynamics abnormalities. *Hum Mol Genet* 18:4552-4564.
- Martin LJ, Pan Y, Price AC, Sterling W, Copeland NG, Jenkins NA, Price DL, Lee MK (2006) Parkinson's disease alpha-synuclein transgenic mice develop neuronal mitochondrial degeneration and cell death. *J Neurosci* 26:41-50.
- Martin M, Iyadurai SJ, Gassman A, Gindhart JG, Hays TS, Saxton WM (1999) Cytoplasmic dynein, the dynactin complex, and kinesin are interdependent and essential for fast axonal transport. *Mol Biol Cell* 10:3717-3728.
- Matsuda N, Sato S, Shiba K, Okatsu K, Saisho K, Gautier CA, Sou YS, Saiki S, Kawajiri S, Sato F, Kimura M, Komatsu M, Hattori N, Tanaka K (2010) PINK1 stabilized by mitochondrial depolarization recruits Parkin to damaged mitochondria and activates latent Parkin for mitophagy. *J Cell Biol* 189:211-221.
- Matsuoka Y, Picciano M, La Francois J, Duff K (2001) Fibrillar beta-amyloid evokes oxidative damage in a transgenic mouse model of Alzheimer's disease. *Neuroscience* 104:609-613.
- Matés JM, Pérez-Gómez C, Núñez de Castro I (1999) Antioxidant enzymes and human diseases. *Clin Biochem* 32:595-603.
- Meissner C, Lorenz H, Weihofen A, Selkoe DJ, Lemberg MK (2011) The mitochondrial intramembrane protease PARL cleaves human Pink1 to regulate Pink1 trafficking. *J Neurochem* 117:856-867.

- Miller KE, Sheetz MP (2004) Axonal mitochondrial transport and potential are correlated. *J Cell Sci* 117:2791-2804.
- Misko A, Jiang S, Wegorzewska I, Milbrandt J, Baloh RH (2010) Mitofusin 2 is necessary for transport of axonal mitochondria and interacts with the Miro/Milton complex. *J Neurosci* 30:4232-4240.
- Misko AL, Sasaki Y, Tuck E, Milbrandt J, Baloh RH (2012) Mitofusin2 mutations disrupt axonal mitochondrial positioning and promote axon degeneration. *J Neurosci* 32:4145-4155.
- Mizuno Y, Sone N, Saitoh T (1987) Effects of 1-methyl-4-phenyl-1,2,3,6-tetrahydropyridine and 1-methyl-4-phenylpyridinium ion on activities of the enzymes in the electron transport system in mouse brain. *J Neurochem* 48:1787-1793.
- Morfini G, Szebenyi G, Elluru R, Ratner N, Brady ST (2002) Glycogen synthase kinase 3 phosphorylates kinesin light chains and negatively regulates kinesin-based motility. *EMBO J* 21:281-293.
- Morfini G, Pigino G, Szebenyi G, You Y, Pollema S, Brady ST (2006) JNK mediates pathogenic effects of polyglutamine-expanded androgen receptor on fast axonal transport. *Nat Neurosci* 9:907-916.
- Morfini GA, You YM, Pollema SL, Kaminska A, Liu K, Yoshioka K, Björkblom B, Coffey ET, Bagnato C, Han D, Huang CF, Banker G, Pigino G, Brady ST (2009) Pathogenic huntingtin inhibits fast axonal transport by activating JNK3 and phosphorylating kinesin. *Nat Neurosci* 12:864-871.
- Morris RL, Hollenbeck PJ (1993) The regulation of bidirectional mitochondrial transport is coordinated with axonal outgrowth. *J Cell Sci* 104 (Pt 3):917-927.
- Morris RL, Hollenbeck PJ (1995) Axonal transport of mitochondria along microtubules and F-actin in living vertebrate neurons. *J Cell Biol* 131:1315-1326.
- Mruk DD, Silvestrini B, Mo MY, Cheng CY (2002) Antioxidant superoxide dismutase - a review: its function, regulation in the testis, and role in male fertility. *Contraception* 65:305-311.

- Munnamalai V, Weaver CJ, Weisheit CE, Venkatraman P, Agim ZS, Quinn MT, Suter DM (2014) Bidirectional interactions between NOX2-type NADPH oxidase and the F-actin cytoskeleton in neuronal growth cones. *J Neurochem* 130:526-540.
- Murakami K, Murata N, Noda Y, Tahara S, Kaneko T, Kinoshita N, Hatsuta H, Murayama S, Barnham KJ, Irie K, Shirasawa T, Shimizu T (2011) SOD1 (copper/zinc superoxide dismutase) deficiency drives amyloid β protein oligomerization and memory loss in mouse model of Alzheimer disease. *J Biol Chem* 286:44557-44568.
- Nagao M, Kaziro Y, Itoh H (1999) The Src family tyrosine kinase is involved in Rho-dependent activation of c-Jun N-terminal kinase by Galpha12. *Oncogene* 18:4425-4434.
- Nakanishi A, Wada Y, Kitagishi Y, Matsuda S (2014) Link between PI3K/AKT/PTEN Pathway and NOX Protein in Diseases. *Aging Dis* 5:203-211.
- Nangaku M, Sato-Yoshitake R, Okada Y, Noda Y, Takemura R, Yamazaki H, Hirokawa N (1994) KIF1B, a novel microtubule plus end-directed monomeric motor protein for transport of mitochondria. *Cell* 79:1209-1220.
- Narendra D, Tanaka A, Suen DF, Youle RJ (2008) Parkin is recruited selectively to impaired mitochondria and promotes their autophagy. *J Cell Biol* 183:795-803.
- Narendra DP, Jin SM, Tanaka A, Suen DF, Gautier CA, Shen J, Cookson MR, Youle RJ (2010) PINK1 is selectively stabilized on impaired mitochondria to activate Parkin. *PLoS Biol* 8:e1000298.
- Nayernia Z, Jaquet V, Krause KH (2014) New insights on NOX enzymes in the central nervous system. *Antioxid Redox Signal* 20:2815-2837.
- Nguyen TT, Oh SS, Weaver D, Lewandowska A, Maxfield D, Schuler MH, Smith NK, Macfarlane J, Saunders G, Palmer CA, Debattisti V, Koshiba T, Pulst S, Feldman EL, Hajnóczky G, Shaw JM (2014) Loss of Miro1-directed mitochondrial movement results in a novel murine model for neuron disease. *Proc Natl Acad Sci U S A* 111:E3631-3640.

- Ogawa F, Murphy LC, Malavasi EL, O'Sullivan ST, Torrance HS, Porteous DJ, Millar JK (2016) NDE1 and GSK3 β Associate with TRAK1 and Regulate Axonal Mitochondrial Motility: Identification of Cyclic AMP as a Novel Modulator of Axonal Mitochondrial Trafficking. *ACS Chem Neurosci*.
- Ohno N, Kidd GJ, Mahad D, Kiryu-Seo S, Avishai A, Komuro H, Trapp BD (2011) Myelination and axonal electrical activity modulate the distribution and motility of mitochondria at CNS nodes of Ranvier. *J Neurosci* 31:7249-7258.
- Orr AL, Li S, Wang CE, Li H, Wang J, Rong J, Xu X, Mastroberardino PG, Greenamyre JT, Li XJ (2008) N-terminal mutant huntingtin associates with mitochondria and impairs mitochondrial trafficking. *J Neurosci* 28:2783-2792.
- Park J, Lee SB, Lee S, Kim Y, Song S, Kim S, Bae E, Kim J, Shong M, Kim JM, Chung J (2006) Mitochondrial dysfunction in *Drosophila* PINK1 mutants is complemented by parkin. *Nature* 441:1157-1161.
- Park JH, Ko J, Park YS, Park J, Hwang J, Koh HC (2016) Clearance of Damaged Mitochondria Through PINK1 Stabilization by JNK and ERK MAPK Signaling in Chlorpyrifos-Treated Neuroblastoma Cells. *Mol Neurobiol*.
- Parkes TL, Elia AJ, Dickinson D, Hilliker AJ, Phillips JP, Boulianne GL (1998) Extension of *Drosophila* lifespan by overexpression of human SOD1 in motoneurons. *Nat Genet* 19:171-174.
- Pathak D, Sepp KJ, Hollenbeck PJ (2010) Evidence that myosin activity opposes microtubule-based axonal transport of mitochondria. *J Neurosci* 30:8984-8992.
- Pilling AD, Horiuchi D, Lively CM, Saxton WM (2006) Kinesin-1 and Dynein are the primary motors for fast transport of mitochondria in *Drosophila* motor axons. *Mol Biol Cell* 17:2057-2068.
- Pukass K, Richter-Landsberg C (2014) Oxidative stress promotes uptake, accumulation, and oligomerization of extracellular α -synuclein in oligodendrocytes. *J Mol Neurosci* 52:339-352.
- Purisai MG, McCormack AL, Cumine S, Li J, Isla MZ, Di Monte DA (2007) Microglial activation as a priming event leading to paraquat-induced dopaminergic cell degeneration. *Neurobiol Dis* 25:392-400.

- Razzell W, Evans IR, Martin P, Wood W (2013) Calcium flashes orchestrate the wound inflammatory response through DUOX activation and hydrogen peroxide release. *Curr Biol* 23:424-429.
- Rintoul GL, Filiano AJ, Brocard JB, Kress GJ, Reynolds IJ (2003) Glutamate decreases mitochondrial size and movement in primary forebrain neurons. *J Neurosci* 23:7881-7888.
- Ritsick DR, Edens WA, Finnerty V, Lambeth JD (2007) Nox regulation of smooth muscle contraction. *Free Radic Biol Med* 43:31-38.
- Royer-Pokora B, Kunkel LM, Monaco AP, Goff SC, Newburger PE, Baehner RL, Cole FS, Curnutte JT, Orkin SH (1986) Cloning the gene for an inherited human disorder--chronic granulomatous disease--on the basis of its chromosomal location. *Nature* 322:32-38.
- Rui Y, Tiwari P, Xie Z, Zheng JQ (2006) Acute impairment of mitochondrial trafficking by beta-amyloid peptides in hippocampal neurons. *J Neurosci* 26:10480-10487.
- Russo GJ, Louie K, Wellington A, Macleod GT, Hu F, Panchumarthi S, Zinsmaier KE (2009) Drosophila Miro is required for both anterograde and retrograde axonal mitochondrial transport. *J Neurosci* 29:5443-5455.
- Saitoh M, Nishitoh H, Fujii M, Takeda K, Tobiume K, Sawada Y, Kawabata M, Miyazono K, Ichijo H (1998) Mammalian thioredoxin is a direct inhibitor of apoptosis signal-regulating kinase (ASK) 1. *EMBO J* 17:2596-2606.
- Saotome M, Safiulina D, Szabadkai G, Das S, Fransson A, Aspenstrom P, Rizzuto R, Hajnóczky G (2008) Bidirectional Ca²⁺-dependent control of mitochondrial dynamics by the Miro GTPase. *Proc Natl Acad Sci U S A* 105:20728-20733.
- Sato T, Ishikawa M, Mochizuki M, Ohta M, Ohkura M, Nakai J, Takamatsu N, Yoshioka K (2015) JSAP1/JIP3 and JLP regulate kinesin-1-dependent axonal transport to prevent neuronal degeneration. *Cell Death Differ* 22:1260-1274.
- Saxton WM, Hollenbeck PJ (2012) The axonal transport of mitochondria. *J Cell Sci* 125:2095-2104.
- Schwarz TL (2013) Mitochondrial trafficking in neurons. *Cold Spring Harb Perspect Biol* 5.

- Sharov VS, Dremina ES, Galeva NA, Williams TD, Schöneich C (2006) Quantitative mapping of oxidation-sensitive cysteine residues in SERCA in vivo and in vitro by HPLC-electrospray-tandem MS: selective protein oxidation during biological aging. *Biochem J* 394:605-615.
- Shen HM, Liu ZG (2006) JNK signaling pathway is a key modulator in cell death mediated by reactive oxygen and nitrogen species. *Free Radic Biol Med* 40:928-939.
- Shen WW, Frieden M, Demaurex N (2011) Remodelling of the endoplasmic reticulum during store-operated calcium entry. *Biol Cell* 103:365-380.
- Sheng ZH, Cai Q (2012) Mitochondrial transport in neurons: impact on synaptic homeostasis and neurodegeneration. *Nat Rev Neurosci* 13:77-93.
- Shidara Y, Hollenbeck PJ (2010) Defects in mitochondrial axonal transport and membrane potential without increased reactive oxygen species production in a *Drosophila* model of Friedreich ataxia. *J Neurosci* 30:11369-11378.
- Shin JE, Miller BR, Babetto E, Cho Y, Sasaki Y, Qayum S, Russler EV, Cavalli V, Milbrandt J, DiAntonio A (2012) SCG10 is a JNK target in the axonal degeneration pathway. *Proc Natl Acad Sci U S A* 109:E3696-3705.
- Smith MA, Hirai K, Hsiao K, Pappolla MA, Harris PL, Siedlak SL, Tabaton M, Perry G (1998) Amyloid-beta deposition in Alzheimer transgenic mice is associated with oxidative stress. *J Neurochem* 70:2212-2215.
- Smith MJ, Pozo K, Brickley K, Stephenson FA (2006) Mapping the GRIF-1 binding domain of the kinesin, KIF5C, substantiates a role for GRIF-1 as an adaptor protein in the anterograde trafficking of cargoes. *J Biol Chem* 281:27216-27228.
- Son Y, Kim S, Chung HT, Pae HO (2013) Reactive oxygen species in the activation of MAP kinases. *Methods Enzymol* 528:27-48.
- Song JJ, Lee YJ (2003) Differential role of glutaredoxin and thioredoxin in metabolic oxidative stress-induced activation of apoptosis signal-regulating kinase 1. *Biochem J* 373:845-853.

- Song JJ, Rhee JG, Suntharalingam M, Walsh SA, Spitz DR, Lee YJ (2002) Role of glutaredoxin in metabolic oxidative stress. Glutaredoxin as a sensor of oxidative stress mediated by H₂O₂. *J Biol Chem* 277:46566-46575.
- Song W, Song Y, Kincaid B, Bossy B, Bossy-Wetzell E (2012) Mutant SOD1(G93A) triggers mitochondrial fragmentation in spinal cord motor neurons: Neuroprotection by SIRT3 and PGC-1 α . *Neurobiol Dis*.
- Stamer K, Vogel R, Thies E, Mandelkow E, Mandelkow EM (2002) Tau blocks traffic of organelles, neurofilaments, and APP vesicles in neurons and enhances oxidative stress. *J Cell Biol* 156:1051-1063.
- Stephen TL, Higgs NF, Sheehan DF, Al Awabdh S, López-Doménech G, Arancibia-Carcamo IL, Kittler JT (2015) Miro1 Regulates Activity-Driven Positioning of Mitochondria within Astrocytic Processes Apposed to Synapses to Regulate Intracellular Calcium Signaling. *J Neurosci* 35:15996-16011.
- Stowers RS, Megeath LJ, Górska-Andrzejak J, Meinertzhagen IA, Schwarz TL (2002) Axonal transport of mitochondria to synapses depends on milton, a novel Drosophila protein. *Neuron* 36:1063-1077.
- Sullivan LB, Chandel NS (2014) Mitochondrial reactive oxygen species and cancer. *Cancer Metab* 2:17.
- Tabet F, Savoia C, Schiffrin EL, Touyz RM (2004) Differential calcium regulation by hydrogen peroxide and superoxide in vascular smooth muscle cells from spontaneously hypertensive rats. *J Cardiovasc Pharmacol* 44:200-208.
- Takahashi N, Mori Y (2011) TRP Channels as Sensors and Signal Integrators of Redox Status Changes. *Front Pharmacol* 2:58.
- Tanaka K, Sugiura Y, Ichishita R, Mihara K, Oka T (2011) KLP6: a newly identified kinesin that regulates the morphology and transport of mitochondria in neuronal cells. *J Cell Sci* 124:2457-2465.
- Taru H, Iijima K, Hase M, Kirino Y, Yagi Y, Suzuki T (2002) Interaction of Alzheimer's beta -amyloid precursor family proteins with scaffold proteins of the JNK signaling cascade. *J Biol Chem* 277:20070-20078.

- Terentyev D, Györke I, Belevych AE, Terentyeva R, Sridhar A, Nishijima Y, de Blanco EC, Khanna S, Sen CK, Cardounel AJ, Carnes CA, Györke S (2008) Redox modification of ryanodine receptors contributes to sarcoplasmic reticulum Ca²⁺ leak in chronic heart failure. *Circ Res* 103:1466-1472.
- Tobiome K, Matsuzawa A, Takahashi T, Nishitoh H, Morita K, Takeda K, Minowa O, Miyazono K, Noda T, Ichijo H (2001) ASK1 is required for sustained activations of JNK/p38 MAP kinases and apoptosis. *EMBO Rep* 2:222-228.
- Valente EM et al. (2004) Hereditary early-onset Parkinson's disease caused by mutations in PINK1. *Science* 304:1158-1160.
- Verburg J, Hollenbeck PJ (2008) Mitochondrial membrane potential in axons increases with local nerve growth factor or semaphorin signaling. *J Neurosci* 28:8306-8315.
- Verstreken P, Ly CV, Venken KJ, Koh TW, Zhou Y, Bellen HJ (2005) Synaptic mitochondria are critical for mobilization of reserve pool vesicles at *Drosophila* neuromuscular junctions. *Neuron* 47:365-378.
- Voets T, Talavera K, Owsianik G, Nilius B (2005) Sensing with TRP channels. *Nat Chem Biol* 1:85-92.
- Vossel KA, Zhang K, Brodbeck J, Daub AC, Sharma P, Finkbeiner S, Cui B, Mucke L (2010) Tau reduction prevents Abeta-induced defects in axonal transport. *Science* 330:198.
- Wang X, Schwarz TL (2009) The mechanism of Ca²⁺ -dependent regulation of kinesin-mediated mitochondrial motility. *Cell* 136:163-174.
- Wang X, Winter D, Ashrafi G, Schlehe J, Wong YL, Selkoe D, Rice S, Steen J, LaVoie MJ, Schwarz TL (2011) PINK1 and Parkin target Miro for phosphorylation and degradation to arrest mitochondrial motility. *Cell* 147:893-906.
- Weihofen A, Thomas KJ, Ostaszewski BL, Cookson MR, Selkoe DJ (2009) Pink1 forms a multiprotein complex with Miro and Milton, linking Pink1 function to mitochondrial trafficking. *Biochemistry* 48:2045-2052.
- Whitmarsh AJ, Kuan CY, Kennedy NJ, Kelkar N, Haydar TF, Mordes JP, Appel M, Rossini AA, Jones SN, Flavell RA, Rakic P, Davis RJ (2001) Requirement of the JIP1 scaffold protein for stress-induced JNK activation. *Genes Dev* 15:2421-2432.

- Wojtczak L, Lebidzińska M, Suski JM, Więckowski MR, Schönfeld P (2011) Inhibition by purine nucleotides of the release of reactive oxygen species from muscle mitochondria: indication for a function of uncoupling proteins as superoxide anion transporters. *Biochem Biophys Res Commun* 407:772-776.
- Wu XF, Block ML, Zhang W, Qin L, Wilson B, Zhang WQ, Veronesi B, Hong JS (2005) The role of microglia in paraquat-induced dopaminergic neurotoxicity. *Antioxid Redox Signal* 7:654-661.
- Xu B, Wu SW, Lu CW, Deng Y, Liu W, Wei YG, Yang TY, Xu ZF (2013) Oxidative stress involvement in manganese-induced alpha-synuclein oligomerization in organotypic brain slice cultures. *Toxicology* 305:71-78.
- Xu KY, Zweier JL, Becker LC (1997) Hydroxyl radical inhibits sarcoplasmic reticulum Ca(2+)-ATPase function by direct attack on the ATP binding site. *Circ Res* 80:76-81.
- Xu SZ, Sukumar P, Zeng F, Li J, Jairaman A, English A, Naylor J, Ciurtin C, Majeed Y, Milligan CJ, Bahnasi YM, Al-Shawaf E, Porter KE, Jiang LH, Emery P, Sivaprasadarao A, Beech DJ (2008) TRPC channel activation by extracellular thioredoxin. *Nature* 451:69-72.
- Yan Y, Liu J, Wei C, Li K, Xie W, Wang Y, Cheng H (2008) Bidirectional regulation of Ca²⁺ sparks by mitochondria-derived reactive oxygen species in cardiac myocytes. *Cardiovasc Res* 77:432-441.
- Yang Y, Gehrke S, Imai Y, Huang Z, Ouyang Y, Wang JW, Yang L, Beal MF, Vogel H, Lu B (2006) Mitochondrial pathology and muscle and dopaminergic neuron degeneration caused by inactivation of *Drosophila* Pink1 is rescued by Parkin. *Proc Natl Acad Sci U S A* 103:10793-10798.
- Yasuda J, Whitmarsh AJ, Cavanagh J, Sharma M, Davis RJ (1999) The JIP group of mitogen-activated protein kinase scaffold proteins. *Mol Cell Biol* 19:7245-7254.
- Yeromin AV, Roos J, Stauderman KA, Cahalan MD (2004) A store-operated calcium channel in *Drosophila* S2 cells. *J Gen Physiol* 123:167-182.
- Yi M, Weaver D, Hajnóczky G (2004) Control of mitochondrial motility and distribution by the calcium signal: a homeostatic circuit. *J Cell Biol* 167:661-672.

- Yoshida T, Inoue R, Morii T, Takahashi N, Yamamoto S, Hara Y, Tominaga M, Shimizu S, Sato Y, Mori Y (2006) Nitric oxide activates TRP channels by cysteine S-nitrosylation. *Nat Chem Biol* 2:596-607.
- Yu Y, Lee HC, Chen KC, Suhan J, Qiu M, Ba Q, Yang G (2016) Inner membrane fusion mediates spatial distribution of axonal mitochondria. *Sci Rep* 6:18981.
- Zaidi A (2010) Plasma membrane Ca-ATPases: Targets of oxidative stress in brain aging and neurodegeneration. *World J Biol Chem* 1:271-280.
- Zhang CL, Ho PL, Kintner DB, Sun D, Chiu SY (2010) Activity-dependent regulation of mitochondrial motility by calcium and Na/K-ATPase at nodes of Ranvier of myelinated nerves. *J Neurosci* 30:3555-3566.
- Zhang J, Wang X, Vikash V, Ye Q, Wu D, Liu Y, Dong W (2016) ROS and ROS-Mediated Cellular Signaling. *Oxid Med Cell Longev* 2016:4350965.
- Zhang Y, Han L, Qi W, Cheng D, Ma X, Hou L, Cao X, Wang C (2015) Eicosapentaenoic acid (EPA) induced apoptosis in HepG2 cells through ROS-Ca(2+)-JNK mitochondrial pathways. *Biochem Biophys Res Commun* 456:926-932.
- Zhao Y, Zhao B (2013) Oxidative stress and the pathogenesis of Alzheimer's disease. *Oxid Med Cell Longev* 2013:316523.

VITA

VITA

Pin-Chao received his B.S. degree in Department of Life Science and M.S. degree in Institute of Biotechnology, National Tsing Hua University, Taiwan. His work focused on the effects of Heat Shock Protein 27 on lifespan and stress resistance in *Drosophila*. After finishing M.S. degree, he joined the lab as a research assistance in Institute of Molecular Medicine, National Tsing Hua University, Taiwan. He examined the mechanisms of delivery of proteins into mitochondria. Later, he joined Dr. Hollenbeck's lab in Department of Biological Sciences at Purdue University in 2011. His study focused on ROS regulation of mitochondrial axonal transport. After finishing Ph.D., he will pursue a postdoctoral position.